Heterogeneous Federated Zeroth-Order Optimization using Gradient Surrogates

Yao Shu [1] **Xiaoqiang Lin** [2] **Zhongxiang Dai** [3] **Bryan Kian Hsiang Low** [2]

Abstract

Federated optimization, an emerging paradigm that finds wide applications, e.g., federated learning, enables multiple clients (e.g., edge devices) to collaboratively optimize a global function by sharing their local gradients. However, the gradient information is not available in many applications, giving rise to the paradigm of federated *zeroth-order optimization* (ZOO). Existing federated ZOO algorithms typically suffer from the limitations of query and communication round inefficiency, which can be attributed to (a) their reliance on a substantial number of function queries for gradient estimation and (b) the significant disparity between their realized local updates and the intended global updates caused by client heterogeneity. To this end, we (a) introduce trajectory-informed gradient surrogates which are capable of using the history of function queries during optimization for accurate and query-efficient gradient estimation, and (b) develop the technique of adaptive gradient correction using these surrogates to mitigate the aforementioned disparity. With these, we propose the *federated zeroth-order optimization using gradient surrogates* (FZooS) algorithm for query- and communication round-efficient heterogeneous federated ZOO, which is supported by our theoretical analyses and extensive experiments.

1. Introduction

Because of the growing computational power of edge devices and increasing privacy concerns, recent years have witnessed a surging interest in federated optimization, which finds real-world applications including federated learning [1]. Particularly, federated optimization allows clients (e.g., edge devices) to retain their local datasets but share their locally computed gradients for optimization. Unfortunately, in many important applications of federated optimization including federated black-box adversarial attack [2], gradient information is not available. This gives rise to the paradigm of federated *zeroth-order optimization* (ZOO) where the global function to be optimized is an aggregation of the local functions on various clients and those local functions are only accessible via function queries. To tackle this problem, existing algorithms [2] follow the framework of applying *finite difference* (FD) for local gradient estimation and resorting to federated *first-order optimization* (FOO) algorithms for optimization. Nevertheless, these algorithms usually suffer from both query and communication round inefficiency for local and global functions that are not only **expensive-to-evaluate** but also **heterogeneous**. This impedes their practical applicability, especially in scenarios with **restricted query times and communication rounds**. However, to the best of our knowledge, little attention has been dedicated to developing both query- and communication round-efficient heterogeneous federated ZOO algorithms in the literature (related work in Appx. A).

To address this problem, it is imperative to first identify the challenges faced by existing federated ZOO algorithms which will be responsible for their query and communication round inefficiency in practice. Federated ZOO typically requires multiple communication rounds for central server aggregation; between consecutive communication rounds, every client performs several iterations of local updates using their estimated gradients that are usually approximated via additional function queries based on FD. We first show that the query inefficiency of existing federated ZOO algorithms arises from their employment of FD for local gradient estimation, which often requires an excessive number of additional function queries. Thus, addressing the challenge of query efficiency in federated ZOO calls for a gradient estimation method that requires minimal (ideally zero) additional function queries. We further show that the communication round inefficiency of these existing algorithms results from the disparity between their realized local updates and the intended global updates, which is typically caused by client heterogeneity. As a consequence, resolving

[1]Guangdong Lab of AI and Digital Economy (SZ) [2]Department of Computer Science, National University of Singapore [3]LIDS and EECS, Massachusetts Institute of Technology. Correspondence to: Zhongxiang Dai <daizx@mit.ed>.

Published at the 2^{nd} Differentiable Almost Everything Workshop at the 41^{st} International Conference on Machine Learning, Vienna, Austria. July 2024.

the challenge of communication round efficiency requires developing a high-quality gradient correction technique to mitigate such a disparity.

So, we propose the *federated zeroth-order optimization using gradient surrogates* (FZooS) algorithm to address the aforementioned challenges, leading to a query- and communication round-efficient heterogeneous federated ZOO algorithm. Firstly, we introduce the recent derived Gaussian process from [3] that only requires the optimization trajectory (i.e., the history of function queries) for gradient estimation, as the local gradient surrogates for the clients, thereby realizing query-efficient gradient estimation in federated ZOO (Sec. 3.1). Secondly, based on these local gradient surrogates, we apply *random Fourier features* (RFF) approximation [4] to produce a transferable global gradient surrogate without the necessity of transferring raw observations, which can be an accurate estimate of the gradient of the global function (Sec. 3.2.1). Using these surrogates, we develop the technique of adaptive gradient correction using adaptive gradient correction vector and length to help mitigate the disparity between our local updates and the intended global updates, and consequently to improve the communication round efficiency of heterogeneous federated ZOO (Sec. 3.2.2). We verify that FZooS has addressed the aforementioned challenges using both theoretical analyses (Sec. 4) and empirical experiments (Sec. 5).

2. Preliminaries

In the federated *zeroth-order optimization* (ZOO) setting [2], we aim to minimize a global function F on $\boldsymbol{x} \in \mathcal{X}$, which is the arithmetic average of N local functions $\{f_1, \cdots, f_N\}$ on N different clients without sharing these local functions:

$$\min_{\boldsymbol{x}\in\mathcal{X}} F(\boldsymbol{x}) \triangleq \textstyle\sum_{i\in[N]} f_i(\boldsymbol{x})/N \ . \tag{1}$$

A central server is typically introduced to periodically aggregate the updated inputs sent from the clients after their several iterations of local optimization. Of note, in this federated ZOO setting, the gradients of the local functions are either not accessible or too computationally expensive to obtain. Consequently, the gradients can not be directly employed for optimization, which is our main difference from the standard federated *first-order optimization* (FOO) setting [5]–[7]. Instead, given an input $\boldsymbol{x} \in \mathcal{X}$, agent i is only allowed to observe a noisy output $y_i(\boldsymbol{x}) \triangleq f_i(\boldsymbol{x}) + \zeta$ of the local function f_i, in which $\zeta \sim \mathcal{N}(0, \sigma^2)$. Moreover, we focus on federated ZOO with heterogeneous clients, i.e., the local functions $\{f_i\}_{i=1}^N$ differ from the global function F. Besides, we adopt a common assumption on $\{f_i\}_{i=1}^N$: We assume that every local function f_i is sampled from a *Gaussian process* (GP), i.e., $f_i \sim \mathcal{GP}(\mu(\cdot), k(\cdot,\cdot))$ [3]. We summarize the framework to solve the heterogeneous federated ZOO problem and identify the challenges faced by existing algorithms in Appx. B.

3. FZooS Algorithm

We hence propose our *federated zeroth-order optimization using gradient surrogates* (FZooS) algorithm (see Algo. 2 in Appendix) to improve the query and communication round efficiency of existing federated ZOO algorithms.

3.1. Trajectory-Informed Gradient Estimation

Of note, we assumed that $f_i \sim \mathcal{GP}(\mu(\cdot), k(\cdot,\cdot)), \forall i \in [N]$ (Sec. 2). Then, in iteration t of communication round r (Algo. 2), conditioned on the optimization trajectory $\mathcal{D}_{r,t-1}^{(i)} \triangleq \{(\boldsymbol{x}_\tau^{(i)}, y_\tau^{(i)})\}_{\tau=1}^{T(r-1)+t-1}$ of client i,[1] ∇f_i follows a *derived posterior Gaussian Process* [3]:

$$\nabla f_i \sim \mathcal{GP}\Big(\nabla\mu_{r,t-1}^{(i)}(\cdot), \partial\left(\sigma_{r,t-1}^{(i)}\right)^2(\cdot,\cdot)\Big) \tag{2}$$

where the mean function $\nabla\mu_{r,t-1}^{(i)}(\cdot)$ and the covariance function $\partial(\sigma_{r,t-1}^{(i)})^2(\cdot,\cdot)$ are defined in (8) from Appx. C.1.

We propose to make use of the posterior mean $\nabla\mu_{r,t-1}^{(i)}(\boldsymbol{x})$ (8) as the local gradient surrogate for client i since it is a prediction of the gradient $\nabla f_i(\boldsymbol{x})$, and $\partial(\sigma_{r,t-1}^{(i)})^2(\boldsymbol{x}) \triangleq \partial(\sigma_{r,t-1}^{(i)})^2(\boldsymbol{x},\boldsymbol{x})$ provides a principled uncertainty measure for this gradient surrogate [3]. Of note, our gradient surrogate only requires the optimization trajectory (i.e., the history of function queries $\mathcal{D}_{r,t-1}^{(i)}$ till iteration $t-1$ of round r) and thus *eliminates the need for additional queries* required by the FD methods adopted by existing federated ZOO (Appx. B.2). This therefore leads to more query-efficient gradient estimations in federated ZOO. Moreover, the aforementioned uncertainty measure can theoretically guarantee the quality of our gradient estimation, and provide theoretical support for our technique of using active queries to further improve the local gradient estimations (Sec. 4).

3.2. Gradient Correction

3.2.1. Global Gradient Surrogate

Note that our local gradient surrogates from Sec. 3.1 can produce not only query-efficient but also accurate gradient estimations [3]. So, these local surrogates can be used to construct an accurate global gradient surrogate, which then satisfies requirement **(A)** for communication round-efficient federated ZOO from Appx. B.2: accurate local and global gradient surrogates. However, due to the non-parametric nature of Gaussian processes, (2) cannot be transferred to the server without sending the raw observations. To this end, we introduce the idea of *random Fourier features* (RFF) approximation from [4] to approximate the mean of (2) and then transfer this approximated mean to server for the construction of high-quality global gradient surrogate.

We firstly approximate the mean of (2) on each client to ease its transfer between the clients and the server. If $k(\cdot,\cdot)$

[1] We slightly abuse notation and use $(\boldsymbol{x}_\tau^{(i)}, y_\tau^{(i)})$ to denote a historical query till iteration $t-1$ of round r.

is assumed to be shift-invariant, it can be approximated by a finite number of random features [4]. That is, we have that $k(\boldsymbol{x}, \boldsymbol{x}') \approx \phi(\boldsymbol{x})^\top \phi(\boldsymbol{x}')$ where pre-defined function $\phi : \mathbb{R}^d \mapsto \mathbb{R}^M$ produces M random features and its parameters are shared across all clients and the server (Appx. D). By incorporating this approximation into (8), the local gradient surrogates on each client i at the end of every round r (i.e., $\nabla\mu^{(i)}_{r,T}(\boldsymbol{x})$) can then be approximated as

$$\nabla\widehat{\mu}^{(i)}_{r,T}(\boldsymbol{x}) \triangleq \nabla\phi(\boldsymbol{x})^\top \boldsymbol{\Phi}^{(i)}_{r,T}\left(\widehat{\mathbf{K}}^{(i)}_{r,T} + \sigma^2\mathbf{I}\right)^{-1}\boldsymbol{y}^{(i)}_{r,T} \quad (3)$$

where $\nabla\phi(\boldsymbol{x})$ is an $M \times d$-dimensional matrix, $\boldsymbol{\Phi}^{(i)}_{r,T} \triangleq [\phi(\boldsymbol{x}^{(i)}_\tau)]^{rT}_{\tau=1}$ is an $M\times rT$-dimensional matrix, and $\widehat{\mathbf{K}}^{(i)}_{r,T} \triangleq [\phi(\boldsymbol{x}^{(i)}_\tau)^\top\phi(\boldsymbol{x}^{(i)}_{\tau'})]^{rT}_{\tau,\tau'=1}$ is an $rT \times rT$-dimensional matrix. Define an M-dimensional column vector $\boldsymbol{w}^{(i)}_{r,T} \triangleq \boldsymbol{\Phi}^{(i)}_{r,T}(\widehat{\mathbf{K}}^{(i)}_{r,T} + \sigma^2\mathbf{I})^{-1}\boldsymbol{y}^{(i)}_{r,T}$, (3) can therefore be rewritten as $\nabla\widehat{\mu}^{(i)}_{r,t-1}(\boldsymbol{x}) = \nabla\phi(\boldsymbol{x})^\top\boldsymbol{w}^{(i)}_{r,T}$ (line 8 of Algo. 2). So, each client only needs to calculate and send the M-dimensional vector $\boldsymbol{w}^{(i)}_{r,T}$ to the server for constructing the global gradient surrogate (line 9 of Algo. 2).

After receiving $\{\boldsymbol{w}^{(i)}_{r,T}\}^N_{i=1}$ from all clients, the server can construct the global gradient surrogate at the end of every round r by averaging these local gradient surrogates via

$$\nabla\widehat{\mu}_r(\boldsymbol{x}) \triangleq \frac{1}{N}\sum_{i\in[N]}\nabla\widehat{\mu}^{(i)}_{r,T}(\boldsymbol{x}) = \nabla\phi(\boldsymbol{x})^\top\Big(\frac{1}{N}\sum_{i\in[N]}\boldsymbol{w}^{(i)}_{r,T}\Big)\,. \quad (4)$$

To transfer this global gradient surrogate to all clients, we only need to send $\boldsymbol{w}_r \triangleq \frac{1}{N}\sum_{i=1}^N \boldsymbol{w}^{(i)}_{r,T}$ back (lines 10-11 of Algo. 2). Importantly, after receiving $\boldsymbol{w}_r$ from the server, each client can calculate the global gradient surrogate *at any input in the domain*. Although this global gradient surrogate incurs an additional transmission of M-dimensional vectors compared with existing federated ZOO algorithms (Algo. 1), it enjoys the advantage of achieving an improved gradient correction with theoretical guarantees (Sec. 4), which is essential for addressing federated ZOO with heterogeneous clients (Appx. B.2) and shall outweigh its drawback of increased transmission burden especially when query- and communication round efficiency are crucial. Besides, this communication burden also occurs in [8]. To further boost the quality of this surrogate, we can actively query in the neighborhood of the updated input $\boldsymbol{x}_r$ on every client (line 7 of Algo. 2) as supported in Sec. 4.

3.2.2. Adaptive Gradient Correction

By using our aforementioned high-quality local and global gradient surrogates, we then develop the technique of adaptive gradient correction to meet requirement **(B)** for communication round-efficient federated ZOO from Appx. B.2. Specifically, thanks to the ability of our gradient surrogates to *estimate the gradient at any input in the domain*, we can let $\boldsymbol{x}' = \boldsymbol{x}'' = \boldsymbol{x}^{(i)}_{r,t-1}$ in (6) to realize a more accurate gradient correction vector during optimization. Moreover, we propose to employ an adaptive gradient correction length $\gamma_{r,t-1}$ (shared across all clients) to better trade off the utilization of our gradient correction vector during optimization. That is, for every iteration t of round r, we propose to use the following $\widehat{\boldsymbol{g}}^{(i)}_{r,t-1}$ on each client for its local update:

$$\widehat{\boldsymbol{g}}^{(i)}_{r,t-1} = \nabla\mu^{(i)}_{r,t-1}(\boldsymbol{x}^{(i)}_{r,t-1}) + \gamma_{r,t-1}\left(\nabla\widehat{\mu}_{r-1}(\boldsymbol{x}^{(i)}_{r,t-1}) - \nabla\widehat{\mu}^{(i)}_{r-1,T}(\boldsymbol{x}^{(i)}_{r,t-1})\right), \quad (5)$$

(i.e., line 6 of Algo. 2) where $\nabla\widehat{\mu}^{(i)}_{r-1,T}$ is the local gradient surrogate of client i with RFF approximation at the end of round $r-1$ from (3), $\nabla\widehat{\mu}_{r-1}$ is our global gradient surrogate from (4), and $\gamma_{r,t-1}$ is a theoretically inspired adaptive gradient correction length which we will discuss in Sec. 4. Of note, the advantage of this adaptive gradient correction can be theoretically justified (Sec. 4).

4. Theoretical Analysis

In this section, we present our theoretical analysis on the gradient disparity (defined as $\Xi^{(i)}_{r,t} \triangleq \|\widehat{\boldsymbol{g}}^{(i)}_{r,t-1} - \nabla F(\boldsymbol{x}^{(i)}_{r,t-1})\|^2$) of our local gradient update (5). The convergence analysis of our FZooS (Algo. 2) is in Appx. C.2. We assume that $\frac{1}{N}\sum_{i=1}^N \|\nabla f_i(\boldsymbol{x}) - \nabla F(\boldsymbol{x})\|^2 \le G$ for any $\boldsymbol{x} \in \mathcal{X}$, which is a common assumption in the analysis of federated optimization [7]. Here a larger G indicates a larger degree of client heterogeneity. We derive an upper bound on the gradient disparity of our (5) in Thm. 1 below (proof in Appx. E.2).

Theorem 1. *Define* $\rho \triangleq \frac{1}{N}\sum_{i=1}^N \rho_i$ *in which* $\rho_i \triangleq \max_{\boldsymbol{x}\in\mathcal{X}, r\ge1, t\ge1} \big\|\partial(\sigma^{(i)}_{r,t})^2(\boldsymbol{x})\big\| / \big\|\partial\left(\sigma^{(i)}_{r,t-1}\right)^2(\boldsymbol{x})\big\|$, *then* $\rho, \rho_i \in [\frac{1}{1+1/\sigma^2}, 1]$. *With constant* $\omega>0$, $\epsilon = \mathcal{O}(\frac{1}{M})$, ① $\triangleq 4\omega\kappa\rho^{(r-1)T+t-1}$, ② $\triangleq 8\omega\kappa\rho^{(r-1)T} + 8N\epsilon$, *and* ③ $\triangleq 4G$, *the following holds with constant probability*

$$\frac{1}{N}\sum_{i\in[N]}\Xi^{(i)}_{r,t} \le ① + \gamma^2_{r,t-1}\times ② + (1-\gamma_{r,t-1})^2 \times ③\,.$$

Corollary 1. *Thm. 1 implies a better-performing choice of* $\gamma_{r,t-1}$, *i.e.,* $\gamma_{r,t-1} = \frac{G}{G+2\omega\kappa\rho^{(r-1)T}+2N\epsilon}$.

In the upper bound of Thm. 1, term ① represents the error of estimating $\{\nabla f_i(\cdot)\}^N_{i=1}$ using our local gradient surrogates in Sec. 3.1, and term ② characterizes the disparity between our gradient correction vector in (5) and its corresponding ground truth $\{\nabla F(\cdot) - \nabla f_i(\cdot)\}^N_{i=1}$. The ϵ within term ② denotes the RFF approximation error for our global gradient surrogate in Sec. 3.2.1 and ϵ decreases with a larger number M of random features. Term ③ results from the client heterogeneity in federated ZOO. Compared with the gradient disparity of existing algorithms (provided in Appx. F), Thm. 1 shows that our (5) enjoys a number of major advantages: ***(a)*** Our (5) is more query-efficient since it does not require any additional function query for gradient estimation, in contrast to existing algorithms which incur $\mathcal{O}(NQ)$ additional function queries in every iteration. ***(b)*** The esti-

mation error in our (5) (i.e., terms ① and ②) can be exponentially decreasing when $\rho < 1$ and ϵ is small, whereas other existing algorithms only achieve a reduction rate of $\mathcal{O}(1/Q)$, which implies that our gradient estimation is significantly more accurate. Of note, $\rho_i < 1$ is likely to be satisfied as justified in [3] and more importantly, $\rho < 1$ is even easier to be realized as it only needs one of the clients to satisfy $\rho_i < 1$. ***(c)*** Our (5) mitigates the disparity caused by the fixed gradient correction vector adopted by existing works, i.e., in contrast to FedProx and SCAFFOLD, our Thm. 1 does not contain an additional disparity term of $\sum_{i=1}^{N} \|\boldsymbol{x}_{r,t-1}^{(i)} - \boldsymbol{x}_{r-1}\|^2$. ***(d)*** Our (5) can trade off between the impacts of our gradient correction vector and client heterogeneity, and can consequently further improve the gradient estimation when $\gamma_{r,t-1}$ is chosen intelligently while accounting for this trade-off. Specifically, the upper bound in Thm. 1 has characterized such a trade-off: When the estimation error of our gradient correction vector (i.e., term ②) is relatively small compared with the client heterogeneity (i.e., term ③), a large γ_{t-1} is preferred to reduce the impact of client heterogeneity and hence to achieve a small gradient disparity. Furthermore, this also implies a theoretically better choice of $\gamma_{r,t-1}$ in our Cor. 1 (refer to Appx. E.3 for a more practical choice of $\gamma_{r,t-1}$).

5. Experiments

In this section, we demonstrate that our FZooS outperforms existing federated ZOO algorithms using synthetic experiments (Sec. 5.1), as well as real-world experiments on federated black-box adversarial attack (Sec. 5.2). More results can be found in Appx. H.

5.1. Synthetic Experiments

We firstly employ federated synthetic functions to illustrate the superiority of our proposed FZooS over a number of existing federated ZOO baselines such as FedZO, FedProx, and SCAFFOLD in the federated ZOO setting (see Appx. F for their specific forms) in Fig. 1. We refer to Appx. G.1 for the details of these synthetic functions and the experimental setting applied here. It shows that our FZooS considerably outperforms the other baselines in terms of both communication round and query efficiency, which can be attributed to the superiority of our (5). When C is increased, a larger number of communication rounds and total queries are required to achieve the same convergence error, which empirically verifies our Thm. C.1.

5.2. Federated Black-Box Adversarial Attack

Following the practice of [2], we then examine the advantages of our FZooS in the task of federated black-box adversarial attack. Here we aim to find a small perturbation $\boldsymbol{x}$ to be added to an input image $\boldsymbol{z}$ such that the perturbed image $\boldsymbol{z} + \boldsymbol{x}$ will be wrongly classified by the *majority* of

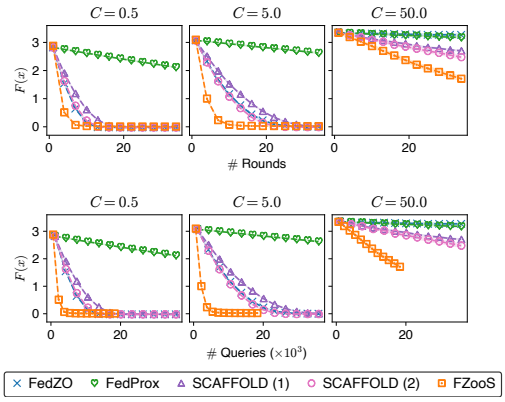

Figure 1. Comparison of the communication round and query efficiency on synthetic function with varying heterogeneity (controlled by $C \geq 0$), where a larger C implies larger heterogeneity.

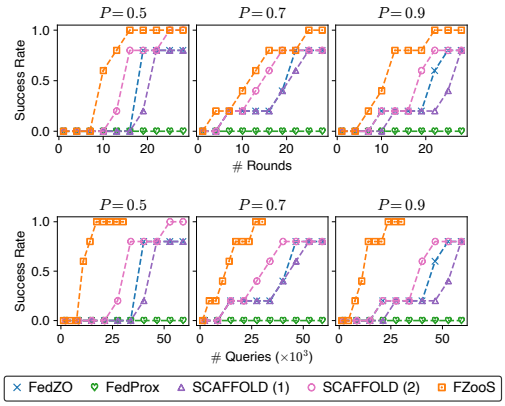

Figure 2. Comparison of the success rate in federated black-box adversarial attack on CIFAR-10 under varying heterogeneity (controlled by $P \in [0, 1]$, a larger P implies smaller heterogeneity).

the private ML models on various clients through only the function queries of these models (refer to Appx. G.2 for more details). Remarkably, Fig. 2 shows that our FZooS again achieves consistently improved communication round efficiency over the other baselines under varying client heterogeneity. Thanks to this improved communication round efficiency and the ability of (5) to avoid a large number of additional function queries in every communication round, FZooS also achieves a substantial improvement in query efficiency. Overall, these results support the superiority of FZooS over the other existing approaches in real-world federated ZOO problems in terms of both communication round and query efficiency.

6. Conclusion

We introduce FZooS to address the challenges of query and communication round inefficiency faced by existing federated ZOO algorithms in the presence of client heterogeneity. We use both theoretical justifications and empirical demonstrations to show that FZooS is indeed able to address these challenges and achieve considerably improved query and communication round efficiency over the existing baselines.

References

[1] B. McMahan, E. Moore, D. Ramage, S. Hampson, and B. A. y Arcas, "Communication-efficient learning of deep networks from decentralized data," in *Proc. AISTATS*, 2017.

[2] W. Fang, Z. Yu, Y. Jiang, Y. Shi, C. N. Jones, and Y. Zhou, "Communication-efficient stochastic zeroth-order optimization for federated learning," *IEEE Trans. Signal Process.*, vol. 70, pp. 5058–5073, 2022.

[3] Y. Shu, Z. Dai, W. Sng, A. Verma, P. Jaillet, and B. K. H. Low, "Zeroth-order optimization with trajectory-informed derivative estimation," in *Proc. ICLR*, 2023.

[4] A. Rahimi and B. Recht, "Random features for large-scale kernel machines," in *Proc. NeurIPS*, 2007.

[5] J. Konečnỳ, B. McMahan, and D. Ramage, "Federated optimization: Distributed optimization beyond the datacenter," arXiv:1511.03575, 2015.

[6] J. Wang, Z. Charles, Z. Xu, *et al.*, "A field guide to federated optimization," arXiv:2107.06917, 2021.

[7] S. J. Reddi, Z. Charles, M. Zaheer, *et al.*, "Adaptive federated optimization," in *Proc. ICLR*, 2021.

[8] S. P. Karimireddy, S. Kale, M. Mohri, S. J. Reddi, S. U. Stich, and A. T. Suresh, "SCAFFOLD: Stochastic controlled averaging for federated learning," in *Proc. ICML*, 2020.

[9] T. Li, A. K. Sahu, A. Talwalkar, and V. Smith, "Federated learning: Challenges, methods, and future directions," *IEEE Signal Process. Mag.*, vol. 37, no. 3, pp. 50–60, 2020.

[10] P. Kairouz, H. B. McMahan, B. Avent, *et al.*, "Advances and open problems in federated learning," *Found. Trends Mach. Learn.*, vol. 14, no. 1-2, pp. 1–210, 2021.

[11] B. McMahan, E. Moore, D. Ramage, S. Hampson, and B. A. y Arcas, "Communication-efficient learning of deep networks from decentralized data," in *Proc. AISTATS*, 2017.

[12] J. Wang, V. Tantia, N. Ballas, and M. G. Rabbat, "SlowMo: Improving communication-efficient distributed SGD with slow momentum," in *Proc. ICLR*, 2020.

[13] H. Yuan and T. Ma, "Federated accelerated stochastic gradient descent," in *Proc. NeurIPS*, 2020.

[14] J. Jin, J. Ren, Y. Zhou, L. Lyu, J. Liu, and D. Dou, "Accelerated federated learning with decoupled adaptive optimization," in *Proc. ICML*, 2022.

[15] M. Al-Shedivat, J. Gillenwater, E. P. Xing, and A. Rostamizadeh, "Federated learning via posterior averaging: A new perspective and practical algorithms," in *Proc. ICLR*, 2021.

[16] T. Li, A. K. Sahu, M. Zaheer, M. Sanjabi, A. Talwalkar, and V. Smith, "Federated optimization in heterogeneous networks," in *Proc. ICML*, 2020.

[17] T. Li, A. K. Sahu, M. Zaheer, M. Sanjabi, A. Talwalkar, and V. Smith, "Feddane: A federated newton-type method," in *ACSSC*, IEEE, 2019, pp. 1227–1231.

[18] S. P. Karimireddy, M. Jaggi, S. Kale, *et al.*, "Mime: Mimicking centralized stochastic algorithms in federated learning," arXiv:2008.03606, 2020.

[19] R. Johnson and T. Zhang, "Accelerating stochastic gradient descent using predictive variance reduction," in *Proc. NeurIPS*, 2013.

[20] Y. E. Nesterov and V. G. Spokoiny, "Random gradient-free minimization of convex functions," *Found. Comput. Math.*, vol. 17, no. 2, pp. 527–566, 2017.

[21] S. Cheng, G. Wu, and J. Zhu, "On the convergence of prior-guided zeroth-order optimization algorithms," in *Proc. NeurIPS*, 2021.

[22] A. S. Berahas, L. Cao, K. Choromanski, and K. Scheinberg, "A theoretical and empirical comparison of gradient approximations in derivative-free optimization," *Found. Comput. Math.*, vol. 22, no. 2, pp. 507–560, 2022.

[23] N. J. Harvey, C. Liaw, Y. Plan, and S. Randhawa, "Tight analyses for non-smooth stochastic gradient descent," in *Proc. COLT*, 2019.

[24] Z. Liu, T. D. Nguyen, T. H. Nguyen, A. Ene, and H. L. Nguyen, "High probability convergence of stochastic gradient methods," arXiv:2302.14843, 2023.

[25] B. Laurent and P. Massart, "Adaptive estimation of a quadratic functional by model selection," *Annals of Statistics*, pp. 1302–1338, 2000.

[26] D. Dua and C. Graff, *UCI machine learning repository*, 2017. [Online]. Available: `http://archive.ics.uci.edu/ml`.

A. Related Work

Federated Learning and Federated First-Order Optimization. Federated learning (FL) has become a paradigm of applying multiple edge devices (i.e., clients) to collaboratively train a global model without sharing the private data on these edge devices [1]. We refer to the surveys [9], [10] for more comprehensive reviews of FL. Such a paradigm then gives rise to recent interest in federated optimization or more precisely federated first-order optimization (FOO) [6] to broaden its real-world application. Since the first federated FOO algorithm FedAvg proposed in [11], a number of techniques have been developed to further improve its performance in different aspects, e.g., federated FOO with momentum [12] and adaptive learning rates [7], [13], [14] for convergence speedup, federated FOO with local posterior sampling for de-biased client updates [15], and federated FOO with regularized functions [16], [17] and control variates [8], [18] for the challenge of heterogeneous clients, in which the global function to be optimized differs from the local functions on clients.

Federated Zeroth-Order Optimization. Despite the success of federated FOO algorithms, some important applications, e.g., federated black-box adversarial attack in [2], suggests the development of federated zeroth-order (ZOO) algorithms for the federated optimization where gradient information is not available. Nevertheless, very limited efforts have been devoted to the development of federated zeroth-order (ZOO) algorithms especially when the clients are heterogeneous. To the best of our knowledge, [2] is the first to consider federated ZOO, in which they simply combine FedAvg with existing FD methods as their FedZO algorithm. Similar to the FedAvg algorithm in federated FOO, the FedZO algorithm also likely performs poorly in the heterogeneous setting. This thus encourages the design of federated ZOO algorithms for heterogeneous federated ZOO problems. Following the practice of FedZO, existing federated FOO algorithms for heterogeneous clients, e.g., [8], [16], can be simply adapted to the corresponding federated ZOO algorithms for this kind of problem. However, these algorithms shall be query- and communication round-inefficient in practice, which therefore raises the question of how to improve query efficiency and the communication round efficiency of these algorithms. To answer this question, we first identify the challenges of such an improvement and then develop a federated ZOO algorithm to overcome these challenges in this paper.

B. Framework and Challenges for Heterogeneous Federated ZOO

Here we firstly summarize the framework to solve the federated ZOO problem (Appx. B.1), and then identify the challenges which existing algorithms following this framework fail to address (Appx. B.2).

B.1. Optimization Framework

To solve (1), a general optimization framework is to estimate the gradients of $\{f_i\}_{i=1}^N$ using only function queries and then employ the standard federated FOO algorithms for the optimization, as in Algo. 1. Specifically, in round r, every client performs T iterations of local gradient decent updates in parallel (line 2-5 of Algo. 1), in which $\widehat{\boldsymbol{g}}_{r,t-1}^{(i)} \in \mathbb{R}^d$ denotes the estimated gradient by client i for the local update in iteration t of round r. After that, each client sends its locally updated input $\boldsymbol{x}_{r,T}^{(i)}$ to server (line 6 of Algo. 1). After receiving the updated inputs from all clients (i.e., $\{\boldsymbol{x}_{r,T}^{(i)}\}_{i=1}^N$), the server aggregates them (e.g., via arithmetic average) to produce a globally updated input $\boldsymbol{x}_r$, and then sends it back to the clients for the optimization in the next round (line 7-8 of Algo. 1).

The aforementioned $\widehat{\boldsymbol{g}}_{r,t-1}^{(i)}$ used in the literature can be summarized into the following general form:

$$\widehat{\boldsymbol{g}}_{r,t-1}^{(i)} \triangleq \boldsymbol{g}_{r,t-1}^{(i)} + \gamma_{r,t-1}^{(i)} \Big(\boldsymbol{g}_{r-1}(\boldsymbol{x}') - \boldsymbol{g}_{r-1}^{(i)}(\boldsymbol{x}'') \Big) \tag{6}$$

where $\boldsymbol{g}_{r,t-1}^{(i)} \in \mathbb{R}^d$ is an estimate of $\nabla f_i(\boldsymbol{x}_{r,t-1}^{(i)})$ and is usually obtained using the *finite difference* (FD) methods (refer to Appx. B.2). In addition, the *gradient correction vector* $\boldsymbol{g}_{r-1}(\boldsymbol{x}') - \boldsymbol{g}_{r-1}^{(i)}(\boldsymbol{x}'') \in \mathbb{R}^d$ is usually obtained from the previous round $r-1$. This aims to make the resulting $\widehat{\boldsymbol{g}}_{r,t-1}^{(i)}$ better aligned with $\nabla F(\boldsymbol{x}_{r,t-1}^{(i)})$, such that the local update on each client (i.e., line 5 of Algo. 1) can better approximate the intended global update along the direction of $\nabla F(\boldsymbol{x}_{r,t-1}^{(i)})$. It is especially important in the presence of client heterogeneity, i.e., $\{\nabla f_i\}_{i=1}^N$ differ from ∇F. Intuitively, to accomplish this alignment, $\boldsymbol{g}_{r-1}(\boldsymbol{x}')$ and $\boldsymbol{g}_{r-1}^{(i)}(\boldsymbol{x}'')$ should be good estimates of $\nabla F(\boldsymbol{x}_{r,t-1}^{(i)})$ and $\nabla f_i(\boldsymbol{x}_{r,t-1}^{(i)})$, respectively, which we theoretically justify in Appx. B.2. Of note, the form of $\boldsymbol{g}_{r-1}(\boldsymbol{x}') - \boldsymbol{g}_{r-1}^{(i)}(\boldsymbol{x}'')$ for gradient correction usually aims to ensure that the estimation biases from $\boldsymbol{g}_{r-1}(\boldsymbol{x}')$ and $\boldsymbol{g}_{r-1}^{(i)}(\boldsymbol{x}'')$ could cancel out [19]. Finally, $\gamma_{r,t-1}^{(i)} \in [0,1]$ denotes the *gradient correction length*, which can be adjusted to trade off the utilization of the gradient correction vector (Appx. B.2).

Remarkably, (6) subsumes the forms of gradient updates employed in many existing federated ZOO algorithms, and hence

Algorithm 1: General Framework for Federated ZOO

Input: Initial $\boldsymbol{x}_0$, rounds R, learning rate η, iterations T for each round, number of clients N

for *each round* $r \in [R]$ **do**
  // Client-Side Update
  for *each client* $i \in [N]$ ***in parallel*** **do**
    $\boldsymbol{x}_{r,0}^{(i)} \leftarrow \boldsymbol{x}_{r-1}$
    for *each iteration* $t \in [T]$ **do**
      $\boldsymbol{x}_{r,t}^{(i)} \leftarrow \boldsymbol{x}_{r,t-1}^{(i)} - \eta\, \widehat{\boldsymbol{g}}_{r,t-1}^{(i)}$
    Send $\boldsymbol{x}_{r,T}^{(i)}$ to receive $\boldsymbol{x}_r$ back
  // Server-Side Update
  $\boldsymbol{x}_r \leftarrow \frac{1}{N}\sum_{i\in[N]} \boldsymbol{x}_{r,T}^{(i)}$
  Send $\boldsymbol{x}_r$ back to each client

Algorithm 2: FZooS

Input: Input of Algo. 1, length γ, M features

for *each round* $r \in [R]$ **do**
  // Client-Side Update
  for *each client* $i \in [N]$ ***in parallel*** **do**
    $\boldsymbol{x}_{r,0}^{(i)} \leftarrow \boldsymbol{x}_{r-1}$, $\nabla\widehat{\mu}_{r-1}$ based on $\boldsymbol{w}_{r-1}$
    for *each iteration* $t \in [T]$ **do**
      $\nabla\mu_{r,t-1}^{(i)}$ conditioned on $\mathcal{D}_{r,t-1}^{(i)}$
      $\boldsymbol{x}_{r,t}^{(i)} \leftarrow \boldsymbol{x}_{r,t-1}^{(i)} - \eta\, \widehat{\boldsymbol{g}}_{r,t-1}^{(i)}$ with (5)
    Send $\boldsymbol{x}_{r,T}^{(i)}$ to receive $\boldsymbol{x}_r$, query around $\boldsymbol{x}_r$
    Approx. $\nabla\mu_{r,T}^{(i)}$ via RFF to get $\boldsymbol{w}_{r,T}^{(i)}$
    Send $\boldsymbol{w}_{r,T}^{(i)}$ to receive $\boldsymbol{w}_r$ back
  // Server-Side Update
  $\boldsymbol{x}_r \leftarrow \frac{1}{N}\sum_{i\in[N]} \boldsymbol{x}_{r,T}^{(i)}$, $\boldsymbol{w}_r \leftarrow \frac{1}{N}\sum_{i\in[N]} \boldsymbol{w}_{r,T}^{(i)}$
  Send $\boldsymbol{x}_r$ back first and then $\boldsymbol{w}_r$ to each client

Algo. 1 can reduce to the corresponding optimization algorithms (more details in Appx. F). E.g., when $\gamma_{r,t-1}^{(i)} = 0$ and $\boldsymbol{g}_{r,t-1}^{(i)}$ is obtained using FD, Algo. 1 becomes the FedZO algorithm [2]; when $\gamma_{r,t-1}^{(i)}=1$, $\boldsymbol{g}_{r-1}(\boldsymbol{x}')=\frac{1}{NT}\sum_{i,t=1}^{N,T} \boldsymbol{g}_{r-1,t-1}^{(i)}$, and $\boldsymbol{g}_{r-1}^{(i)}(\boldsymbol{x}'') = \frac{1}{T}\sum_{t=1}^{T} \boldsymbol{g}_{r-1,t-1}^{(i)}$, (6) reduces to the gradient update in [8] and hence Algo. 1 becomes the SCAFFOLD (Type II) algorithm in the federated ZOO setting; let the gradient correction vector $\boldsymbol{g}_{r-1}(\boldsymbol{x}') - \boldsymbol{g}_{r-1}^{(i)}(\boldsymbol{x}'')$ in (6) be $\boldsymbol{x}_{r,t-1}^{(i)} - \boldsymbol{x}_r$, Algo. 1 is then equivalent to FedProx [16] in the federated ZOO setting.

B.2. Existing Challenges

Existing federated ZOO algorithms aiming to solve the problem in Sec. 2 typically fail to address the challenges of query efficiency and communication round efficiency, which we discuss in detail below.

Challenge of Query Efficiency. Similar to standard ZOO algorithms [20], [21], existing federated ZOO algorithms (e.g., [2]) also commonly apply the FD methods [22] for gradient estimation. Specifically, given a parameter $\lambda > 0$ and directions $\{\boldsymbol{u}_q\}_{q=1}^{Q}$, the gradient of the function f_i on client i at $\boldsymbol{x}$ can be estimated as

$$\nabla f_i(\boldsymbol{x}) \approx \boldsymbol{\Delta}^{(i)}(\boldsymbol{x}) \triangleq \frac{1}{Q}\sum_{q\in[Q]} \frac{y_i(\boldsymbol{x}+\lambda\boldsymbol{u}_q) - y_i(\boldsymbol{x})}{\lambda}\boldsymbol{u}_q\,. \tag{7}$$

That is, for existing federated ZOO algorithms, $\boldsymbol{g}_{r,t-1}^{(i)} = \boldsymbol{\Delta}^{(i)}(\boldsymbol{x}_{r,t-1}^{(i)})$ in (6). As implied in (7), Q additional function queries are required for the gradient estimation at every local updated input $\boldsymbol{x}_{r,t-1}^{(i)}$. This therefore results in $NTQ\times$ more function queries than the standard federated FOO algorithms [8], [16] in every communication round, which is unsatisfying

in practice especially when $\{f_i\}_{i=1}^N$ are prohibitively costly to evaluate. So, tackling the challenge of query efficiency in federated ZOO requires designing query-efficient gradient estimators.

Challenge of Communication Round Efficiency. When $\widehat{\boldsymbol{g}}_{r,t-1}^{(i)} = \nabla F(\boldsymbol{x}_{r,t-1}^{(i)})$ in (6), Algo. 1 is then able to attain the convergence of centralized FOO algorithms, which is known to be better than the one in the federated setting [8]. Therefore, intuitively, the convergence or the communication round efficiency (i.e., the number of communication rounds R required to achieve an ϵ convergence error) of Algo. 1 depends on the disparity between (6) and $\nabla F(\boldsymbol{x}_{r,t-1}^{(i)})$. Define the gradient disparity $\Xi_{r,t}^{(i)} \triangleq \|\widehat{\boldsymbol{g}}_{r,t-1}^{(i)} - \nabla F(\boldsymbol{x}_{r,t-1}^{(i)})\|^2$, we propose the following Prop. B.1 (proof in Appx. E.1) to show the condition for the best-performing (6) and thus to justify the challenge in communication round efficiency that existing federated ZOO algorithms typically fail to address well.

Proposition B.1. *Let $\boldsymbol{g}_{r-1}^{(i)}(\boldsymbol{x}'') \neq \boldsymbol{g}_{r-1}(\boldsymbol{x}')$, the minimum of $\Xi_{r,t}^{(i)}$ w.r.t $\gamma_{r,t-1}^{(i)}$ is achieved when*

$$\gamma_{r,t-1}^{(i)} = \gamma_{r,t-1}^{(i)*} \triangleq \left(\nabla F(\boldsymbol{x}_{r,t-1}^{(i)}) - \boldsymbol{g}_{r,t-1}^{(i)}\right)^\top \left(\boldsymbol{g}_{r-1}(\boldsymbol{x}') - \boldsymbol{g}_{r-1}^{(i)}(\boldsymbol{x}'')\right) \left\|\boldsymbol{g}_{r-1}(\boldsymbol{x}') - \boldsymbol{g}_{r-1}^{(i)}(\boldsymbol{x}'')\right\|^{-2}.$$

When $\gamma_{r,t-1}^{(i)*} = 1$, $\Xi_{r,t}^{(i)} = 0$ iff we have $\boldsymbol{g}_{r-1}(\boldsymbol{x}') - \boldsymbol{g}_{r-1}^{(i)}(\boldsymbol{x}'') = \nabla F(\boldsymbol{x}_{r,t-1}^{(i)}) - \boldsymbol{g}_{r,t-1}^{(i)}$.

Prop. B.1 shows that to achieve a small gradient disparity, $\gamma_{r,t-1}^{(i)}$ should be adaptive w.r.t. the alignment between the *gradient correction vector* $\boldsymbol{g}_{r-1}(\boldsymbol{x}') - \boldsymbol{g}_{r-1}^{(i)}(\boldsymbol{x}'')$ and the *drift* $\nabla F(\boldsymbol{x}_{r,t-1}^{(i)}) - \boldsymbol{g}_{r,t-1}^{(i)}$. We have shown (Appx. E.1) that a better alignment between the gradient correction vector and the drift leads to a smaller gradient disparity, Prop. B.1 further shows that a zero gradient disparity (i.e., $\Xi_{r,t}^{(i)} = 0$ for any $r \in [R], t \in [T]$) can be reached when these two are perfectly aligned. To achieve such an alignment, i.e., to make $\boldsymbol{g}_{r-1}(\boldsymbol{x}') = \nabla F(\boldsymbol{x}_{r,t-1}^{(i)})$ and $\boldsymbol{g}_{r-1}^{(i)}(\boldsymbol{x}'') = \boldsymbol{g}_{r,t-1}^{(i)}$ hold more likely, it requires not only *(a)* accurate gradient surrogates $\boldsymbol{g}_{r-1}$ and $\boldsymbol{g}_{r-1}^{(i)}$ to accurately represent ∇F and ∇f_i, respectively, but also *(b)* adaptive $\boldsymbol{x}', \boldsymbol{x}''$ to avoid the discrepancy between $\boldsymbol{x}_{r,t-1}^{(i)}$ and $\boldsymbol{x}', \boldsymbol{x}''$.

Consequently, resolving the challenge of communication round efficiency in federated ZOO mainly requires **(A)** *accurate* local and global surrogates (i.e., $\boldsymbol{g}_{r-1}^{(i)}$ and $\boldsymbol{g}_{r-1}$) for the gradient correction in (6), and **(B)** *adaptive* gradient correction in (6) with both adaptive $\boldsymbol{x}', \boldsymbol{x}''$ and adaptive $\gamma_{r,t-1}^{(i)}$. However, existing federated ZOO algorithms usually fail to address them well: Firstly, these algorithms rely on the FD methods for gradient estimation, which usually lead to poor estimation quality and consequently inaccurate gradient correction vectors in (6) when the query budget is very limited. Secondly, although $\boldsymbol{x}_{r,t-1}^{(i)}$ changes during local updates, existing algorithms typically rely on $\boldsymbol{g}_{r-1}, \boldsymbol{g}_{r-1}^{(i)}$ evaluated at a fixed input $\boldsymbol{x}_{r-1} = \boldsymbol{x}' = \boldsymbol{x}''$ to estimate ∇F or ∇f_i (e.g., [8], [16]), leading to large discrepancies between $\boldsymbol{x}_{r,t-1}^{(i)}$ and $\boldsymbol{x}', \boldsymbol{x}''$. Thirdly, existing algorithms use a fixed gradient correction length (e.g., $\gamma_{r,t-1}^{(i)} = 0$ in [2] and $\gamma_{r,t-1}^{(i)} = 1$ in [8]), which is likely to result in misspecified gradient correction length.

C. More Details of FZooS

C.1. Exact Form of Derived Gaussian Process

$$\begin{aligned}
\nabla \mu_{r,t-1}^{(i)}(\boldsymbol{x}) &\triangleq \partial_{\boldsymbol{x}} \boldsymbol{k}_{r,t-1}^{(i)}(\boldsymbol{x})^\top \left(\mathbf{K}_{r,t-1}^{(i)} + \sigma^2 \mathbf{I}\right)^{-1} \boldsymbol{y}_{r,t-1}^{(i)}, \\
\partial \left(\sigma_{r,t-1}^{(i)}\right)^2 (\boldsymbol{x}, \boldsymbol{x}') &\triangleq \partial_{\boldsymbol{x}} \partial_{\boldsymbol{x}'} k(\boldsymbol{x}, \boldsymbol{x}') - \partial_{\boldsymbol{x}} \boldsymbol{k}_{r,t-1}^{(i)}(\boldsymbol{x})^\top \left(\mathbf{K}_{r,t-1}^{(i)} + \sigma^2 \mathbf{I}\right)^{-1} \partial_{\boldsymbol{x}'} \boldsymbol{k}_{r,t-1}^{(i)}(\boldsymbol{x}').
\end{aligned} \tag{8}$$

Both $\boldsymbol{k}_{r,t-1}^{(i)}(\boldsymbol{x})^\top \triangleq [k(\boldsymbol{x}, \boldsymbol{x}_\tau^{(i)})]_{\tau=1}^{T(r-1)+t-1}$ and $(\boldsymbol{y}_{r,t-1}^{(i)})^\top \triangleq [y_\tau^{(i)}]_{\tau=1}^{T(r-1)+t-1}$ are $[T(r-1)+t-1]$-dimensional row vectors, and $\mathbf{K}_{r,t-1}^{(i)} \triangleq [k(\boldsymbol{x}_\tau^{(i)}, \boldsymbol{x}_{\tau'}^{(i)})]_{\tau,\tau'=1}^{T(r-1)+t-1}$ is a $[T(r-1)+t-1] \times [T(r-1)+t-1]$-dimensional matrix.

C.2. Convergence Analysis

We prove the convergence of our FZooS (measured by the number of communication rounds to achieve ϵ convergence error) under different assumptions, in addition to assuming that F is β-smooth, $\mathcal{X} \triangleq [0,1]^d$, and $|f_i(\boldsymbol{x})| \leq 1$ for any $\boldsymbol{x} \in \mathcal{X}$ and $i \in [N]$.

Theorem C.1. *Define $D_0 \triangleq \|\boldsymbol{x}_0 - \boldsymbol{x}^*\|^2$ and $D_1 \triangleq F(\boldsymbol{x}_0) - F(\boldsymbol{x}^*)$, to achieve an ϵ convergence error for our FZooS (Algo. 2) with a constant probability when $\rho < 1$, the number M of random features and the number R of communication rounds need to satisfy the following,*

(i) *If F is strongly convex and $\eta \leq \frac{1}{10\beta T}$, $M = \mathcal{O}\left(\frac{NG}{\epsilon^2}\right)$ and $R = \mathcal{O}\left(\frac{1}{\eta T} \ln \frac{D_0}{\epsilon} + \ln \frac{\sqrt{G}}{\epsilon}\right)$.*

(ii) *If F is convex and $\eta \leq \frac{1}{10\beta T}$, $M = \mathcal{O}\left(\frac{NG}{\epsilon^2} + \frac{d^2 NG}{\epsilon^4}\right)$ and $R = \mathcal{O}\left(\frac{D_0}{\eta T \epsilon} + \frac{\sqrt{G} + \sqrt[4]{d^2 G}}{\epsilon}\right)$.*

(iii) *If F is non-convex and $\eta \leq \frac{7}{100\beta T}$, $M = \mathcal{O}\left(\frac{NG}{\epsilon^2}\right)$ and $R = \mathcal{O}\left(\frac{D_1}{\eta T \epsilon} + \frac{\sqrt{G}}{\epsilon}\right)$.*

The proof is in Appx. E.5.[2] Thm. C.1 suggests that the learning rate η in FZooS should be proportionally reduced w.r.t. the number T of local updates, which is in fact consistent with the results in federated FOO [8]. Thm. C.1 also shows that when client heterogeneity (i.e., measured by G) increases, both the number M of random features and the number R of communication rounds in our FZooS should be increased in order to achieve the same convergence error, which is also empirically verified in our Sec. 5 and Appx. H. Moreover, Thm. C.1 has revealed that given a constant learning rate η that satisfies the conditions in Thm. C.1 under various T, a larger T usually improves the communication round efficiency (i.e., R) of our FZooS (see Appx. H). More importantly, compared with the convergence of other existing algorithms (provided in Appx. F), FZooS enjoys an improved communication round efficiency, which can be attributed to the advantages of our (5) as discussed in Sec. 4 (see Appx. F for a detailed comparison).

D. Random Fourier Features

According to [4], the random Fourier features can usually be represented as a M-dimensional row vector $\phi(\boldsymbol{x})^\top = \left[\frac{2}{\sqrt{M}}\cos(\boldsymbol{v}_j \boldsymbol{x} + b_j)\right]_{j=1}^{M}$ where every $\boldsymbol{v}_j$ is independently randomly sampled from a distribution $p(\boldsymbol{v})$ and every b_j is independently randomly sampled from the uniform distribution over $[0, 2\pi]$. Particularly, for the squared exponential kernel $k(\boldsymbol{x}, \boldsymbol{x}') = \exp\left(-\|\boldsymbol{x} - \boldsymbol{x}'\|^2 / (2l^2)\right)$ in which l is the length scale, $p(\boldsymbol{v}) = \mathcal{N}(0, \frac{1}{l^2}\mathbf{I})$. In FZooS, we typically adopt the squared exponential kernel for the optimization. Importantly, before the start of our FZooS, $\{\boldsymbol{v}_j\}_{j=1}^M$ and $\{b_j\}_{j=1}^M$ need to be sampled and shared across all clients as well as server (as mentioned in Sec. 3.2.1), which however will only happen once for whole optimization process.

[2] The poor convergence of our FZooS under convex F (vs. the one under non-convex F) results from the drawback of the commonly applied proof technique for convex F rather than the algorithm itself. This has been widely recognized in the literature [23], [24].

E. Theoretical Analyses

E.1. Proof of Proposition B.1

Based on the definition of $\Xi_{r,t}^{(i)}$ in Appx. B.2, we have that

$$\begin{aligned}\Xi_{r,t}^{(i)} &= \left\|\widehat{\boldsymbol{g}}_{r,t-1}^{(i)} - \nabla F(\boldsymbol{x}_{r,t-1}^{(i)})\right\|^2 \\ &= \left\|\boldsymbol{g}_{r,t-1}^{(i)} + \gamma_{r,t-1}^{(i)}\left(\boldsymbol{g}_{r-1}(\boldsymbol{x}') - \boldsymbol{g}_{r-1}^{(i)}(\boldsymbol{x}'')\right) - \nabla F(\boldsymbol{x}_{r,t-1}^{(i)})\right\|^2 \\ &= \left\|\boldsymbol{g}_{r,t-1}^{(i)} - \nabla F(\boldsymbol{x}_{r,t-1}^{(i)})\right\|^2 - 2\gamma_{r,t-1}^{(i)}\left(\nabla F(\boldsymbol{x}_{r,t-1}^{(i)}) - \boldsymbol{g}_{r,t-1}^{(i)}\right)^\top\left(\boldsymbol{g}_{r-1}(\boldsymbol{x}') - \boldsymbol{g}_{r-1}^{(i)}(\boldsymbol{x}'')\right) + \\ &\qquad \left(\gamma_{r,t-1}^{(i)}\right)^2\left\|\boldsymbol{g}_{r-1}(\boldsymbol{x}') - \boldsymbol{g}_{r-1}^{(i)}(\boldsymbol{x}'')\right\|^2,\end{aligned} \tag{9}$$

which is a quadratic function w.r.t. $\gamma_{r,t-1}^{(i)}$. It is easy to show that when

$$\gamma_{r,t-1}^{(i)} = \gamma_{r,t-1}^{(i)*} \triangleq \frac{\left(\nabla F(\boldsymbol{x}_{r,t-1}^{(i)}) - \boldsymbol{g}_{r,t-1}^{(i)}\right)^\top\left(\boldsymbol{g}_{r-1}(\boldsymbol{x}') - \boldsymbol{g}_{r-1}^{(i)}(\boldsymbol{x}'')\right)}{\left\|\boldsymbol{g}_{r-1}(\boldsymbol{x}') - \boldsymbol{g}_{r-1}^{(i)}(\boldsymbol{x}'')\right\|}, \tag{10}$$

$\Xi_{r,t}^{(i)}$ can achieve its global minimum w.r.t. $\gamma_{r,t-1}^{(i)}$ as

$$\Xi_{r,t}^{(i)} = \left\|\boldsymbol{g}_{r,t-1}^{(i)} - \nabla F(\boldsymbol{x}_{r,t-1}^{(i)})\right\|^2 - \frac{\left\|\left(\nabla F(\boldsymbol{x}_{r,t-1}^{(i)}) - \boldsymbol{g}_{r,t-1}^{(i)}\right)^\top\left(\boldsymbol{g}_{r-1}(\boldsymbol{x}') - \boldsymbol{g}_{r-1}^{(i)}(\boldsymbol{x}'')\right)\right\|^2}{\left\|\boldsymbol{g}_{r-1}(\boldsymbol{x}') - \boldsymbol{g}_{r-1}^{(i)}(\boldsymbol{x}'')\right\|^2}. \tag{11}$$

This therefore finishes the proof of the fist-part result in Prop. B.1. Interestingly, (11) implies that given the $\gamma_{r,t-1}^{(i)}$ in (10), a better alignment between the gradient correction vector $\boldsymbol{g}_{r-1}(\boldsymbol{x}') - \boldsymbol{g}_{r-1}^{(i)}(\boldsymbol{x}'')$ and the shift $\nabla F(\boldsymbol{x}_{r,t-1}^{(i)}) - \boldsymbol{g}_{r,t-1}^{(i)}$ leads to a smaller gradient disparity $\Xi_{r,t}^{(i)}$.

Given the $\gamma_{r,t-1}^{(i)*} = 1$ in (10), when $\boldsymbol{g}_{r-1}(\boldsymbol{x}') - \boldsymbol{g}_{r-1}^{(i)}(\boldsymbol{x}'') = \nabla F(\boldsymbol{x}_{r,t-1}^{(i)}) - \boldsymbol{g}_{r,t-1}^{(i)}$, we can easily verify that $\Xi_{r,t}^{(i)}$ in (10) has $\Xi_{r,t}^{(i)} = 0$. On the contrary, when $\Xi_{r,t}^{(i)} = 0$, we have that

$$\left\|\boldsymbol{g}_{r,t-1}^{(i)} - \nabla F(\boldsymbol{x}_{r,t-1}^{(i)})\right\| = \frac{\left\|\left(\nabla F(\boldsymbol{x}_{r,t-1}^{(i)}) - \boldsymbol{g}_{r,t-1}^{(i)}\right)^\top\left(\boldsymbol{g}_{r-1}(\boldsymbol{x}') - \boldsymbol{g}_{r-1}^{(i)}(\boldsymbol{x}'')\right)\right\|}{\left\|\boldsymbol{g}_{r-1}(\boldsymbol{x}') - \boldsymbol{g}_{r-1}^{(i)}(\boldsymbol{x}'')\right\|}, \tag{12}$$

which implies that $\nabla F(\boldsymbol{x}_{r,t-1}^{(i)}) - \boldsymbol{g}_{r,t-1}^{(i)}$ and $\boldsymbol{g}_{r-1}(\boldsymbol{x}') - \boldsymbol{g}_{r-1}^{(i)}(\boldsymbol{x}'')$ are linear dependent according to the Cauchy-Schwarz inequality. Since $\gamma_{r,t-1}^{(i)*} = 1$, we further have

$$\left\|\nabla F(\boldsymbol{x}_{r,t-1}^{(i)}) - \boldsymbol{g}_{r,t-1}^{(i)}\right\| = \left\|\boldsymbol{g}_{r-1}(\boldsymbol{x}') - \boldsymbol{g}_{r-1}^{(i)}(\boldsymbol{x}'')\right\|. \tag{13}$$

These two results, i.e., (12) and (13) thus imply that $\nabla F(\boldsymbol{x}_{r,t-1}^{(i)}) - \boldsymbol{g}_{r,t-1}^{(i)} = \boldsymbol{g}_{r-1}(\boldsymbol{x}') - \boldsymbol{g}_{r-1}^{(i)}(\boldsymbol{x}'')$, which therefore concludes our proof.

E.2. Proof of Theorem 1

E.2.1. Gradient Estimation Error Using Uncertainty

We introduce the following lemma that is adapted from [3] to bound the estimation error of our local gradient surrogates using the uncertainty measure in our (8).

Lemma E.1. *Let $\delta \in (0,1)$ and $\omega \triangleq d + 2(\sqrt{d}+1)\ln(1/\delta)$. For any $\boldsymbol{x} \in \mathcal{X}$, $i \in [N]$, $r \geq 1$ and $t \geq 1$, the following holds with probability of at least $1-\delta$,*

$$\left\|\nabla \mu_{r,t}^{(i)}(\boldsymbol{x}) - \nabla f_i(\boldsymbol{x})\right\|^2 \leq \omega \left\|\partial\left(\sigma_{r,t}^{(i)}\right)^2(\boldsymbol{x})\right\| .$$

E.2.2. RFF Approximation Error for Global Gradient Surrogate

Lemma E.2 ([25])**.** *If $\mathrm{x}_1, \cdots, \mathrm{x}_k$ are independent standard normal random variables, for $\mathrm{y} = \sum_{i=1}^k \mathrm{x}_i^2$ and any ϵ,*

$$\mathbb{P}(\mathrm{y} - k \geq 2\sqrt{k\epsilon} + 2\epsilon) \leq \exp(-\epsilon) .$$

Following the general idea in [4], we present the following Lemma E.3 to bound the difference of our approximated kernel using random features and the ground truth kernel k, as well as the difference between their partial derivatives first. To ease our presentation, we let the kernel k be defined by an infinite dimensional vector $\psi(\boldsymbol{x})$, which is defined by the corresponding infinite number of features for k, throughout this section. That is, $k(\boldsymbol{x}, \boldsymbol{x}') = \psi(\boldsymbol{x})^\top \psi(\boldsymbol{x}')$ for any $\boldsymbol{x}, \boldsymbol{x}' \in \mathcal{X}$.

Lemma E.3. *Let $\delta \in (0,1)$. Assume that $\mathbb{E}\left[\|\boldsymbol{v}\|^2\right] \leq V$, for any $\boldsymbol{x}, \boldsymbol{x}' \in \mathcal{X}$, the following holds with probability of at least $1-\delta$,*

$$\begin{aligned} \left|\boldsymbol{\phi}(\boldsymbol{x})^\top \boldsymbol{\phi}(\boldsymbol{x}') - \boldsymbol{\psi}(\boldsymbol{x})^\top \boldsymbol{\psi}(\boldsymbol{x}')\right| &\leq \sqrt{8\ln(2/\delta)/M} , \\ \left\|\nabla\boldsymbol{\phi}(\boldsymbol{x})^\top \boldsymbol{\phi}(\boldsymbol{x}') - \nabla\boldsymbol{\psi}(\boldsymbol{x})^\top \boldsymbol{\psi}(\boldsymbol{x}')\right\| &\leq \sqrt{4V/(M\delta)} \end{aligned}$$

where M is the number of random Fourier features.

Proof. Recall that $\boldsymbol{\phi}(\boldsymbol{x})^\top \boldsymbol{\phi}(\boldsymbol{x}') = 1/M \sum_{j=1}^M 2\cos(\boldsymbol{v}_j^\top \boldsymbol{x} + b_j)\cos(\boldsymbol{v}_j^\top \boldsymbol{x}' + b_j)$ as shown in Appx. D. Then, according to [4], for any $j \in [M]$,

$$\begin{aligned} \mathbb{E}\left[2\cos(\boldsymbol{v}_j^\top \boldsymbol{x} + b_j)\cos(\boldsymbol{v}_j^\top \boldsymbol{x}' + b_j)\right] &= \boldsymbol{\psi}(\boldsymbol{x})^\top \boldsymbol{\psi}(\boldsymbol{x}') , \\ \mathbb{E}\left[\boldsymbol{\phi}(\boldsymbol{x})^\top \boldsymbol{\phi}(\boldsymbol{x}')\right] &= \boldsymbol{\psi}(\boldsymbol{x})^\top \boldsymbol{\psi}(\boldsymbol{x}') . \end{aligned} \tag{14}$$

Since $2\cos(\boldsymbol{v}_j^\top \boldsymbol{x} + b_j)\cos(\boldsymbol{v}_j^\top \boldsymbol{x}' + b_j) \in [-2, 2]$ and both $\{\boldsymbol{v}_1, \cdots, \boldsymbol{v}_M\}$ and $\{b_1, \cdots, b_M\}$ are randomly independently sampled, according to Hoeffding's inequality, the following inequality holds for any $\epsilon > 0$

$$\mathbb{P}\left(\left|\boldsymbol{\phi}(\boldsymbol{x})^\top \boldsymbol{\phi}(\boldsymbol{x}') - \boldsymbol{\psi}(\boldsymbol{x})^\top \boldsymbol{\psi}(\boldsymbol{x}')\right| \geq \epsilon\right) \leq 2\exp\left(-\frac{M\epsilon^2}{8}\right) . \tag{15}$$

Choose $\delta = 2\exp(M\epsilon^2)$, the following holds with a probability of at least $1-\delta$,

$$\left|\boldsymbol{\phi}(\boldsymbol{x})^\top \boldsymbol{\phi}(\boldsymbol{x}') - \boldsymbol{\psi}(\boldsymbol{x})^\top \boldsymbol{\psi}(\boldsymbol{x}')\right| \leq \sqrt{\frac{8\ln(2/\delta)}{M}} . \tag{16}$$

Moreover, based on the interchangeability of derivative and expectation, we then have the following results derived from (14)

$$\begin{aligned} \mathbb{E}\left[-2\sin(\boldsymbol{v}_j^\top \boldsymbol{x} + b_j)\cos(\boldsymbol{v}_j^\top \boldsymbol{x}' + b_j)\boldsymbol{v}_j^\top\right] &= \nabla\boldsymbol{\psi}(\boldsymbol{x})^\top \boldsymbol{\psi}(\boldsymbol{x}') , \\ \mathbb{E}\left[\nabla\boldsymbol{\phi}(\boldsymbol{x})^\top \boldsymbol{\phi}(\boldsymbol{x}')\right] &= \nabla\boldsymbol{\psi}(\boldsymbol{x})^\top \boldsymbol{\psi}(\boldsymbol{x}') . \end{aligned} \tag{17}$$

Since both $\{\boldsymbol{v}_1, \cdots, \boldsymbol{v}_M\}$ and $\{b_1, \cdots, b_M\}$ are randomly independently sampled, we then can bound the variance

$\mathbb{E}\left[\left\|\nabla\boldsymbol{\phi}(\boldsymbol{x})^\top\boldsymbol{\phi}(\boldsymbol{x}')-\nabla\boldsymbol{\psi}(\boldsymbol{x})^\top\boldsymbol{\psi}(\boldsymbol{x}')\right\|^2\right]$ as below

$$
\begin{aligned}
&\mathbb{E}\left[\left\|\nabla\boldsymbol{\phi}(\boldsymbol{x})^\top\boldsymbol{\phi}(\boldsymbol{x}')-\nabla\boldsymbol{\psi}(\boldsymbol{x})^\top\boldsymbol{\psi}(\boldsymbol{x}')\right\|^2\right]\\
\overset{(a)}{=}&\mathbb{E}\left[\left\|\frac{1}{M}\sum_{j=1}^{M}\left(-2\sin(\boldsymbol{v}_j^\top\boldsymbol{x}+b_j)\cos(\boldsymbol{v}_j^\top\boldsymbol{x}'+b_j)\boldsymbol{v}_j-\nabla\boldsymbol{\psi}(\boldsymbol{x})^\top\boldsymbol{\psi}(\boldsymbol{x}')\right)\right\|^2\right]\\
\overset{(b)}{=}&\frac{1}{M^2}\mathbb{E}\left[\sum_{j=1}^{M}\left\|-2\sin(\boldsymbol{v}_j^\top\boldsymbol{x}+b_j)\cos(\boldsymbol{v}_j^\top\boldsymbol{x}'+b_j)\boldsymbol{v}_j-\nabla\boldsymbol{\psi}(\boldsymbol{x})^\top\boldsymbol{\psi}(\boldsymbol{x}')\right\|^2\right]\\
\overset{(c)}{=}&\frac{1}{M^2}\sum_{j=1}^{M}\left(\mathbb{E}\left[\left\|-2\sin(\boldsymbol{v}_j^\top\boldsymbol{x}+b_j)\cos(\boldsymbol{v}_j^\top\boldsymbol{x}'+b_j)\boldsymbol{v}_j\right\|^2\right]-\mathbb{E}\left[\left\|\nabla\boldsymbol{\psi}(\boldsymbol{x})^\top\boldsymbol{\psi}(\boldsymbol{x}')\right\|^2\right]\right)\\
\overset{(d)}{\leq}&\frac{1}{M^2}\sum_{j=1}^{M}\mathbb{E}\left[\left\|-2\sin(\boldsymbol{v}_j^\top\boldsymbol{x}+b_j)\cos(\boldsymbol{v}_j^\top\boldsymbol{x}'+b_j)\boldsymbol{v}_j\right\|^2\right]\\
\overset{(e)}{\leq}&\frac{4}{M^2}\sum_{j=1}^{M}\mathbb{E}\left[\left\|\boldsymbol{v}_j\right\|^2\right]\\
\overset{(f)}{\leq}&\frac{4V}{M}
\end{aligned}
\tag{18}
$$

where (b) is from the independence among $\{\boldsymbol{v}_1,\cdots,\boldsymbol{v}_M\}$ and $\{b_1,\cdots,b_M\}$ for variance derivation and (c) is based on the definition of variance. In addition, (e) is due to the fact that $\sin(\boldsymbol{v}_j^\top\boldsymbol{x}+b_j),\cos(\boldsymbol{v}_j^\top\boldsymbol{x}'+b_j)\in[-1,1]$ and (f) is because of the assumption that $\mathbb{E}\left[\left\|\boldsymbol{v}\right\|^2\right]\leq V$.

Therefore, according to Chebyshev's inequality, we have the following inequalities for any $\epsilon>0$

$$
\begin{aligned}
\mathbb{P}\left(\left\|\nabla\boldsymbol{\phi}(\boldsymbol{x})^\top\boldsymbol{\phi}(\boldsymbol{x}')-\nabla\boldsymbol{\psi}(\boldsymbol{x})^\top\boldsymbol{\psi}(\boldsymbol{x}')\right\|>\epsilon\right)&\leq\frac{\mathbb{E}\left[\left\|\nabla\boldsymbol{\phi}(\boldsymbol{x})^\top\boldsymbol{\phi}(\boldsymbol{x}')-\nabla\boldsymbol{\psi}(\boldsymbol{x})^\top\boldsymbol{\psi}(\boldsymbol{x}')\right\|^2\right]}{\epsilon^2}\\
&\leq\frac{4V}{M\epsilon^2}\,.
\end{aligned}
\tag{19}
$$

Choose $\epsilon=\sqrt{4V/(M\delta)}$, the following holds for a probability of at least $1-\delta$,

$$
\left\|\nabla\boldsymbol{\phi}(\boldsymbol{x})^\top\boldsymbol{\phi}(\boldsymbol{x}')-\nabla\boldsymbol{\psi}(\boldsymbol{x})^\top\boldsymbol{\psi}(\boldsymbol{x}')\right\|\leq\sqrt{\frac{4V}{M\delta}}\,,
\tag{20}
$$

which finally completes the proof. □

Lemma E.4. *For any $\boldsymbol{x},\boldsymbol{x}'\in\mathcal{X}$ and $i\in[N]$, assume that $\mathbb{E}\left[\left\|\boldsymbol{v}\right\|^2\right]\leq V$, $\left\|\nabla\boldsymbol{\psi}(\boldsymbol{x})^\top\boldsymbol{\psi}(\boldsymbol{x}')\right\|\leq L$ and $|f_i(\boldsymbol{x})|\leq 1$, then the following holds with a constant probability for all $r\in[R]$,*

$$
\left\|\nabla\widehat{\mu}_{r,T}^{(i)}(\boldsymbol{x})-\nabla\mu_{r,T}^{(i)}(\boldsymbol{x})\right\|^2\leq\mathcal{O}\left(\frac{1}{M}\right)\,.
$$

Proof. Based on the definition in (8) and (3), we have that:

$$\begin{aligned}
&\left\|\nabla\widehat{\mu}_{r,T}^{(i)}(\boldsymbol{x})-\nabla\mu_{r,T}^{(i)}(\boldsymbol{x})\right\| \\
&\overset{(a)}{=}\left\|\nabla\boldsymbol{\phi}(\boldsymbol{x})^{\top}\boldsymbol{\Phi}_{r,t-1}^{(i)}\left(\widehat{\mathbf{K}}_{r,T}^{(i)}+\sigma^2\mathbf{I}\right)^{-1}\boldsymbol{y}_{r,T}^{(i)}-\nabla\boldsymbol{\psi}(\boldsymbol{x})^{\top}\boldsymbol{\Psi}_{r,T}^{(i)}\left(\mathbf{K}_{r,T}^{(i)}+\sigma^2\mathbf{I}\right)^{-1}\boldsymbol{y}_{r,T}^{(i)}\right\| \\
&\overset{(b)}{\leq}\left\|\nabla\boldsymbol{\phi}(\boldsymbol{x})^{\top}\boldsymbol{\Phi}_{r,T}^{(i)}\left(\widehat{\mathbf{K}}_{r,T}^{(i)}+\sigma^2\mathbf{I}\right)^{-1}-\nabla\boldsymbol{\psi}(\boldsymbol{x})^{\top}\boldsymbol{\Psi}_{r,T}^{(i)}\left(\mathbf{K}_{r,T}^{(i)}+\sigma^2\mathbf{I}\right)^{-1}\right\|\left\|\boldsymbol{y}_{r,T}^{(i)}\right\| \\
&\overset{(c)}{=}\underbrace{\left\|\nabla\boldsymbol{\phi}(\boldsymbol{x})^{\top}\boldsymbol{\Phi}_{r,T}^{(i)}\left(\widehat{\mathbf{K}}_{r,T}^{(i)}+\sigma^2\mathbf{I}\right)^{-1}-\nabla\boldsymbol{\psi}(\boldsymbol{x})^{\top}\boldsymbol{\Psi}_{r,T}^{(i)}\left(\widehat{\mathbf{K}}_{r,T}^{(i)}+\sigma^2\mathbf{I}\right)^{-1}\right\|}_{①}\left\|\boldsymbol{y}_{r,T}^{(i)}\right\|+ \\
&\qquad\underbrace{\left\|\nabla\boldsymbol{\psi}(\boldsymbol{x})^{\top}\boldsymbol{\Psi}_{r,T}^{(i)}\left(\widehat{\mathbf{K}}_{r,T}^{(i)}+\sigma^2\mathbf{I}\right)^{-1}-\nabla\boldsymbol{\psi}(\boldsymbol{x})^{\top}\boldsymbol{\Psi}_{r,T}^{(i)}\left(\mathbf{K}_{r,T}^{(i)}+\sigma^2\mathbf{I}\right)^{-1}\right\|}_{②}\left\|\boldsymbol{y}_{r,T}^{(i)}\right\|
\end{aligned} \tag{21}$$

where (b) and (c) are from the Cauchy–Schwarz inequality and the triangle inequality, respectively.

We bound term ①, term ② and $\left\|\boldsymbol{y}_{r,T}^{(i)}\right\|$ above separately. Firstly, the following holds with probability of at least $1-rT\delta'$

$$\begin{aligned}
① &\overset{(a)}{=}\left\|\nabla\boldsymbol{\phi}(\boldsymbol{x})^{\top}\boldsymbol{\Phi}_{r,T}^{(i)}\left(\widehat{\mathbf{K}}_{r,T}^{(i)}+\sigma^2\mathbf{I}\right)^{-1}-\nabla\boldsymbol{\psi}(\boldsymbol{x})^{\top}\boldsymbol{\Psi}_{r,T}^{(i)}\left(\widehat{\mathbf{K}}_{r,T}^{(i)}+\sigma^2\mathbf{I}\right)^{-1}\right\| \\
&\overset{(b)}{\leq}\left\|\nabla\boldsymbol{\phi}(\boldsymbol{x})^{\top}\boldsymbol{\Phi}_{r,T}^{(i)}-\nabla\boldsymbol{\psi}(\boldsymbol{x})^{\top}\boldsymbol{\Psi}_{r,T}^{(i)}\right\|\left\|\left(\widehat{\mathbf{K}}_{r,T}^{(i)}+\sigma^2\mathbf{I}\right)^{-1}\right\| \\
&\overset{(c)}{\leq}\sqrt{\sum_{\tau=1}^{rT}\left\|\nabla\boldsymbol{\phi}(\boldsymbol{x})^{\top}\boldsymbol{\phi}(\boldsymbol{x}_{\tau}^{(i)})-\nabla\boldsymbol{\psi}(\boldsymbol{x})^{\top}\boldsymbol{\psi}(\boldsymbol{x}_{\tau}^{(i)})\right\|^2}\left\|\left(\widehat{\mathbf{K}}_{r,T}^{(i)}+\sigma^2\mathbf{I}\right)^{-1}\right\| \\
&\overset{(d)}{\leq}\frac{1}{\sigma^2}\sqrt{\frac{4rTV}{M\delta'}}
\end{aligned} \tag{22}$$

Where (b) comes from the Cauchy–Schwarz inequality and (c) follows from the fact that for any matrix A with n rows and each row identified as $\boldsymbol{a}_i$ we have $\|A\|\leq\|A\|_{\mathrm{F}}\triangleq\sqrt{\sum_{i=1}^{n}\|\boldsymbol{a}_i\|^2}$. Finally, (d) is due to the fact that $\widehat{\mathbf{K}}_{r,T}^{(i)}$ is positive semi-definite and therefore $\widehat{\mathbf{K}}_{r,T}^{(i)}+\sigma^2\mathbf{I}\succcurlyeq\sigma^2\mathbf{I}$ as well as the results in Lemma E.3.

Secondly, the following holds with probability of at least $1-r^2T^2\delta''$,

$$\begin{aligned}
② &\overset{(a)}{=}\left\|\nabla\boldsymbol{\psi}(\boldsymbol{x})^{\top}\boldsymbol{\Psi}_{r,T}^{(i)}\left(\widehat{\mathbf{K}}_{r,T}^{(i)}+\sigma^2\mathbf{I}\right)^{-1}-\nabla\boldsymbol{\psi}(\boldsymbol{x})^{\top}\boldsymbol{\Psi}_{r,T}^{(i)}\left(\mathbf{K}_{r,T}^{(i)}+\sigma^2\mathbf{I}\right)^{-1}\right\| \\
&\overset{(b)}{\leq}\left\|\nabla\boldsymbol{\psi}(\boldsymbol{x})^{\top}\boldsymbol{\Psi}_{r,t-1}^{(i)}\right\|\left\|\left(\widehat{\mathbf{K}}_{r,T}^{(i)}+\sigma^2\mathbf{I}\right)^{-1}-\left(\mathbf{K}_{r,T}^{(i)}+\sigma^2\mathbf{I}\right)^{-1}\right\| \\
&\overset{(c)}{=}\left\|\nabla\boldsymbol{\psi}(\boldsymbol{x})^{\top}\boldsymbol{\Psi}_{r,T}^{(i)}\right\|\left\|\left(\mathbf{K}_{r,T}^{(i)}-\widehat{\mathbf{K}}_{r,T}^{(i)}\right)\left(\widehat{\mathbf{K}}_{r,T}^{(i)}+\sigma^2\mathbf{I}\right)^{-1}\left(\mathbf{K}_{r,T}^{(i)}+\sigma^2\mathbf{I}\right)^{-1}\right\| \\
&\overset{(d)}{\leq}\sqrt{\sum_{\tau=1}^{rT}\left\|\nabla\boldsymbol{\psi}(\boldsymbol{x})^{\top}\boldsymbol{\psi}(\boldsymbol{x}_{\tau}^{(i)})\right\|^2}\left\|\mathbf{K}_{r,T}^{(i)}-\widehat{\mathbf{K}}_{r,T}^{(i)}\right\|\left\|\left(\widehat{\mathbf{K}}_{r,T}^{(i)}+\sigma^2\mathbf{I}\right)^{-1}\right\|\left\|\left(\mathbf{K}_{r,T}^{(i)}+\sigma^2\mathbf{I}\right)^{-1}\right\| \\
&\overset{(e)}{\leq}\frac{L}{\sigma^4}\sqrt{rT}\sqrt{\sum_{\tau,\tau'=1}^{rT}\left\|\boldsymbol{\psi}(\boldsymbol{x}_{\tau}^{(i)})^{\top}\boldsymbol{\psi}(\boldsymbol{x}_{\tau'}^{(i)})-\boldsymbol{\phi}(\boldsymbol{x}_{\tau}^{(i)})^{\top}\boldsymbol{\phi}(\boldsymbol{x}_{\tau'}^{(i)})\right\|^2} \\
&\overset{(f)}{\leq}\frac{L\,(rT)^{3/2}}{\sigma^4}\sqrt{\frac{8\ln(2/\delta'')}{M}}
\end{aligned} \tag{23}$$

where (b) is from the Cauchy–Schwarz inequality. Besides, (c) and (e) come from the aforementioned inequality $\|A\|\leq$

$\|A\|_{\mathrm{F}}$. In addition, (f) is based on the assumption that $\left\|\nabla\boldsymbol{\psi}(\boldsymbol{x})^{\top}\boldsymbol{\psi}(\boldsymbol{x}')\right\| \leq L$, $\|A\| \leq \|A\|_{\mathrm{F}}$, $\widehat{\mathbf{K}}_{r,T}^{(i)} + \sigma^2\mathbf{I} \succcurlyeq \sigma^2\mathbf{I}$ and $\mathbf{K}_{r,T}^{(i)} + \sigma^2\mathbf{I} \succcurlyeq \sigma^2\mathbf{I}$.

Thirdly, the following holds with probability of at least $1 - rT\delta'''$,

$$\begin{aligned}\left\|\boldsymbol{y}_{r,T}^{(i)}\right\| &\overset{(a)}{=} \sqrt{\sum_{\tau=1}^{rT}\left(f_i(\boldsymbol{x}_\tau)+\zeta_\tau\right)^2} \\ &\overset{(b)}{\leq} \sqrt{\sum_{\tau=1}^{rT} 2f_i^2(\boldsymbol{x}_\tau)+2\zeta_\tau^2} \\ &\overset{(c)}{\leq} \sqrt{2rT + 2\sigma^2\sum_{\tau=1}^{rT}\left(\frac{\zeta_\tau}{\sigma}\right)^2} \\ &\overset{(d)}{\leq} \sqrt{2rT + 2\sigma^2\left(rT + 2\sqrt{rT\ln(1/\delta''')} + 2\ln(1/\delta''')\right)}\end{aligned} \tag{24}$$

where ζ_τ denote the observation noise associated with the input $\boldsymbol{x}_\tau$. Besides, (c) is from the assumption that $\zeta_\tau \sim \mathcal{N}(0,\sigma^2)$ for any τ in Sec. 2 and $|f_i(\boldsymbol{x})| \leq 1$ for any $\boldsymbol{x} \in \mathcal{X}$. Finally, (d) comes from our Lemma E.2.

By introducing (22), (23) and (24) with $\delta' = \frac{\delta}{3rT}$, $\delta'' = \frac{\delta}{3r^2T^2}$ and $\delta''' = \frac{\delta}{3rT}$ into (21), the following then holds with probability of at least $1-\delta$,

$$\begin{aligned}&\left\|\nabla\widehat{\mu}_{r,T}^{(i)}(\boldsymbol{x}) - \nabla\mu_{r,T}^{(i)}(\boldsymbol{x})\right\| \\ \leq&\left(\frac{rT}{\sigma^2}\sqrt{\frac{12V}{M\delta}} + \frac{4L\,(rT)^{3/2}}{\sigma^4}\sqrt{\frac{\ln(6rT/\delta)}{M}}\right)\sqrt{2rT + 2\sigma^2\left(rT + 2\sqrt{rT\ln(3rT/\delta)} + 2\ln(3rT/\delta)\right)} \\ =&\mathcal{O}\left(\frac{rT\sqrt{rT}}{\sqrt{M}} + \frac{r^2T^2\sqrt{\ln(rT)}}{\sqrt{M}}\right).\end{aligned} \tag{25}$$

Of note, it is easy to show that when (25) holds for $r = R$, it must hold for any $r \leq R$. Therefore, the following finally holds with a constant probability for all $r \in [R]$,

$$\left\|\nabla\widehat{\mu}_{r,T}^{(i)}(\boldsymbol{x}) - \nabla\mu_{r,T}^{(i)}(\boldsymbol{x})\right\|^2 \leq \mathcal{O}\left(\frac{1}{M}\right), \tag{26}$$

which concludes our proof. □

Remark. Note that the assumption $\mathbb{E}\left[\|\boldsymbol{v}\|^2\right] \leq V$ implies that the distribution $p(\boldsymbol{v})$ in Appx. D has a bounded mean and covariance since $\mathbb{E}\left[\|\boldsymbol{v}\|^2\right] = \|\mathbb{E}[\boldsymbol{v}]\|^2 + \mathbb{E}\left[\|\boldsymbol{v} - \mathbb{E}[\boldsymbol{v}]\|^2\right]$. This is usually valid for the widely applied kernels (e.g., the squared exponential kernel in Appx. D) in practice.

Remarkably, (25) with $r = R$ has demonstrated that a larger number M of random features is preferred to maintain the approximation quality of $\nabla\widehat{\mu}_{R,T}^{(i)}(\boldsymbol{x}) \approx \nabla\mu_{R,T}^{(i)}$ when the number R of communication rounds and the number T of local iterations increase. This in fact aligns with the intuition that a larger hypothesis space (defined by the M random features) should be used when the target function (defined by the existing RT function queries) becomes more complex. However, for any communication round $r+1 \in [R]$ in our FZooS, the approximation of $\nabla\mu_{r,T}^{(i)}$ using $\nabla\widehat{\mu}_{r,T}^{(i)}(\boldsymbol{x})$ needs to be accurate only at the local updated inputs $\{\boldsymbol{x}_{r+1,t-1}^{(i)}\}_{t\in[T],i\in[N]}$ with a relatively small T (i.e., $T \leq 20$), which consequently usually does not requires an extremely large M to realize a good approximation quality in practice. This has actually been supported by the empirical results in our Sec. 5 and Appx. H.

E.2.3. Final Gradient Disparity Analysis Using Uncertainty

We introduce the following Lemma E.5 and Lemma E.6 from [3] to ease our proof of Thm. 1:

Lemma E.5. *Let $\{\boldsymbol{v}_1, \ldots, \boldsymbol{v}_\tau\}$ be any τ vectors in $\mathbb{R}^d$. Then the following holds for any $a > 0$:*

$$\|\boldsymbol{v}_i\| \|\boldsymbol{v}_j\| \leq \frac{a}{2} \|\boldsymbol{v}_i\|^2 + \frac{1}{2a} \|\boldsymbol{v}_j\|^2 \ , \tag{27}$$

$$\|\boldsymbol{v}_i + \boldsymbol{v}_j\|^2 \leq (1+a) \|\boldsymbol{v}_i\|^2 + \left(1 + \frac{1}{a}\right) \|\boldsymbol{v}_j\|^2 \ , \tag{28}$$

$$\left\| \sum_{i=1}^{\tau} \boldsymbol{v}_i \right\|^2 \leq \tau \sum_{i=1}^{\tau} \|\boldsymbol{v}_i\|^2 \ . \tag{29}$$

Proof. For (27), we have that

$$\frac{a}{2} \|\boldsymbol{v}_i\|^2 + \frac{1}{2a} \|\boldsymbol{v}_j\|^2 \geq 2\sqrt{\frac{a}{2} \|\boldsymbol{v}_i\|^2 \cdot \frac{1}{2a} \|\boldsymbol{v}_j\|^2} = \|\boldsymbol{v}_i\| \|\boldsymbol{v}_j\| \ . \tag{30}$$

For (28), we have that

$$\begin{aligned} (1+a) \|\boldsymbol{v}_i\|^2 + \left(1 + \frac{1}{a}\right) \|\boldsymbol{v}_j\|^2 &= \|\boldsymbol{v}_i\|^2 + \|\boldsymbol{v}_j\|^2 + \left(a \|\boldsymbol{v}_i\|^2 + \frac{1}{a} \|\boldsymbol{v}_j\|^2\right) \\ &\geq \|\boldsymbol{v}_i\|^2 + \|\boldsymbol{v}_j\|^2 + 2\sqrt{a \|\boldsymbol{v}_i\|^2 \cdot \frac{1}{a} \|\boldsymbol{v}_j\|^2} \\ &= \|\boldsymbol{v}_i + \boldsymbol{v}_j\|^2 \ . \end{aligned} \tag{31}$$

For (29), we can directly employ the convexity of function $h(\boldsymbol{x}) = \|\boldsymbol{x}\|^2$ and Jensen's inequality:

$$\left\| \frac{1}{\tau} \sum_{i=1}^{\tau} \boldsymbol{v}_i \right\|^2 \leq \frac{1}{\tau} \sum_{i=1}^{\tau} \|\boldsymbol{v}_i\|^2 \ . \tag{32}$$

By multiplying the inequality above with τ^2, we conclude the proof. □

Lemma E.6. *Define $\rho_i \triangleq \max_{\boldsymbol{x} \in \mathcal{X}, r \geq 1, t \geq 1} \left\| \partial \left(\sigma_{r,t}^{(i)}\right)^2 (\boldsymbol{x}) \right\| \Big/ \left\| \partial \left(\sigma_{r,t-1}^{(i)}\right)^2 (\boldsymbol{x}) \right\|$, we have that $\rho_i \in \left[1/(1+1/\sigma^2), 1\right]$, and that for any $\boldsymbol{x} \in \mathcal{X}, r \geq 1, t \geq 1$ the following holds,*

$$\left\| \partial \left(\sigma_{r,t}^{(i)}\right)^2 (\boldsymbol{x}) \right\| \leq \kappa \rho_i^{(r-1)T+t} \ .$$

Let $\delta \in (0,1)$, $\epsilon = \mathcal{O}(\frac{1}{M})$ and $\omega = d + 2(\sqrt{d}+1)\ln(2NRT/\delta)$, the following inequalities then hold with a probability of at least $1-\delta$:

$$\begin{aligned} &\left\| \frac{1}{N} \sum_{j=1, j\neq i}^{N} \left(\nabla \widehat{\mu}_{r-1,T}^{(j)}(\boldsymbol{x}_{r,t-1}^{(i)}) - \nabla f_j(\boldsymbol{x}_{r,t-1}^{(i)}) \right) \right\|^2 \\ &\overset{(a)}{\leq} \frac{N-1}{N^2} \sum_{j=1, j\neq i}^{N} \left\| \nabla \widehat{\mu}_{r-1,T}^{(j)}(\boldsymbol{x}_{r,t-1}^{(i)}) - \nabla f_j(\boldsymbol{x}_{r,t-1}^{(i)}) \right\|^2 \\ &\overset{(b)}{=} \frac{N-1}{N^2} \sum_{j=1, j\neq i}^{N} \left\| \nabla \widehat{\mu}_{r-1,T}^{(j)}(\boldsymbol{x}_{r,t-1}^{(i)}) - \nabla \mu_{r-1,T}^{(j)}(\boldsymbol{x}_{r,t-1}^{(i)}) + \nabla \mu_{r-1,T}^{(j)}(\boldsymbol{x}_{r,t-1}^{(i)}) - \nabla f_j(\boldsymbol{x}_{r,t-1}^{(i)}) \right\|^2 \\ &\overset{(c)}{\leq} \frac{N-1}{N^2} \sum_{j=1, j\neq i}^{N} \left(\frac{N}{N-1} \left\| \nabla \mu_{r-1,T}^{(j)}(\boldsymbol{x}_{r,t-1}^{(i)}) - \nabla f_j(\boldsymbol{x}_{r,t-1}^{(i)}) \right\|^2 + N \left\| \nabla \widehat{\mu}_{r-1,T}^{(j)}(\boldsymbol{x}_{r,t-1}^{(i)}) - \nabla \mu_{r-1,T}^{(j)}(\boldsymbol{x}_{r,t-1}^{(i)}) \right\|^2 \right) \\ &\overset{(d)}{\leq} \frac{\omega}{N} \sum_{j=1, j\neq i}^{N} \left\| \partial \left(\sigma_{r-1,T}^{(j)}\right)^2 (\boldsymbol{x}_{r,t-1}^{(i)}) \right\| + \frac{(N-1)^2}{N} \epsilon \ , \end{aligned} \tag{33}$$

in which (a) is from (29) and (c) is from (28) with $a = \frac{1}{N-1}$. In addition, (d) comes from Lemma E.1 and Lemma E.4.

$$
\begin{aligned}
&\frac{(N-1)^2}{N^2}\left\|\nabla f_i(\boldsymbol{x}_{r,t-1}^{(i)}) - \nabla\widehat{\mu}_{r-1,T}^{(i)}(\boldsymbol{x}_{r,t-1}^{(i)})\right\|^2 \\
&\overset{(a)}{=}\frac{(N-1)^2}{N^2}\left\|\nabla f_i(\boldsymbol{x}_{r,t-1}^{(i)}) - \nabla\mu_{r-1,T}^{(i)}(\boldsymbol{x}_{r,t-1}^{(i)}) + \nabla\mu_{r-1,T}^{(i)}(\boldsymbol{x}_{r,t-1}^{(i)}) - \nabla\widehat{\mu}_{r-1,T}^{(i)}(\boldsymbol{x}_{r,t-1}^{(i)})\right\|^2 \\
&\overset{(b)}{\leq}\frac{(N-1)^2}{N^2}\left(\frac{N}{N-1}\left\|\nabla f_i(\boldsymbol{x}_{r,t-1}^{(i)}) - \nabla\mu_{r-1,T}^{(i)}(\boldsymbol{x}_{r,t-1}^{(i)})\right\|^2 + N\left\|\nabla\mu_{r-1,T}^{(i)}(\boldsymbol{x}_{r,t-1}^{(i)})\nabla\widehat{\mu}_{r-1,T}^{(i)}(\boldsymbol{x}_{r,t-1}^{(i)})\right\|^2\right) \\
&\overset{(c)}{\leq}\left(\frac{\omega(N-1)}{N}\left\|\partial\left(\sigma_{r-1,T}^{(i)}\right)^2(\boldsymbol{x}_{r,t-1}^{(i)})\right\| + \frac{(N-1)^2}{N}\epsilon\right),
\end{aligned}
\tag{34}
$$

in which (c) is from (28) with $a = \frac{1}{N-1}$. In addition, (d) comes from Lemma E.1 and Lemma E.4.

By exploiting the inequalities above, we have

$$
\begin{aligned}
&\frac{1}{N}\sum_{i=1}^{N}\Xi_{r,t}^{(i)} \\
&\overset{(a)}{=}\frac{1}{N}\sum_{i=1}^{N}\left\|\nabla\mu_{r,t-1}^{(i)}(\boldsymbol{x}_{r,t-1}^{(i)}) + \gamma_{r,t-1}\left(\nabla\widehat{\mu}_{r-1}(\boldsymbol{x}_{r,t-1}^{(i)}) - \nabla\widehat{\mu}_{r-1,T}^{(i)}(\boldsymbol{x}_{r,t-1}^{(i)})\right) - \nabla F(\boldsymbol{x}_{r,t-1}^{(i)})\right\|^2 \\
&\overset{(b)}{=}\frac{1}{N}\sum_{i=1}^{N}\left\|\nabla\mu_{r,t-1}^{(i)}(\boldsymbol{x}_{r,t-1}^{(i)}) - \nabla f_i(\boldsymbol{x}_{r,t-1}^{(i)}) + \gamma_{r,t-1}\left(\frac{1}{N}\sum_{j=1,j\neq i}^{N}\left(\nabla\widehat{\mu}_{r-1,T}^{(j)}(\boldsymbol{x}_{r,t-1}^{(i)}) - \nabla f_j(\boldsymbol{x}_{r,t-1}^{(i)})\right)\right) + \right. \\
&\qquad\left.\frac{\gamma_{r,t-1}(N-1)}{N}\left(\nabla f_i(\boldsymbol{x}_{r,t-1}^{(i)}) - \nabla\widehat{\mu}_{r-1,T}^{(i)}(\boldsymbol{x}_{r,t-1}^{(i)})\right) + (1-\gamma_{r,t-1})\left(\nabla f_i(\boldsymbol{x}_{r,t-1}^{(i)}) - \nabla F(\boldsymbol{x}_{r,t-1}^{(i)})\right)\right\|^2 \\
&\overset{(c)}{\leq}\frac{1}{N}\sum_{i=1}^{N}\left(4\left\|\nabla\mu_{r,t-1}^{(i)}(\boldsymbol{x}_{r,t-1}^{(i)}) - \nabla f_i(\boldsymbol{x}_{r,t-1}^{(i)})\right\|^2 + 4\gamma_{r,t-1}^2\left\|\frac{1}{N}\sum_{j=1,j\neq i}^{N}\left(\nabla\widehat{\mu}_{r-1,T}^{(j)}(\boldsymbol{x}_{r,t-1}^{(i)}) - \nabla f_j(\boldsymbol{x}_{r,t-1}^{(i)})\right)\right\|^2 + \right. \\
&\qquad\left.\frac{4\gamma_{r,t-1}^2(N-1)^2}{N^2}\left\|\nabla f_i(\boldsymbol{x}_{r,t-1}^{(i)}) - \nabla\widehat{\mu}_{r-1,T}^{(i)}(\boldsymbol{x}_{r,t-1}^{(i)})\right\|^2 + 4(1-\gamma_{r,t-1})^2\left\|\nabla f_i(\boldsymbol{x}_{r,t-1}^{(i)}) - \nabla F(\boldsymbol{x}_{r,t-1}^{(i)})\right\|^2\right) \\
&\overset{(d)}{\leq}\frac{4\omega}{N}\sum_{i=1}^{N}\left\|\partial\left(\sigma_{r,t-1}^{(i)}\right)(\boldsymbol{x}_{r,t-1}^{(i)})\right\| + 4\gamma_{r,t-1}^2\left(\frac{\omega}{N^2}\sum_{i=1}^{N}\sum_{j=1,j\neq i}^{N}\left\|\partial\left(\sigma_{r-1,T}^{(j)}\right)^2(\boldsymbol{x}_{r,t-1}^{(i)})\right\| + \frac{(N-1)^2}{N}\epsilon\right) + \\
&\qquad 4\gamma_{r,t-1}^2\left(\frac{\omega(N-1)}{N^2}\sum_{i=1}^{N}\left\|\partial\left(\sigma_{r-1,T}^{(i)}\right)^2(\boldsymbol{x}_{r,t-1}^{(i)})\right\| + \frac{(N-1)^2}{N}\epsilon\right) + 4(1-\gamma_{r,t-1})^2G
\end{aligned}
\tag{35}
$$

where (c) is from the (29). In addition, (d) is from Lemma E.1, (33) and (34).

By introducing the results in Lemma E.6 into (35), we have

$$
\begin{aligned}
\frac{1}{N}\sum_{i=1}^{N}\Xi_{r,t}^{(i)} &\overset{(a)}{\leq}\frac{4\omega}{N}\sum_{i=1}^{N}\kappa\rho_i^{(r-1)T+t-1} + 4\gamma_{r,t-1}^2\left(\frac{2\omega(N-1)}{N^2}\sum_{i=1}^{N}\kappa\rho_i^{(r-1)T} + \frac{2(N-1)^2}{N}\epsilon\right) \\
&\qquad + 4(1-\gamma_{r,t-1})^2G \\
&\overset{(b)}{\leq}\frac{4\omega}{N}\sum_{i=1}^{N}\kappa\rho_i^{(r-1)T+t-1} + 4\gamma_{r,t-1}^2\left(\frac{2\omega}{N}\sum_{i=1}^{N}\kappa\rho_i^{(r-1)T} + 2N\epsilon\right) + 4(1-\gamma_{r,t-1})^2G \\
&\overset{(c)}{\leq} 4\omega\kappa\rho^{(r-1)T+t-1} + 4\gamma_{r,t-1}^2\left(2\omega\kappa\rho^{(r-1)T} + 2N\epsilon\right) + 4(1-\gamma_{r,t-1})^2G
\end{aligned}
\tag{36}
$$

where (c) is from Jansen's inequality with $\rho \triangleq \frac{1}{N}\sum_{i=1}^{N}\rho_i$. This finally concludes our proof.

Remark. Of note, the upper bound in our Thm. 1 is a quadratic function w.r.t. the gradient correction length $\gamma_{r,t-1}$. As a consequence, it is easy to verify that in order to minimize the upper bound in our Thm. 1 (i.e., to achieve a better-performing (5)) w.r.t. $\gamma_{r,t-1}$, $\gamma_{r,t-1}$ needs to be chosen as

$$\gamma_{r,t-1} = \frac{G}{G + 2\omega\rho^{(r-1)T} + 2N\epsilon}, \tag{37}$$

as shown in our Cor. 1. This better-performing $\gamma_{r,t-1}$ therefore implies that ***(a)*** an adaptive $\gamma_{r,t-1}$ is indeed able to theoretically reduce the gradient disparity, which therefore aligns with the conclusion from our Prop. B.1 and ***(b)*** when the estimation error of our gradient correction vector (characterized by $2\omega\rho^{rT} + 2N\epsilon$) in (5) is smaller than the client heterogeneity (characterized by G), a large γ_{t-1} is suggested to be applied in order to minimize the gradient disparity $\frac{1}{N}\sum_{i=1}^{N}\Xi_{r,t}^{(i)}$, as shown in our Sec. 4.

By introducing this $\gamma_{r,t-1}$ into the upper bound in Thm. 1, we have

$$\begin{aligned}
\frac{1}{N}\sum_{i=1}^{N}\Xi_{r,t}^{(i)} &\overset{(a)}{\leq} 4\omega\kappa\rho^{(r-1)T+t-1} + 4\gamma_{r,t-1}^{2}\left(2\omega\kappa\rho^{(r-1)T} + 2N\epsilon\right) + 4(1-\gamma_{r,t-1})^{2}G \\
&\overset{(b)}{=} 4\omega\kappa\rho^{(r-1)T+t-1} + \frac{4G\left(2\omega\kappa\rho^{(r-1)T} + 2N\epsilon\right)}{G + \left(2\omega\rho^{(r-1)T} + 2N\epsilon\right)} \\
&\overset{(c)}{\leq} 4\omega\kappa\rho^{(r-1)T+t-1} + 2\sqrt{2G(\omega\kappa\rho^{(r-1)T} + N\epsilon)} \\
&\overset{(d)}{\leq} 4\omega\kappa\rho^{(r-1)T+t-1} + 2\sqrt{2\omega\kappa\rho^{(r-1)T}G} + 2\sqrt{2NG\epsilon}
\end{aligned} \tag{38}$$

where (c) is from the inequality of $G + 2\omega\rho^{(r-1)T} + 2N\epsilon \geq 2\sqrt{G(2\omega\rho^{(r-1)T} + 2N\epsilon)}$ (i.e., the relationship between the geometric mean and arithmetic mean of G and $2\omega\rho^{(r-1)T} + 2N\epsilon$) and (d) is from the fact that $(\sqrt{2\omega\kappa\rho^{(r-1)T}G} + \sqrt{2NG\epsilon})^2 > 2\omega\kappa\rho^{(r-1)T}G + 2NG\epsilon$. Interestingly, (38) enjoys two major aspects. ***(a)*** In contrast to the algorithm where $\gamma_{r,t-1} = 0$ (e.g., FedZO), the impact of client heterogeneity (i.e., G) is able to be reduced in our FZooS through decreasing the estimation error of our gradient surrogates (i.e., $\omega\kappa\rho^{(r-1)T}$) and the RFF approximation error (i.e., ϵ) for our global gradient surrogates. ***(b)*** In contrast to the federated ZOO algorithms where $\gamma_{r,t-1} = 1$ (e.g., SCAFFOLD), the impact of the large estimation error of our gradient surrogates (i.e., $\omega\kappa\rho^{(r-1)T}$) is also able to be mitigated in our FZooS through a small client heterogeneity (i.e., G) in practice. As a result, these advantages will intuitively make our FZooS produce more robust optimization performance under different scenarios in practice, as supported by our Sec. 5 and Appx. H.

E.3. Gradient Estimation Analysis Based on Euclidean Distance

Of note, for every iteration t of round r, our global gradient surrogate in Sec. 3.2.1 is obtained based on the optimization trajectory $\mathcal{D}^{(i)}_{r-1,T} = \{(\boldsymbol{x}^{(i)}_\tau, y^{(i)}_\tau)\}_{\tau=1}^{T(r-1)}$ and is not capable of being updated immediately although $t-1$ new function queries are given at this time. This is because the update of our global gradient surrogate only occurs when clients and server can communicate with each other, i.e., at the end of each round. Intuitively, this will result in the phenomenon that the quality of our global gradient surrogate and hence the quality of our (5) decays w.r.t. the iterations of local updates, as empirically supported in Appx. H.1. This is likely because the Euclidean distance between the input to be evaluated in our global gradient surrogate and the queried inputs from the optimization trajectory becomes larger and consequently the optimization trajectory becomes less informative. Unfortunately, such a quality decay within the local updates fails to be captured in Thm. 1 and hence may result in an impractical choice of $\gamma_{r,t-1}$ in Cor. 1. To this end, we develop another uncertainty analysis of our global gradient surrogate that is based on Euclidean distance to capture such a phenomenon in this section, which finally gives us a more practical choice of gradient correction length.

We first introduce the following lemma to ease our proof in this section.

Lemma E.7. *For any matrix $\mathbf{A}$, $\mathbf{A}^\top\mathbf{A}$ and $\mathbf{A}\mathbf{A}^\top$ share the same non-zero eigenvalues.*

Proof. Let λ be any non-zero eigenvalue of $\mathbf{A}^\top\mathbf{A}$, for some $\boldsymbol{x} \neq \mathbf{0}$, we have

$$\mathbf{A}^\top\mathbf{A}\boldsymbol{x} = \lambda\boldsymbol{x} \; . \tag{39}$$

By multiplying $\mathbf{A}$ on both sides above, we have

$$\mathbf{A}\mathbf{A}^\top(\mathbf{A}\boldsymbol{x}) = \lambda(\mathbf{A}\boldsymbol{x}) \; , \tag{40}$$

which implies that λ is also the eigenvalue of $\mathbf{A}\mathbf{A}^\top$ with $\mathbf{A}\boldsymbol{x}$ being the eigenvector. Following the same proof, it is easy to show that any non-zero eigenvalue of $\mathbf{A}\mathbf{A}^\top$ remains the eigenvalue of $\mathbf{A}^\top\mathbf{A}$, which therefore concludes the proof. □

We then introduce another estimation error analysis (different from the one presented in Appx. E.2) of our global gradient surrogate as follows where we slightly abuse the notation and use $\boldsymbol{x}^{(i)}_\tau \in \mathcal{D}^{(i)}_{r,T}$ to denote that $\boldsymbol{x}^{(i)}_\tau$ is from the optimization trajectory $\mathcal{D}^{(i)}_{r,T}$.

Proposition E.1. *Let the shift-invariant kernel $k(\boldsymbol{x},\boldsymbol{x}') = k(\|\boldsymbol{x}-\boldsymbol{x}'\|^2)$ where $k(\cdot)$ is assumed to be non-increasing and function $h(\iota) = \iota\nabla k(\iota)^2$ is assumed to be convex, the following then holds with a probability of at least $1-\delta$ for any $\boldsymbol{x} \in \mathcal{X}$,*

$$\|\nabla\mu_r(\boldsymbol{x}) - \nabla F(\boldsymbol{x})\|^2 \leq \omega\kappa - \frac{4\omega\iota_r^2\nabla k(\iota_r)^2}{k(0)d + \sigma^2 d/(rT)}$$

where $\omega = d + 2(\sqrt{d}+1)\ln(1/\delta)$, $\iota_r \triangleq \frac{1}{rNT}\sum_{i=1}^N \sum_{\boldsymbol{x}^{(i)}_\tau \in \mathcal{D}^{(i)}_{r,T}} \left\|\boldsymbol{x} - \boldsymbol{x}^{(i)}_\tau\right\|^2$, and $k(0) = k(\boldsymbol{x},\boldsymbol{x})$.

Proof. Recall that the uncertainty measure function (see (8)) of our local gradient surrogate on client i for iteration T of round r will be

$$\begin{aligned}
\partial\left(\sigma^{(i)}_{r,T}\right)^2(\boldsymbol{x}) &= \partial_{\boldsymbol{z}}\partial_{\boldsymbol{z}'}k(\boldsymbol{z},\boldsymbol{z}') - \partial_{\boldsymbol{z}}\boldsymbol{k}^{(i)}_{r,T}(\boldsymbol{z})^\top\left(\mathbf{K}^{(i)}_{r,T} + \sigma^2\mathbf{I}\right)^{-1}\partial_{\boldsymbol{z}'}\boldsymbol{k}^{(i)}_{r,T}(\boldsymbol{z}')\Big|_{\boldsymbol{z}=\boldsymbol{z}'=\boldsymbol{x}} \\
&\overset{(a)}{\preccurlyeq} \kappa\mathbf{I} - \left(\lambda_{\max}(\mathbf{K}^{(i)}_{r,T}) + \sigma^2\right)^{-1}\partial_{\boldsymbol{z}}\boldsymbol{k}^{(i)}_{r,T}(\boldsymbol{z})^\top\partial_{\boldsymbol{z}'}\boldsymbol{k}^{(i)}_{r,T}(\boldsymbol{z}')\Big|_{\boldsymbol{z}=\boldsymbol{z}'=\boldsymbol{x}} \\
&\overset{(b)}{\preccurlyeq} \kappa\mathbf{I} - \frac{\partial_{\boldsymbol{z}}\boldsymbol{k}^{(i)}_{r,T}(\boldsymbol{z})^\top\partial_{\boldsymbol{z}'}\boldsymbol{k}^{(i)}_{r,T}(\boldsymbol{z}')\big|_{\boldsymbol{z}=\boldsymbol{z}'=\boldsymbol{x}}}{rT\max_{\boldsymbol{x},\boldsymbol{x}'\in\mathcal{D}^{(i)}_{r,T}} k(\boldsymbol{x},\boldsymbol{x}') + \sigma^2}
\end{aligned} \tag{41}$$

where (a) is based on the assumption on $\partial_{\boldsymbol{z}}\partial_{\boldsymbol{z}'}k(\boldsymbol{z},\boldsymbol{z}')$ in our Sec. 2 and the definition of maximum eigenvalue. In addition, (b) comes from $\lambda_{\max}(\mathbf{K}^{(i)}_{r,T}) \leq rT\max_{\boldsymbol{x},\boldsymbol{x}'\in\mathcal{D}^{(i)}_{r,T}} k(\boldsymbol{x},\boldsymbol{x}')$ (i.e., the Gershgorin theorem).

Based on the assumption that $k(\boldsymbol{x},\boldsymbol{x}') = k(\|\boldsymbol{x}-\boldsymbol{x}'\|^2)$ and $k(\cdot)$ is non-increasing, we have

$$\max_{\boldsymbol{x},\boldsymbol{x}'\in\mathcal{D}^{(i)}_{r,T}} k(\boldsymbol{x},\boldsymbol{x}') \leq k(\boldsymbol{x},\boldsymbol{x}) = k(0) \; . \tag{42}$$

Moreover, define $\iota \triangleq \|\boldsymbol{z}-\boldsymbol{z}'\|^2$, the partial derivative of kernel $k(\cdot,\cdot)$ will be

$$\begin{aligned}\partial_{\boldsymbol{z}} k(\boldsymbol{z},\boldsymbol{z}') &= 2\left(\boldsymbol{z}-\boldsymbol{z}'\right)\nabla k(\iota)\\ \partial_{\boldsymbol{z}'} k(\boldsymbol{z},\boldsymbol{z}') &= 2\left(\boldsymbol{z}'-\boldsymbol{z}\right)\nabla k(\iota)\,.\end{aligned} \tag{43}$$

Therefore, the each element in the $rT\times rT$ matrix $\partial_{\boldsymbol{z}}\boldsymbol{k}^{(i)}_{r,T}(\boldsymbol{z})\partial_{\boldsymbol{z}'}\boldsymbol{k}^{(i)}_{r,T}(\boldsymbol{z}')^\top\big|_{\boldsymbol{z}=\boldsymbol{z}'=\boldsymbol{x}}$ that is induced by the input pair $(\boldsymbol{x}^{(i)}_\tau,\boldsymbol{x}^{(i)}_{\tau'})$ with $\boldsymbol{x}^{(i)}_\tau,\boldsymbol{x}^{(i)}_{\tau'}\in\mathcal{D}^{(i)}_{r,T}$ and $\tau,\tau'\in[rT]$ will be:

$$4\left(\boldsymbol{x}-\boldsymbol{x}^{(i)}_\tau\right)^\top\left(\boldsymbol{x}-\boldsymbol{x}^{(i)}_{\tau'}\right)\nabla k(\iota^{(i)}_\tau)\nabla k(\iota^{(i)}_{\tau'}) \tag{44}$$

where $\iota^{(i)}_\tau \triangleq \left\|\boldsymbol{x}-\boldsymbol{x}^{(i)}_\tau\right\|^2, \iota^{(i)}_{\tau'} \triangleq \left\|\boldsymbol{x}-\boldsymbol{x}^{(i)}_{\tau'}\right\|^2$. Based on these results, the trace norm $\|\cdot\|_{\text{tr}}$ of $\partial_{\boldsymbol{z}}\boldsymbol{k}^{(i)}_{r,T}(\boldsymbol{z})\partial_{\boldsymbol{z}'}\boldsymbol{k}^{(i)}_{r,T}(\boldsymbol{z}')^\top\big|_{\boldsymbol{z}=\boldsymbol{z}'=\boldsymbol{x}}$ will be

$$\begin{aligned}\left\|\partial_{\boldsymbol{z}}\boldsymbol{k}^{(i)}_{r,T}(\boldsymbol{z})\partial_{\boldsymbol{z}'}\boldsymbol{k}^{(i)}_{r,T}(\boldsymbol{z}')^\top\big|_{\boldsymbol{z}=\boldsymbol{z}'=\boldsymbol{x}}\right\|_{\text{tr}} &= \sum_{\tau=1}^{rT} 4\left\|\boldsymbol{x}-\boldsymbol{x}_\tau\right\|^2\nabla k(\iota_\tau)^2\\ &= \sum_{\tau=1}^{rT} 4\iota_\tau\nabla k(\iota_\tau)^2\,.\end{aligned} \tag{45}$$

By further assuming that the function $h(\iota)=\iota\nabla k(\iota)^2$ is convex, we then have

$$\begin{aligned}\left\|\partial_{\boldsymbol{z}}\boldsymbol{k}^{(i)}_{r,T}(\boldsymbol{z})^\top\partial_{\boldsymbol{z}'}\boldsymbol{k}^{(i)}_{r,T}(\boldsymbol{z}')\big|_{\boldsymbol{z}=\boldsymbol{z}'=\boldsymbol{x}}\right\| &\overset{(a)}{\geq} \frac{1}{d}\left\|\partial_{\boldsymbol{z}}\boldsymbol{k}^{(i)}_{r,T}(\boldsymbol{z})^\top\partial_{\boldsymbol{z}'}\boldsymbol{k}^{(i)}_{r,T}(\boldsymbol{z}')\big|_{\boldsymbol{z}=\boldsymbol{z}'=\boldsymbol{x}}\right\|_{\text{tr}}\\ &\overset{(b)}{=} \frac{1}{d}\left\|\partial_{\boldsymbol{z}}\boldsymbol{k}^{(i)}_{r,T}(\boldsymbol{z})\partial_{\boldsymbol{z}'}\boldsymbol{k}^{(i)}_{r,T}(\boldsymbol{z}')^\top\big|_{\boldsymbol{z}=\boldsymbol{z}'=\boldsymbol{x}}\right\|_{\text{tr}}\\ &\overset{(c)}{=} \frac{1}{d}\sum_{\tau=1}^{rT}4\iota^{(i)}_\tau\nabla k(\iota^{(i)}_\tau)^2\\ &\overset{(d)}{\geq} \frac{4rT}{d}\iota^{(i)}_r\nabla k(\iota^{(i)}_r)^2\end{aligned} \tag{46}$$

where (a) comes from the fact the maximum eigenvalue of a matrix is always larger or equal to its averaged eigenvalues and (b) is based on Lemma E.7. In addition, (c) is obtained from (45) while (d) results from the definition of $\iota^{(i)}_r \triangleq \frac{1}{rT}\sum_{\boldsymbol{x}^{(i)}_\tau\in\mathcal{D}^{(i)}_{r,T}}\left\|\boldsymbol{x}-\boldsymbol{x}^{(i)}_\tau\right\|^2$ as well as the Jansen's inequality for the convex function $h(\cdot)$.

Finally, by introducing the results above, i.e., (42) and (46), into (41), we have

$$\left\|\partial\left(\sigma^{(i)}_{r,T}\right)^2(\boldsymbol{x})\right\| \leq \kappa - \frac{4\iota^{(i)}_r\nabla k(\iota^{(i)}_r)^2}{k(0)d+\sigma^2 d/(rT)}\,. \tag{47}$$

Define $\iota_r \triangleq \frac{1}{N}\sum_{i=1}^N \iota^{(i)}_r$, we then have

$$\begin{aligned}\|\nabla\mu_r(\boldsymbol{x})-\nabla F(\boldsymbol{x})\|^2 &\overset{(a)}{=} \left\|\frac{1}{N}\sum_{i=1}^N\left(\nabla\mu^{(i)}_{r,T}(\boldsymbol{x})-\nabla f_i(\boldsymbol{x})\right)\right\|^2\\ &\overset{(b)}{\leq} \frac{1}{N}\sum_{i=1}^N\left\|\nabla\mu^{(i)}_{r,T}(\boldsymbol{x})-\nabla f_i(\boldsymbol{x})\right\|^2\\ &\overset{(c)}{\leq} \frac{1}{N}\sum_{i=1}^N \omega\kappa - \frac{4\omega\iota^{(i)}_r\nabla k(\iota^{(i)}_r)^2}{k(0)d+\sigma^2 d/(rT)}\\ &\overset{(d)}{\leq} \omega\kappa - \frac{4\omega\iota_r\nabla k(\iota_r)^2}{k(0)d+\sigma^2 d/(rT)}\end{aligned} \tag{48}$$

where (b) is from the Cauchy-Schwarz inequality, (c) derives from Lemma E.1, and (d) results from the Jansen's inequality for convex function $h(\cdot)$. which finally concludes the proof. □

Remark. Of note, the assumption that $k(\boldsymbol{x}, \boldsymbol{x}') = k(\|\boldsymbol{x} - \boldsymbol{x}'\|^2)$ where $k(\cdot)$ is non-increasing and function $h(\iota) = \iota \nabla k(\iota)^2$ is convex can be satisfied by the widely applied squared exponential kernel $k(\boldsymbol{x}, \boldsymbol{x}') = \exp\left(-\|\boldsymbol{x} - \boldsymbol{x}'\|^2 / (2l^2)\right)$, which has also been applied in our FZooS. To justify the validity of these assumptions on the squared exponential kernel, we first show that this kernel can be represented as $k(\iota) = \exp\left(-\iota/(2l^2)\right)$, which is non-increasing w.r.t. its input ι, and $h(\iota) = \iota \exp\left(-\iota/l^2\right)/(4l^4)$ is convex when $\iota \geq 2l^2$.

Remarkably, Prop. E.1 reveals that the quality of the gradient estimation at an input $\boldsymbol{x} \in \mathcal{X}$ when using our global gradient surrogate without RFF approximation is highly related to the averaged Euclidean distance between $\boldsymbol{x}$ and $\boldsymbol{x}_\tau \in \bigcup_{i=1}^N \mathcal{D}_{r,T}^{(i)}$ (i.e., ι_r in Prop. E.1). Specifically, when the input $\boldsymbol{x}$ to be evaluated in our global gradient surrogate leads to a larger value of $\iota_r \nabla k(\iota_r)^2$, the upper bound in our Prop. E.1 demonstrates that the gradient estimation error of our global gradient surrogate tends to be more accurate. Note that when the kernel is the squared exponential kernel, we have that $h(\iota) = \iota \nabla k(\iota)^2 = \iota \exp\left(-\iota/l^2\right)/(4l^4)$ decreases w.r.t. ι and that a smaller averaged Euclidean distance between $\boldsymbol{x}$ and $\boldsymbol{x}_\tau \in \bigcup_{i=1}^N \mathcal{D}_{r,T}^{(i)}$ likely enjoys a smaller gradient estimation error. This is intuitively aligned with the common practice that $\boldsymbol{x}_\tau \in \bigcup_{i=1}^N \mathcal{D}_{r,T}^{(i)}$ is more informative when it achieves a smaller averaged Euclidean distance with $\boldsymbol{x}$. Intuitively, when the iteration t of local updates is increased, the input $\boldsymbol{x}_{r,t-1}$ to be evaluated in our global gradient surrogate likely achieves a larger distance with the history of function queries $\bigcup_{i=1}^N \mathcal{D}_{r,T}^{(i)}$ and consequently the quality of our global gradient surrogate likely decays, which finally aligns with the phenomenon that we have mentioned at the beginning of this section.

More Practical Choice of $\gamma_{r,t-1}$. Finally, by introducing Prop. E.1 into the analysis in Appx. E.2, we achieve the following better-performing choice of gradient correction length $\gamma_{r,t-1}$:

Corollary E.1. *Based on our Prop. E.1, a better-performing choice choice of $\gamma_{r,t-1}$ should be*

$$\gamma_{r,t-1} = \frac{G}{G + 2\left(\omega\kappa - \frac{4\omega\iota_r \nabla k(\iota_r)^2}{k(0)d + \sigma^2 d/(rT)} + N\epsilon\right)}.$$

Cor. E.1 implies that $\gamma_{r,t-1}$ should decay w.r.t the iteration t of local updates if $\iota_r \nabla k(\iota_r)^2$ decreases w.r.t. t. Particularly, when $k(\boldsymbol{x}, \boldsymbol{x}') = \exp\left(-\|\boldsymbol{x} - \boldsymbol{x}'\|^2 / (2l^2)\right)$ and $\iota_r \nabla k(\iota_r)^2$ decreases at a rate of $\mathcal{O}(\frac{1}{t})$ for the iteration t of local updates, we then have that better-performing choice of $\gamma_{r,t-1}$ in Prop. E.1 has the form of $\gamma_{r,t-1} = \frac{G}{G + C_0 - C_1/t}$ for some constant $C_0 \geq C_1 > 0$. Since we usually have no prior knowledge of client heterogeneity G as well as the constants C_0, C_1, we commonly apply the approximated form of $\gamma_{r,t-1} = 1/t$, which will be widely applied in our experiments as shown in our Appx. G.

E.4. Convergence of Algo. 1

We first introduce the following lemmas that are inspired by the results in [8].

Lemma E.8. *For any α-strongly convex and β-smooth function f, and any $\boldsymbol{x}, \boldsymbol{y}, \boldsymbol{z}$ in the domain of f, we have*

$$\nabla f(\boldsymbol{x})^\top (\boldsymbol{y} - \boldsymbol{z}) \leq f(\boldsymbol{y}) - f(\boldsymbol{z}) - \alpha \|\boldsymbol{y} - \boldsymbol{z}\|^2/4 + \beta \|\boldsymbol{z} - \boldsymbol{x}\|^2$$

Proof. Since f is both α-strongly convex and β-smooth, we have that

$$\begin{aligned} f(\boldsymbol{z}) - f(\boldsymbol{x}) &\leq \nabla f(\boldsymbol{x})^\top (\boldsymbol{z} - \boldsymbol{x}) + \frac{\beta}{2} \|\boldsymbol{z} - \boldsymbol{x}\|^2 \\ f(\boldsymbol{y}) - f(\boldsymbol{x}) &\geq \nabla f(\boldsymbol{x})^\top (\boldsymbol{y} - \boldsymbol{x}) + \frac{\alpha}{2} \|\boldsymbol{y} - \boldsymbol{x}\|^2 \ . \end{aligned} \tag{49}$$

Note that when $\alpha = 0$, the inequalities above still hold. By aggregating the results above, we have

$$\begin{aligned} f(\boldsymbol{z}) - f(\boldsymbol{y}) &= f(\boldsymbol{z}) - f(\boldsymbol{x}) + f(\boldsymbol{x}) - f(\boldsymbol{y}) \\ &\leq \nabla f(\boldsymbol{x})^\top (\boldsymbol{z} - \boldsymbol{x}) + \nabla f(\boldsymbol{x})^\top (\boldsymbol{x} - \boldsymbol{y}) + \frac{\beta}{2} \|\boldsymbol{z} - \boldsymbol{x}\|^2 - \frac{\alpha}{2} \|\boldsymbol{y} - \boldsymbol{x}\|^2 \\ &\leq \nabla f(\boldsymbol{x})^\top (\boldsymbol{z} - \boldsymbol{y}) + \frac{\beta}{2} \|\boldsymbol{z} - \boldsymbol{x}\|^2 - \frac{\alpha}{4} \|\boldsymbol{y} - \boldsymbol{z}\|^2 + \frac{\alpha}{2} \|\boldsymbol{x} - \boldsymbol{z}\|^2 \\ &= \nabla f(\boldsymbol{x})^\top (\boldsymbol{z} - \boldsymbol{y}) + \frac{\beta + \alpha}{2} \|\boldsymbol{z} - \boldsymbol{x}\|^2 - \frac{\alpha}{4} \|\boldsymbol{y} - \boldsymbol{z}\|^2 \end{aligned} \tag{50}$$

where the second inequality comes from $\alpha \|\boldsymbol{y} - \boldsymbol{x}\|^2 /2 \geq \alpha \|\boldsymbol{y} - \boldsymbol{z}\|^2 /4 - \alpha \|\boldsymbol{x} - \boldsymbol{z}\|^2 /2$ (triangle inequality). When $\alpha > 0$, since $\beta > \alpha$, we have

$$f(\boldsymbol{z}) - f(\boldsymbol{y}) \leq \nabla f(\boldsymbol{x})^\top (\boldsymbol{z} - \boldsymbol{y}) + \beta \|\boldsymbol{z} - \boldsymbol{x}\|^2 - \frac{\alpha}{4} \|\boldsymbol{y} - \boldsymbol{z}\|^2 \ . \tag{51}$$

By rearranging the inequality above, we can directly derive the result in Lemma E.8 with $\alpha > 0$. Even when $\alpha = 0$, since $\|\boldsymbol{z} - \boldsymbol{x}\|^2 \geq 0$, we have

$$\begin{aligned} f(\boldsymbol{z}) - f(\boldsymbol{y}) &\leq \nabla f(\boldsymbol{x})^\top (\boldsymbol{z} - \boldsymbol{y}) + \frac{\beta}{2} \|\boldsymbol{z} - \boldsymbol{x}\|^2 \\ &\leq \nabla f(\boldsymbol{x})^\top (\boldsymbol{z} - \boldsymbol{y}) + \beta \|\boldsymbol{z} - \boldsymbol{x}\|^2 \ . \end{aligned} \tag{52}$$

By rearranging the inequality above, we show that the result in Lemma E.8 also holds for $\alpha = 0$. □

Lemma E.9. *For any β-smooth function f, inputs $\boldsymbol{x}, \boldsymbol{y}$ in the domain of f, the following holds for any $\eta > 0$*

$$\|\boldsymbol{x} - \eta \nabla f(\boldsymbol{x}) - \boldsymbol{y} + \eta \nabla f(\boldsymbol{y})\|^2 \leq (1 + \eta\beta)^2 \|\boldsymbol{x} - \boldsymbol{y}\|^2 \ .$$

Proof. Since f is β-smooth, we have

$$\begin{aligned} \|\boldsymbol{x} - \eta \nabla f(\boldsymbol{x}) - \boldsymbol{y} + \eta \nabla f(\boldsymbol{y})\|^2 &\leq \left(1 + \frac{1}{a}\right) \|\boldsymbol{x} - \boldsymbol{y}\|^2 + (1 + a)\, \eta^2 \|\nabla f(\boldsymbol{x}) - \nabla f(\boldsymbol{y})\|^2 \\ &\leq \left(1 + \frac{1}{a} + (1 + a)\, \eta^2 \beta^2\right) \|\boldsymbol{x} - \boldsymbol{y}\|^2 \end{aligned} \tag{53}$$

where the first inequality derives from Lemma E.5 and the second inequality comes from the smoothness of f. By choosing $a = 1/(\eta\beta)$, we conclude our proof. □

Remark. Lemma E.9 only requires the smoothness of function f. When f is both β-smooth and α-strongly convex ($\alpha > 0$), we will have a tighter bound as below when $\eta < \alpha/\beta^2$ (see proof below),

$$\|\boldsymbol{x} - \eta \nabla f(\boldsymbol{x}) - \boldsymbol{y} + \eta \nabla f(\boldsymbol{y})\|^2 \leq (1 - \eta\alpha) \|\boldsymbol{x} - \boldsymbol{y}\|^2 \ , \tag{54}$$

which can lead to a better convergence (by achieving a smaller constant term) compared with the inequality (62) we will prove later. However, for simplicity and consistency under various assumptions on the function to be optimized, we only use Lemma E.9 for the convergence analysis of our Thm. C.1 in the main paper.

Proof. Based on the strong convexity of f, for any inputs $\boldsymbol{x}, \boldsymbol{y}$ in the domain of f, we have

$$\begin{aligned} f(\boldsymbol{y}) - f(\boldsymbol{x}) &\geq \nabla f(\boldsymbol{x})^\top (\boldsymbol{y} - \boldsymbol{x}) + \frac{\alpha}{2} \|\boldsymbol{y} - \boldsymbol{x}\|^2 \ , \\ f(\boldsymbol{x}) - f(\boldsymbol{y}) &\geq \nabla f(\boldsymbol{y})^\top (\boldsymbol{x} - \boldsymbol{y}) + \frac{\alpha}{2} \|\boldsymbol{y} - \boldsymbol{x}\|^2 \ . \end{aligned} \tag{55}$$

By summing up these inequalities, we have

$$\left(\nabla f(\boldsymbol{y}) - \nabla f(\boldsymbol{x})\right)^\top (\boldsymbol{y} - \boldsymbol{x}) \geq \alpha \|\boldsymbol{y} - \boldsymbol{x}\|^2 \ . \tag{56}$$

Finally, we have

$$\begin{aligned} &\|\boldsymbol{x} - \eta \nabla f(\boldsymbol{x}) - \boldsymbol{y} + \eta \nabla f(\boldsymbol{y})\|^2 \\ \overset{(a)}{=} &\|\boldsymbol{x} - \boldsymbol{y}\|^2 + \eta^2 \|\nabla f(\boldsymbol{x}) - \nabla f(\boldsymbol{y})\|^2 - 2\eta \left(\nabla f(\boldsymbol{x}) - \nabla f(\boldsymbol{y})\right)^\top (\boldsymbol{x} - \boldsymbol{y}) \\ \overset{(b)}{\leq} &\|\boldsymbol{x} - \boldsymbol{y}\|^2 + \eta^2 \beta^2 \|\boldsymbol{x} - \boldsymbol{y}\|^2 - 2\eta\alpha \|\boldsymbol{x} - \boldsymbol{y}\|^2 \\ \overset{(c)}{=} &\left(1 + \eta^2\beta^2 - 2\eta\alpha\right) \|\boldsymbol{x} - \boldsymbol{y}\|^2 \end{aligned} \tag{57}$$

where (b) comes from the smoothness of f and (56). Since $\alpha > 0$, by introducing $\eta \leq \alpha/\beta^2$ into (57), we can complete our proof. □

Lemma E.10. *Let f be β-smooth and $\boldsymbol{x}^* = \arg\min f(\boldsymbol{x})$, then for any input $\boldsymbol{x}$ in the domain of f, the following holds*

$$\|\nabla f(\boldsymbol{x})\|^2 \leq 2\beta \left(f(\boldsymbol{x}) - f(\boldsymbol{x}^*)\right)$$

Proof. Since f is β-smooth, we have the following inequality for any x, y in the domain of f

$$f(\boldsymbol{y}) \leq f(\boldsymbol{x}) + \nabla f(\boldsymbol{x})^\top (\boldsymbol{y} - \boldsymbol{x}) + \frac{\beta}{2} \|\boldsymbol{y} - \boldsymbol{x}\|^2 \ . \tag{58}$$

By setting $\boldsymbol{y} = \boldsymbol{x} - \nabla f(\boldsymbol{x})/\beta$, we have

$$\begin{aligned} f(\boldsymbol{x}^*) &\leq f(\boldsymbol{x} - \frac{1}{\beta} \nabla f(\boldsymbol{x})) \\ &\leq f(\boldsymbol{x}) + \nabla f(\boldsymbol{x})^\top \left(\boldsymbol{x} - \frac{1}{\beta} \nabla f(\boldsymbol{x}) - \boldsymbol{x}\right) + \frac{\beta}{2} \left\| \boldsymbol{x} - \frac{1}{\beta} \nabla f(\boldsymbol{x}) - \boldsymbol{x} \right\|^2 \\ &= f(\boldsymbol{x}) - \frac{1}{2\beta} \|\nabla f(\boldsymbol{x})\|^2 \ . \end{aligned} \tag{59}$$

We finally conclude our proof by rearranging the inequality above. □

We then bound the drift between $\boldsymbol{x}_{r,t}^{(i)}$ and $\boldsymbol{x}_r$ for every iteration t of any round r as below, which is the key difference between the convergence of general federated ZOO and centralized optimization.

Lemma E.11. *Assume that F is β-smooth. Then the updated input $\boldsymbol{x}_{r,t}^{(i)}$ at any iteration $t \geq 1$ of round $r \geq 1$ on client i in Algo. 1 has the following bounded drift with $\eta \leq \frac{1}{\beta T}$*

$$\left\| \boldsymbol{x}_{r+1,t}^{(i)} - \boldsymbol{x}_r \right\|^2 \leq 2\eta^2 T \sum_{\tau=1}^{t} S^{t-\tau} \Xi_{r+1,\tau}^{(i)} + 22\eta^2 T^2 \|\nabla F(\boldsymbol{x}_r)\|^2$$

where $S \triangleq (T+1)^2/(T(T-1))$.

Proof. Since $\boldsymbol{x}_{r+1,t}^{(i)} = \boldsymbol{x}_{r+1,t-1}^{(i)} - \eta \widehat{\boldsymbol{g}}_{r+1,t-1}^{(i)}$, we have the following inequalities when $T > 1$

$$
\begin{aligned}
&\left\| \boldsymbol{x}_{r+1,t}^{(i)} - \boldsymbol{x}_r \right\|^2 \\
&\overset{(a)}{=} \left\| \boldsymbol{x}_{r+1,t-1}^{(i)} - \eta \widehat{\boldsymbol{g}}_{r+1,t-1}^{(i)} - \boldsymbol{x}_r \right\|^2 \\
&\overset{(b)}{=} \left\| \boldsymbol{x}_{r+1,t-1}^{(i)} - \eta \nabla F(\boldsymbol{x}_{r+1,t-1}^{(i)}) + \eta \nabla F(\boldsymbol{x}_r) - \boldsymbol{x}_r + \eta \left(\nabla F(\boldsymbol{x}_{r+1,t-1}^{(i)}) - \widehat{\boldsymbol{g}}_{r+1,t-1}^{(i)} - \nabla F(\boldsymbol{x}_r) \right) \right\|^2 \\
&\overset{(c)}{\leq} \frac{T}{T-1} \left\| \boldsymbol{x}_{r+1,t-1}^{(i)} - \eta \nabla F(\boldsymbol{x}_{r+1,t-1}^{(i)}) + \eta \nabla F(\boldsymbol{x}_r) - \boldsymbol{x}_r \right\|^2 \\
&\qquad\qquad + \eta^2 T \left\| \nabla F(\boldsymbol{x}_{r+1,t-1}^{(i)}) - \widehat{\boldsymbol{g}}_{r+1,t-1}^{(i)} - \nabla F(\boldsymbol{x}_r) \right\|^2 \\
&\overset{(d)}{\leq} \frac{T}{T-1} \left\| \boldsymbol{x}_{r+1,t-1}^{(i)} - \eta \nabla F(\boldsymbol{x}_{r+1,t-1}^{(i)}) + \eta \nabla F(\boldsymbol{x}_r) - \boldsymbol{x}_r \right\|^2 \\
&\qquad\qquad + 2\eta^2 T \left[\left\| \nabla F(\boldsymbol{x}_{r+1,t-1}^{(i)}) - \widehat{\boldsymbol{g}}_{r+1,t-1}^{(i)} \right\|^2 + \left\| \nabla F(\boldsymbol{x}_r) \right\|^2 \right]
\end{aligned}
\tag{60}
$$

where (c) and (d) come from the (28) in Lemma E.5 by setting $a = 1/(T-1)$ and $a = 1$, respectively. Since F is β-smooth, we can introduce Lemma E.9 into (60) to obtain the following result given the constant $S \triangleq (T+1)^2/(T(T-1))$

$$
\begin{aligned}
&\left\| \boldsymbol{x}_{r+1,t}^{(i)} - \boldsymbol{x}_r \right\|^2 \\
&\overset{(a)}{\leq} \frac{T(1+\eta\beta)^2}{T-1} \left\| \boldsymbol{x}_{r+1,t-1}^{(i)} - \boldsymbol{x}_r \right\|^2 + 2\eta^2 T \left[\left\| \nabla F(\boldsymbol{x}_{r+1,t-1}^{(i)}) - \widehat{\boldsymbol{g}}_{r+1,t-1}^{(i)} \right\|^2 + \left\| \nabla F(\boldsymbol{x}_r) \right\|^2 \right] \\
&\overset{(b)}{=} 2\eta^2 T \sum_{\tau=0}^{t-1} \left(\frac{T(1+\eta\beta)^2}{T-1} \right)^{t-\tau-1} \left\| \nabla F(\boldsymbol{x}_{r+1,\tau}^{(i)}) - \widehat{\boldsymbol{g}}_{r+1,\tau}^{(i)} \right\|^2 + 2\eta^2 T \left\| \nabla F(\boldsymbol{x}_r) \right\|^2 \sum_{\tau=0}^{t-1} \left(\frac{(1+\eta\beta)^2 T}{T-1} \right)^{\tau} \\
&\overset{(c)}{\leq} 2\eta^2 T \sum_{\tau=0}^{t-1} \left(\frac{(T+1)^2}{T(T-1)} \right)^{t-\tau-1} \left\| \nabla F(\boldsymbol{x}_{r+1,\tau}^{(i)}) - \widehat{\boldsymbol{g}}_{r+1,\tau}^{(i)} \right\|^2 + 2\eta^2 T \left\| \nabla F(\boldsymbol{x}_r) \right\|^2 \sum_{\tau=0}^{t-1} \left(\frac{(T+1)^2}{T(T-1)} \right)^{\tau} \\
&\overset{(d)}{\leq} 2\eta^2 T \sum_{\tau=0}^{t-1} S^{t-\tau-1} \left\| \nabla F(\boldsymbol{x}_{r+1,\tau}^{(i)}) - \widehat{\boldsymbol{g}}_{r+1,\tau}^{(i)} \right\|^2 + 22\eta^2 T^2 \left\| \nabla F(\boldsymbol{x}_r) \right\|^2 \\
&\overset{(e)}{=} 2\eta^2 T \sum_{\tau=1}^{t} S^{t-\tau} \Xi_{r+1,\tau}^{(i)} + 22\eta^2 T^2 \left\| \nabla F(\boldsymbol{x}_r) \right\|^2
\end{aligned}
\tag{61}
$$

where (b) comes from the summation of geometric series and (c) is from the fact that $\eta \leq 1/(\beta T)$. In addition, (d) results from the definition of S as well as the following results

$$
\begin{aligned}
\sum_{\tau=0}^{t-1} \left(\frac{(T+1)^2}{T(T-1)} \right)^{\tau} &\leq \sum_{\tau=0}^{T-1} \left(\frac{(T+1)^2}{T(T-1)} \right)^{\tau} \\
&= \frac{\left((T+1)^2/[T(T-1)] \right)^T - 1}{(T+1)^2/[T(T-1)] - 1} \\
&= \frac{T(T-1)}{3T+1} \left(\left(1 + \frac{3T+1}{T(T-1)} \right)^T - 1 \right) \\
&< \frac{T(T-1)}{3T+1} \left(\exp\left(\frac{3T+1}{T} \right) - 1 \right) \\
&< \frac{T}{3} \left(\exp\left(\frac{7}{2} \right) - 1 \right) \\
&< 11T \,.
\end{aligned}
\tag{62}
$$

Finally, (e) results from the definition of $\Xi_{r+1,t}^{(i)} \triangleq \left\|\widehat{\boldsymbol{g}}_{r+1,t-1} - \nabla F(\boldsymbol{x}_{r+1,t-1}^{(i)})\right\|^2$ in our Appx. B.2.

□

We finally present the convergence of Algo. 1 in the following theorem for the general federated ZOO framework, which then can be easily applied to prove the convergence of our FZooS in Appx. E.5 and the convergence of existing federated ZOO algorithms in Appx. F.

Theorem E.1. *Define* $\Xi_{r,t}^{(i)} \triangleq \sum_{t=1}^{T} \left\|\widehat{\boldsymbol{g}}_{r,t-1}^{(i)} - \nabla F(\boldsymbol{x}_{r,t-1}^{(i)})\right\|^2$, $S \triangleq (T+1)^2/(T(T-1))$, *and* $\boldsymbol{x}^* \triangleq \arg\min F(\boldsymbol{x})$. *Algo. 1 then has the following convergence when* F *is under different assumptions:*

(i) *When* F *is* β*-smooth and* α*-strongly convex, by defining* $p_r \triangleq \frac{(1-\alpha\eta T/4)^{R-r}}{\sum_{r=0}^{R}(1-\alpha\eta T/4)^{R-r}}$ *and choosing a constant learning rate* $\eta \leq \frac{1}{10\beta T}$,

$$\min_{r\in[R+1)} F(\boldsymbol{x}_r) - F(\boldsymbol{x}^*) \leq 2\alpha \exp\left(-\frac{\alpha\eta TR}{4}\right) \|\boldsymbol{x}_0 - \boldsymbol{x}^*\|^2 + \sum_{r=0}^{R}\sum_{i=1}^{N}\sum_{t=1}^{T} p_r \left(\frac{\eta}{NT}\sum_{\tau=1}^{t} S^{t-\tau}\Xi_{r+1,\tau}^{(i)} + \frac{8(\eta T + 1/\alpha)}{\alpha NT}\Xi_{r+1,t}^{(i)}\right) .$$

(ii) *When* F *is* β*-smooth and convex, by choosing a constant learning rate* $\eta \leq \frac{1}{10\beta T}$,

$$\min_{r\in[R+1)} F(\boldsymbol{x}_r) - F(\boldsymbol{x}^*) \leq \frac{2\|\boldsymbol{x}_0 - \boldsymbol{x}^*\|^2}{\eta RT} + \frac{1}{R}\sum_{r=0}^{R}\sum_{i=1}^{N}\sum_{t=1}^{T}\left(\frac{\eta}{NT}\sum_{\tau=1}^{t} S^{t-\tau}\Xi_{r+1,\tau}^{(i)} + \frac{8\eta}{N}\Xi_{r+1,t}^{(i)} + \frac{4\sqrt{d}}{NT}\sqrt{\Xi_{r+1,t}^{(i)}}\right) .$$

(iii) *When* F *is only* β*-smooth, by choosing a constant learning rate* $\eta \leq \frac{7}{100\beta T}$,

$$\min_{r\in[R+1)} \|\nabla F(\boldsymbol{x}_r)\|^2 \leq \frac{13(F(\boldsymbol{x}_0) - F(\boldsymbol{x}^*))}{\eta RT} + \frac{13}{\eta RT}\sum_{r=0}^{R}\sum_{i=1}^{N}\sum_{t=1}^{T}\left(\frac{(0.14\eta + 1/(2\beta T))}{N}\Xi_{r+1,t}^{(i)} + \frac{1.02\eta^2\beta}{N}\sum_{\tau=1}^{t} S^{t-\tau}\Xi_{r+1,\tau}^{(i)}\right) .$$

Proof. Recall that the global update on server in Algo. 1 is given as

$$\boldsymbol{x}_{r+1} = \frac{1}{N}\sum_{i=1}^{N}\boldsymbol{x}_{r+1}^{(i)} = \frac{1}{N}\sum_{i=1}^{N}\left(\boldsymbol{x}_r^{(i)} - \eta\sum_{t=1}^{T}\widehat{\boldsymbol{g}}_{r+1,t-1}^{(i)}\right) = \boldsymbol{x}_r - \frac{\eta}{N}\sum_{i=1}^{N}\sum_{t=1}^{T}\widehat{\boldsymbol{g}}_{r+1,t-1}^{(i)} . \tag{63}$$

Therefore, we have

$$\begin{aligned}\|\boldsymbol{x}_{r+1} - \boldsymbol{x}^*\|^2 &= \left\|\boldsymbol{x}_r - \frac{\eta}{N}\sum_{i=1}^{N}\sum_{t=1}^{T}\widehat{\boldsymbol{g}}_{r+1,t-1}^{(i)} - \boldsymbol{x}^*\right\|^2 \\ &= \|\boldsymbol{x}_r - \boldsymbol{x}^*\|^2 \underbrace{-2\left(\boldsymbol{x}_r - \boldsymbol{x}^*\right)^\top \frac{\eta}{N}\sum_{i=1}^{N}\sum_{t=1}^{T}\widehat{\boldsymbol{g}}_{r+1,t-1}^{(i)}}_{①} + \underbrace{\left\|\frac{\eta}{N}\sum_{i=1}^{N}\sum_{t=1}^{T}\widehat{\boldsymbol{g}}_{r+1,t-1}^{(i)}\right\|^2}_{②} .\end{aligned} \tag{64}$$

We then bound ① and ② based on the different assumptions on F separately.

Strongly Convex F. Since F is β-smooth and α-strongly convex, we have

$$
\begin{aligned}
① &\overset{(a)}{=} 2\left(\boldsymbol{x}^* - \boldsymbol{x}_r\right)^\top \frac{\eta}{N}\sum_{i=1}^{N}\sum_{t=1}^{T}\left(\widehat{\boldsymbol{g}}_{r+1,t-1}^{(i)} - \nabla F(\boldsymbol{x}_{r+1,t-1}^{(i)})\right) + 2\left(\boldsymbol{x}^* - \boldsymbol{x}_r\right)^\top \frac{\eta}{N}\sum_{i=1}^{N}\sum_{t=1}^{T}\nabla F(\boldsymbol{x}_{r+1,t-1}^{(i)}) \\
&\overset{(b)}{\le} 2\left\|\boldsymbol{x}^* - \boldsymbol{x}_r\right\| \frac{\eta}{N}\sum_{i=1}^{N}\sum_{t=1}^{T}\left\|\widehat{\boldsymbol{g}}_{r+1,t-1}^{(i)} - \nabla F(\boldsymbol{x}_{r+1,t-1}^{(i)})\right\| \\
&\qquad + \frac{2\eta}{N}\sum_{i=1}^{N}\sum_{t=1}^{T}\left[F(\boldsymbol{x}^*) - F(\boldsymbol{x}_r) - \frac{\alpha}{4}\left\|\boldsymbol{x}_r - \boldsymbol{x}^*\right\|^2 + \beta\left\|\boldsymbol{x}_{r,t-1}^{(i)} - \boldsymbol{x}_r\right\|^2\right] \\
&\overset{(c)}{\le} \frac{2\eta}{N}\left\|\boldsymbol{x}^* - \boldsymbol{x}_r\right\|\sum_{i=1}^{N}\sum_{t=1}^{T}\sqrt{\Xi_{r+1,t}^{(i)}} + 2\eta T\big[F(\boldsymbol{x}^*) - F(\boldsymbol{x}_r)\big] - \frac{\alpha\eta T}{2}\left\|\boldsymbol{x}_r - \boldsymbol{x}^*\right\|^2 \\
&\qquad + \frac{4\eta^3 T\beta}{N}\sum_{i=1}^{N}\sum_{t=1}^{T}\sum_{\tau=1}^{t} S^{t-\tau}\Xi_{r+1,\tau}^{(i)} + 44\eta^3 T^3\beta\left\|\nabla F(\boldsymbol{x}_r)\right\|^2 \\
&\overset{(d)}{\le} -\frac{\alpha\eta T}{4}\left\|\boldsymbol{x}^* - \boldsymbol{x}_r\right\|^2 + 2\eta T\big[F(\boldsymbol{x}^*) - F(\boldsymbol{x}_r)\big] + 44\eta^3 T^3\beta\left\|\nabla F(\boldsymbol{x}_r)\right\|^2 + \\
&\qquad \sum_{i=1}^{N}\sum_{t=1}^{T}\left(\frac{4\eta^3 T\beta}{N}\sum_{\tau=1}^{t} S^{t-\tau}\Xi_{r+1,\tau}^{(i)} + \frac{4\eta}{\alpha N}\Xi_{r+1,t}^{(i)}\right).
\end{aligned} \tag{65}
$$

where (b) is from Lemma E.8 by setting $\boldsymbol{y} = \boldsymbol{x}^*$, $\boldsymbol{z} = \boldsymbol{x}_r$ and $\boldsymbol{x} = \boldsymbol{x}_{r,t-1}^{(i)}$ in Lemma E.8. In addition, (c) comes from the definition of $\Xi_{r+1,t}^{(i)} \triangleq \left\|\widehat{\boldsymbol{g}}_{r+1,t-1} - \nabla F(\boldsymbol{x}_{r+1,t-1}^{(i)})\right\|^2$ in our Appx. B.2 and Lemma E.11. Finally, (d) comes from the following results

$$
\begin{aligned}
\frac{2\eta}{N}\left\|\boldsymbol{x}^* - \boldsymbol{x}_r\right\|\sum_{i=1}^{N}\sum_{t=1}^{T}\sqrt{\Xi_{r+1,t}^{(i)}} &= \frac{2\eta}{N}\sum_{i=1}^{N}\sum_{t=1}^{T}\left\|\boldsymbol{x}^* - \boldsymbol{x}_r\right\|\sqrt{\Xi_{r+1,t}^{(i)}} \\
&\le \frac{\eta}{N}\sum_{i=1}^{N}\sum_{t=1}^{T}\left(\frac{\alpha}{4}\left\|\boldsymbol{x}^* - \boldsymbol{x}_r\right\|^2 + \frac{4}{\alpha}\Xi_{r+1,t}^{(i)}\right) \\
&= \frac{\alpha\eta T}{4}\left\|\boldsymbol{x}^* - \boldsymbol{x}_r\right\|^2 + \frac{4\eta}{\alpha N}\sum_{i=1}^{N}\sum_{t=1}^{T}\Xi_{r+1,t}^{(i)}.
\end{aligned} \tag{66}
$$

We then bound term ② in (64) as below

$$
\begin{aligned}
② &\overset{(a)}{=} \left\|\frac{\eta}{N}\sum_{i=1}^{N}\sum_{t=1}^{T}\widehat{\boldsymbol{g}}_{r+1,t-1}^{(i)}\right\|^2 \\
&\overset{(b)}{=} \left\|\frac{\eta}{N}\sum_{i=1}^{N}\sum_{t=1}^{T}\left(\widehat{\boldsymbol{g}}_{r+1,t-1}^{(i)} - \nabla F(\boldsymbol{x}_{r+1,t-1}^{(i)}) + \nabla F(\boldsymbol{x}_{r+1,t-1}^{(i)}) - \nabla F(\boldsymbol{x}_r)\right) + \eta T\nabla F(\boldsymbol{x}_r)\right\|^2 \\
&\overset{(c)}{\le} \frac{2\eta^2 T}{N}\sum_{i=1}^{N}\sum_{t=1}^{T}\left(2\left\|\widehat{\boldsymbol{g}}_{r+1,t-1}^{(i)} - \nabla F(\boldsymbol{x}_{r+1,t-1}^{(i)})\right\|^2 + 2\left\|\nabla F(\boldsymbol{x}_{r+1,t-1}^{(i)}) - \nabla F(\boldsymbol{x}_r)\right\|^2\right) + \\
&\qquad 2\eta^2 T^2\left\|\nabla F(\boldsymbol{x}_r)\right\|^2 \\
&\overset{(d)}{\le} \frac{4\eta^2 T}{N}\sum_{i=1}^{N}\sum_{t=1}^{T}\Xi_{r+1,t}^{(i)} + \frac{4\eta^2 T\beta^2}{N}\sum_{i=1}^{N}\sum_{t=1}^{T}\left\|\boldsymbol{x}_{r+1,t-1}^{(i)} - \boldsymbol{x}_r\right\|^2 + 2\eta^2 T^2\left\|\nabla F(\boldsymbol{x}_r)\right\|^2 \\
&\overset{(e)}{\le} \sum_{i=1}^{N}\sum_{t=1}^{T}\left(\frac{8\eta^4 T^2\beta^2}{N}\sum_{\tau=1}^{t} S^{t-\tau}\Xi_{r+1,\tau}^{(i)} + \frac{4\eta^2 T}{N}\Xi_{r+1,t}^{(i)}\right) + \left(88\eta^4 T^4\beta^2 + 2\eta^2 T^2\right)\left\|\nabla F(\boldsymbol{x}_r)\right\|^2
\end{aligned} \tag{67}
$$

where (c) is obtained by applying Lemma E.5 multiple times and (d) is from the smoothness of F. Besides, (e) comes from our Lemma E.11 and the fact that $\eta \le 1/(\beta T)$.

By combining (65) and (67), we have

$$
\begin{aligned}
&\left\|\boldsymbol{x}_{R+1}-\boldsymbol{x}^*\right\|^2 \\
&\overset{(a)}{\leq}\left(1-\frac{\alpha\eta T}{4}\right)\left\|\boldsymbol{x}_R-\boldsymbol{x}^*\right\|^2+2\eta T\big[F(\boldsymbol{x}^*)-F(\boldsymbol{x}_R)\big] \\
&\quad+2\eta^2T^2\left(44\eta^2T^2\beta^2+22\eta T\beta+1\right)\left\|\nabla F(\boldsymbol{x}_R)\right\|^2 \\
&\quad+\sum_{i=1}^{N}\sum_{t=1}^{T}\left(\frac{4\eta^3T\beta(2\eta T\beta+1)}{N}\sum_{\tau=1}^{t}S^{t-\tau}\Xi_{R+1,\tau}^{(i)}+\frac{4\eta(\eta T+1/\alpha)}{\alpha N}\Xi_{R+1,t}^{(i)}\right) \\
&\overset{(b)}{\leq}\left(1-\frac{\alpha\eta T}{4}\right)\left\|\boldsymbol{x}_R-\boldsymbol{x}^*\right\|^2+2\eta T\left(1-2\eta T\beta\left(44\eta^2T^2\beta^2+22\eta T\beta+1\right)\right)\big[F(\boldsymbol{x}^*)-F(\boldsymbol{x}_R)\big] \\
&\quad+\sum_{i=1}^{N}\sum_{t=1}^{T}\left(\frac{4\eta^3T\beta(2\eta T\beta+1)}{N}\sum_{\tau=1}^{t}S^{t-\tau}\Xi_{r+1,\tau}^{(i)}+\frac{4\eta(\eta T+1/\alpha)}{\alpha N}\Xi_{r+1,t}^{(i)}\right) \\
&\overset{(c)}{=}\left(1-\frac{\alpha\eta T}{4}\right)^{R+1}\left\|\boldsymbol{x}_0-\boldsymbol{x}^*\right\|^2+\sum_{r=0}^{R}\left(1-\frac{\alpha\eta T}{4}\right)^{R-r}H\big[F(\boldsymbol{x}^*)-F(\boldsymbol{x}_r)\big] \\
&\quad+\sum_{r=0}^{R}\left(1-\frac{\alpha\eta T}{4}\right)^{R-r}\sum_{i=1}^{N}\sum_{t=1}^{T}\left(\frac{4\eta^3T\beta(2\eta T\beta+1)}{N}\sum_{\tau=1}^{t}S^{t-\tau}\Xi_{r+1,\tau}^{(i)}+\frac{4\eta(\eta T+1/\alpha)}{\alpha N}\Xi_{r+1,t}^{(i)}\right)
\end{aligned}
\tag{68}
$$

where (b) is from Lemma E.10 and (c) is from $H\triangleq 2\eta T\left(1-2\eta T\beta\left(44\eta^2T^2\beta^2+22\eta T\beta+1\right)\right)$ as well as the repeated application of (b).

Define $p_r\triangleq\frac{(1-\alpha\eta T/4)^{R-r}}{\sum_{r=0}^{R}(1-\alpha\eta T/4)^{R-r}}$. Note that when choose the learning rate η that satisfies $\eta\leq\frac{1}{10\beta T}$, we have $H\geq 0.544\,\eta T$. Based on this and $\left\|\boldsymbol{x}_{R+1}-\boldsymbol{x}^*\right\|^2\geq 0$ for (68), we further have

$$
\begin{aligned}
\min_{r\in[R+1)}F(\boldsymbol{x}_r)-F(\boldsymbol{x}^*)&\overset{(a)}{\leq}\sum_{r=0}^{R}p_r\big[F(\boldsymbol{x}_r)-F(\boldsymbol{x}^*)\big] \\
&\overset{(b)}{\leq}\frac{\left(1-\alpha\eta T/4\right)^{R+1}\left\|\boldsymbol{x}_0-\boldsymbol{x}^*\right\|^2}{H\sum_{r=0}^{R}\left(1-\alpha\eta T/4\right)^{r}} \\
&\quad+\frac{1}{H}\sum_{r=0}^{R}\sum_{i=1}^{N}\sum_{t=1}^{T}p_r\left(\frac{\eta^2}{2N}\sum_{\tau=1}^{t}S^{t-\tau}\Xi_{r+1,\tau}^{(i)}+\frac{4\eta(\eta T+1/\alpha)}{\alpha N}\Xi_{r+1,t}^{(i)}\right) \\
&\overset{(c)}{\leq}\frac{\alpha\eta T}{H}\exp\left(-\frac{\alpha\eta TR}{4}\right)\left\|\boldsymbol{x}_0-\boldsymbol{x}^*\right\|^2 \\
&\quad+\frac{1}{H}\sum_{r=0}^{R}\sum_{i=1}^{N}\sum_{t=1}^{T}p_r\left(\frac{\eta^2}{2N}\sum_{\tau=1}^{t}S^{t-\tau}\Xi_{r+1,\tau}^{(i)}+\frac{4\eta(\eta T+1/\alpha)}{\alpha N}\Xi_{r+1,t}^{(i)}\right) \\
&\overset{(d)}{\leq}2\alpha\exp\left(-\frac{\alpha\eta TR}{4}\right)\left\|\boldsymbol{x}_0-\boldsymbol{x}^*\right\|^2 \\
&\quad+\sum_{r=0}^{R}\sum_{i=1}^{N}\sum_{t=1}^{T}p_r\left(\frac{\eta}{NT}\sum_{\tau=1}^{t}S^{t-\tau}\Xi_{r+1,\tau}^{(i)}+\frac{8(\eta T+1/\alpha)}{\alpha NT}\Xi_{r+1,t}^{(i)}\right)
\end{aligned}
\tag{69}
$$

where (b) is from the rearrangement of (68) and the fact that $\eta\leq\frac{1}{10\beta T}$. Besides, (c) comes from the inequality $1-x\leq$

$\exp(-x)$ as well as the following results when $R+1 \geq 4\ln(3/4)/(\alpha\eta T)$

$$\begin{aligned}\sum_{r=0}^{R}\left(1-\frac{\alpha\eta T}{4}\right)^{r} &= \frac{1-(1-\alpha\eta T/4)^{R+1}}{1-(1-\alpha\eta T/4)} \\ &\geq \frac{4\left[1-\exp(-\alpha\eta T(R+1)/4)\right]}{\alpha\eta T} \\ &\geq \frac{1}{\alpha\eta T}\,.\end{aligned} \tag{70}$$

Finally, (d) is due to the fact that $H \geq 0.544\,\eta T$.

Convex F. When $\alpha = 0$, following the derivation in (65), we have

$$\begin{aligned}① &\overset{(a)}{\leq} \frac{2\eta}{N}\left\|\boldsymbol{x}^* - \boldsymbol{x}_r\right\| \sum_{i=1}^{N}\sum_{t=1}^{T}\sqrt{\Xi_{r+1,t}^{(i)}} + 2\eta T\left[F(\boldsymbol{x}^*) - F(\boldsymbol{x}_r)\right] + 44\eta^3T^3\beta\left\|\nabla F(\boldsymbol{x}_r)\right\|^2 \\ &\qquad + \frac{4\eta^3T\beta}{N}\sum_{i=1}^{N}\sum_{t=1}^{T}\sum_{\tau=1}^{t} S^{t-\tau}\Xi_{r+1,\tau}^{(i)} \\ &\overset{(b)}{\leq} \frac{2\eta\sqrt{d}}{N}\sum_{i=1}^{N}\sum_{t=1}^{T}\sqrt{\Xi_{r+1,t}^{(i)}} + 2\eta T\left[F(\boldsymbol{x}^*) - F(\boldsymbol{x}_r)\right] + 44\eta^3T^3\beta\left\|\nabla F(\boldsymbol{x}_r)\right\|^2 \\ &\qquad + \frac{4\eta^3T\beta}{N}\sum_{i=1}^{N}\sum_{t=1}^{T}\sum_{\tau=1}^{t} S^{t-\tau}\Xi_{r+1,\tau}^{(i)} \\ &\overset{(c)}{=} 2\eta T\left[F(\boldsymbol{x}^*) - F(\boldsymbol{x}_r)\right] + 44\eta^3T^3\beta\left\|\nabla F(\boldsymbol{x}_r)\right\|^2 \\ &\qquad + \sum_{i=1}^{N}\sum_{t=1}^{T}\left(\frac{4\eta^3T\beta}{N}\sum_{\tau=1}^{t} S^{t-\tau}\Xi_{r+1,\tau}^{(i)} + \frac{2\eta\sqrt{d}}{N}\sqrt{\Xi_{r+1,t}^{(i)}}\right)\end{aligned} \tag{71}$$

where the (b) comes from the diameter of $\mathcal{X}$, i.e., $\|\boldsymbol{x}-\boldsymbol{x}'\| \leq \sqrt{d}$ for any $\boldsymbol{x}, \boldsymbol{x}' \in \mathcal{X} = [0,1]^d$.

For term ② in (64), similar to (67), we also have

$$② \leq \sum_{i=1}^{N}\sum_{t=1}^{T}\left(\frac{8\eta^4T^2\beta^2}{N}\sum_{\tau=1}^{t} S^{t-\tau}\Xi_{r+1,\tau}^{(i)} + \frac{4\eta^2T}{N}\Xi_{r+1,t}^{(i)}\right) + \left(88\eta^4T^4\beta^2 + 2\eta^2T^2\right)\left\|\nabla F(\boldsymbol{x}_r)\right\|^2\,. \tag{72}$$

By combining (71) and (72), we have

$$\begin{aligned}&\left\|\boldsymbol{x}_{R+1} - \boldsymbol{x}^*\right\|^2 \\ &\overset{(a)}{\leq} \left\|\boldsymbol{x}_R - \boldsymbol{x}^*\right\|^2 + 2\eta T\left(1 - 2\eta T\beta\left(44\eta^2T^2\beta^2 + 22\eta T\beta + 1\right)\right)\left[F(\boldsymbol{x}^*) - F(\boldsymbol{x}_R)\right] \\ &\qquad + \sum_{i=1}^{N}\sum_{t=1}^{T}\left(\frac{4\eta^3T\beta(2\eta T\beta+1)}{N}\sum_{\tau=1}^{t} S^{t-\tau}\Xi_{R+1,\tau}^{(i)} + \frac{4\eta^2T}{N}\Xi_{R+1,t}^{(i)} + \frac{2\eta\sqrt{d}}{N}\sqrt{\Xi_{R+1,t}^{(i)}}\right) \\ &\overset{(b)}{\leq} \left\|\boldsymbol{x}_0 - \boldsymbol{x}^*\right\|^2 + \sum_{r=0}^{R} H\left[F(\boldsymbol{x}^*) - F(\boldsymbol{x}_r)\right] \\ &\qquad + \sum_{i=1}^{N}\sum_{t=1}^{T}\left(\frac{4\eta^3T\beta(2\eta T\beta+1)}{N}\sum_{\tau=1}^{t} S^{t-\tau}\Xi_{r+1,\tau}^{(i)} + \frac{4\eta^2T}{N}\Xi_{r+1,t}^{(i)} + \frac{2\eta\sqrt{d}}{N}\sqrt{\Xi_{r+1,t}^{(i)}}\right)\end{aligned} \tag{73}$$

where (a) is from Lemma E.10 and (b) is from $H \triangleq 2\eta T\left(1 - 2\eta T\beta\left(44\eta^2T^2\beta^2 + 22\eta T\beta + 1\right)\right)$ as well as the repeated application of (a).

Note that when choose the learning rate η that satisfies $\eta \leq \frac{1}{10\beta T}$, we have $H \geq 0.544\,\eta T$. Based on this and $\|\boldsymbol{x}_{R+1} - \boldsymbol{x}^*\|^2 \geq 0$ for (73), we further have

$$\begin{aligned}
\min_{r\in[R+1)} F(\boldsymbol{x}_r) - F(\boldsymbol{x}^*) &\overset{(a)}{\leq} \frac{1}{R}\sum_{r=0}^{R}\left[F(\boldsymbol{x}_r) - F(\boldsymbol{x}^*)\right] \\
&\overset{(b)}{\leq} \frac{\|\boldsymbol{x}_0 - \boldsymbol{x}^*\|^2}{RH} + \frac{1}{RH}\sum_{r=0}^{R}\sum_{i=1}^{N}\sum_{t=1}^{T}\left(\frac{\eta^2}{2N}\sum_{\tau=1}^{t} S^{t-\tau}\Xi_{r+1,\tau}^{(i)}\right. \\
&\qquad \left. + \frac{4\eta^2 T}{N}\Xi_{r+1,t}^{(i)} + \frac{2\eta\sqrt{d}}{N}\sqrt{\Xi_{r+1,t}^{(i)}}\right) \\
&\overset{(c)}{\leq} \frac{2\|\boldsymbol{x}_0 - \boldsymbol{x}^*\|^2}{\eta R} + \frac{1}{R}\sum_{r=0}^{R}\sum_{i=1}^{N}\sum_{t=1}^{T}\left(\frac{\eta}{NT}\sum_{\tau=1}^{t} S^{t-\tau}\Xi_{r+1,\tau}^{(i)}\right. \\
&\qquad \left. + \frac{8\eta}{N}\Xi_{r+1,t}^{(i)} + \frac{4\sqrt{d}}{NT}\sqrt{\Xi_{r+1,t}^{(i)}}\right)
\end{aligned} \tag{74}$$

where (c) is due to the fact that $H \geq 0.544\,\eta T$.

Non-Convex F. When F is only β-smooth, we have

$$\begin{aligned}
&F(\boldsymbol{x}_{r+1}) - F(\boldsymbol{x}_r) \\
&\overset{(a)}{\leq} \nabla F(\boldsymbol{x}_r)^\top(\boldsymbol{x}_{r+1} - \boldsymbol{x}_r) + \frac{\beta}{2}\|\boldsymbol{x}_{r+1} - \boldsymbol{x}_r\|^2 \\
&\overset{(b)}{=} -\frac{\eta}{N}\nabla F(\boldsymbol{x}_r)^\top\sum_{i=1}^{N}\sum_{t=1}^{T}\widehat{\boldsymbol{g}}_{r+1,t-1}^{(i)} + \frac{\beta}{2}\left\|\frac{\eta}{N}\sum_{i=1}^{N}\sum_{t=1}^{T}\widehat{\boldsymbol{g}}_{r+1,t-1}^{(i)}\right\|^2 \\
&\overset{(c)}{\leq} -\frac{\eta}{N}\nabla F(\boldsymbol{x}_r)^\top\sum_{i=1}^{N}\sum_{t=1}^{T}\left(\widehat{\boldsymbol{g}}_{r+1,t-1}^{(i)} - \nabla F(\boldsymbol{x}_{r+1,t-1}^{(i)}) + \nabla F(\boldsymbol{x}_{r+1,t-1}^{(i)}) - \nabla F(\boldsymbol{x}_r) + \nabla F(\boldsymbol{x}_r)\right) \\
&\qquad + \frac{\beta}{2}\left[\sum_{i=1}^{N}\sum_{t=1}^{T}\left(\frac{8\eta^4T^2\beta^2}{N}\sum_{\tau=1}^{t}S^{t-\tau}\Xi_{r+1,\tau}^{(i)} + \frac{4\eta^2T}{N}\Xi_{r+1,t}^{(i)}\right) + \left(88\eta^4T^4\beta^2 + 2\eta^2T^2\right)\|\nabla F(\boldsymbol{x}_r)\|^2\right] \\
&\overset{(d)}{\leq} \frac{\eta}{N}\sum_{i=1}^{N}\sum_{t=1}^{T}\|\nabla F(\boldsymbol{x}_r)\|\left(\left\|\widehat{\boldsymbol{g}}_{r+1,t-1}^{(i)} - \nabla F(\boldsymbol{x}_{r+1,t-1}^{(i)})\right\| + \left\|\nabla F(\boldsymbol{x}_{r+1,t-1}^{(i)}) - \nabla F(\boldsymbol{x}_r)\right\|\right) \\
&\qquad + \sum_{i=1}^{N}\sum_{t=1}^{T}\left(\frac{4\eta^4T^2\beta^3}{N}\sum_{\tau=1}^{t}S^{t-\tau}\Xi_{r+1,\tau}^{(i)} + \frac{2\eta^2\beta T}{N}\Xi_{r+1,t}^{(i)}\right) + \left(44\eta^4T^4\beta^3 + \eta^2T^2\beta - \eta T\right)\|\nabla F(\boldsymbol{x}_r)\|^2 \\
&\overset{(e)}{\leq} \frac{\eta}{N}\sum_{i=1}^{N}\sum_{t=1}^{T}\left(\eta\beta T\|\nabla F(\boldsymbol{x}_r)\|^2 + \frac{1}{2\eta\beta T}\left\|\widehat{\boldsymbol{g}}_{r+1,t-1}^{(i)} - \nabla F(\boldsymbol{x}_{r+1,t-1}^{(i)})\right\|^2 + \frac{\beta}{2\eta T}\left\|\boldsymbol{x}_{r+1,t-1}^{(i)} - \boldsymbol{x}_r\right\|^2\right) + \\
&\qquad + \sum_{i=1}^{N}\sum_{t=1}^{T}\left(\frac{4\eta^4T^2\beta^3}{N}\sum_{\tau=1}^{t}S^{t-\tau}\Xi_{r+1,\tau}^{(i)} + \frac{2\eta^2\beta T}{N}\Xi_{r+1,t}^{(i)}\right) + \left(44\eta^4T^4\beta^3 + \eta^2T^2\beta - \eta T\right)\|\nabla F(\boldsymbol{x}_r)\|^2 \\
&\overset{(f)}{\leq} \left(44\eta^4T^4\beta^3 + 13\eta^2T^2\beta - \eta T\right)\|\nabla F(\boldsymbol{x}_r)\|^2 + \sum_{i=1}^{N}\sum_{t=1}^{T}\left(\frac{\left(4\eta^4T^2\beta^3 + \eta^2\beta\right)}{N}\sum_{\tau=1}^{t}S^{t-\tau}\Xi_{r+1,\tau}^{(i)}\right. \\
&\qquad \left. + \frac{\left(2\eta^2\beta T + 1/(2\beta T)\right)}{N}\Xi_{r+1,t}^{(i)}\right)
\end{aligned} \tag{75}$$

where (a) comes from the smoothness of F and (b) is from the one-round update (63) for input $\boldsymbol{x}$. In addition, (c) derives from (67) and (e) results from (27) in Lemma E.5 by setting $a = \eta\beta T$ in (27). Finally, (f) comes from Lemma E.11.

Define $H \triangleq \eta T - 44\eta^4 T^4 \beta^3 - 13\eta^2 T^2 \beta$ and choose $\eta \leq \frac{7}{100\beta T}$, we have that $H > 0.08\eta T$. Based on this, we further have

$$\begin{aligned}
\min_{r\in[R+1)} \|\nabla F(\boldsymbol{x}_r)\|^2 &\overset{(a)}{\leq} \frac{1}{R}\sum_{r=0}^{R} \|\nabla F(\boldsymbol{x}_r)\|^2 \\
&\overset{(b)}{\leq} \frac{1}{RH}\sum_{r=0}^{R}\big[F(\boldsymbol{x}_r) - F(\boldsymbol{x}_{r+1})\big] + \frac{1}{RH}\sum_{r=0}^{R}\sum_{i=1}^{N}\sum_{t=1}^{T}\Bigg(\frac{\big(2\eta^2\beta T + 1/(2\beta T)\big)}{N}\Xi_{r+1,t}^{(i)} \\
&\qquad + \frac{\big(4\eta^4 T^2\beta^3 + \eta^2\beta\big)}{N}\sum_{\tau=1}^{t} S^{t-\tau}\Xi_{r+1,\tau}^{(i)}\Bigg) \\
&\overset{(c)}{\leq} \frac{13(F(\boldsymbol{x}_0) - F(\boldsymbol{x}^*))}{\eta RT} + \frac{13}{\eta RT}\sum_{r=0}^{R}\sum_{i=1}^{N}\sum_{t=1}^{T}\Bigg(\frac{(0.14\eta + 1/(2\beta T))}{N}\Xi_{r+1,t}^{(i)} \\
&\qquad + \frac{1.02\eta^2\beta}{N}\sum_{\tau=1}^{t} S^{t-\tau}\Xi_{r+1,\tau}^{(i)}\Bigg)
\end{aligned} \tag{76}$$

where (c) is due to the fact that $H \geq 0.08\,\eta T$. □

Remark. Of note, Thm. E.1 has presented the convergence of the general optimization framework for federated ZOO problems (i.e., Algo. 1). So, it can be easily adapted to provide the convergence for those algorithms that follow this optimization framework (e.g., our Thm. C.1 and the results in Appx. F). This advancement demonstrates superiority over existing federated optimization approaches, such as FedZO, FedProx, and SCAFFOLD, in terms of universality. Notably, these prior works primarily focus on providing convergence guarantees exclusively for their specific algorithmic designs.

E.5. Proof of Theorem C.1

To establish the proof for Thm. C.1, we introduce the upper bound of gradient disparity $\frac{1}{N}\sum_{i=1}^{N}\Xi_{r,t}^{(i)}$ derived from our Thm. 1, into Thm. E.1. This is in fact facilitated by leveraging the gradient correction length in our Cor. 1 to improve the bound in our Thm. 1 (refer to the remark of Appx. E.2). To begin with, we first derive a set of inequalities below based on our (38) since they are frequently required in the results of Thm. E.1. It is important to note that for the sake of simplicity in our proof, we present the validity of these inequalities with a constant probability, without explicitly providing the exact form of this probability.

$$
\begin{aligned}
&\frac{1}{NR}\sum_{r=0}^{R}\sum_{t=1}^{T}\sum_{i=1}^{N}\sum_{\tau=1}^{t}S^{t-\tau}\Xi_{r+1,\tau}^{(i)}\\
&\overset{(a)}{=}\frac{1}{R}\sum_{r=0}^{R}\sum_{t=1}^{T}\sum_{\tau=1}^{t}S^{t-\tau}\left(4\omega\kappa\rho^{rT+\tau-1}+2\sqrt{2\omega\kappa\rho^{rT}G}+2\sqrt{2NG\epsilon}\right)\\
&\overset{(b)}{=}\sum_{t=1}^{T}\frac{1}{R}\sum_{r=0}^{R}\left(\frac{4\omega\kappa\rho^{rT}\left(S^t-\rho^t\right)}{S-\rho}+\left(2\sqrt{2\omega\kappa\rho^{rT}G}+2\sqrt{2NG\epsilon}\right)\frac{S^t-1}{S-1}\right)\\
&\overset{(c)}{=}\sum_{t=1}^{T}\left[\frac{4\omega\kappa\left(S^t-\rho^t\right)\left(1-\rho^{(R+1)T}\right)}{R(S-\rho)(1-\rho^T)}+\left(\frac{2\sqrt{2\omega\kappa G}(1-\rho^{(R+1)T/2})}{R(1-\rho^{T/2})(S-1)}+\frac{2\sqrt{2NG\epsilon}}{S-1}\right)\left(S^t-1\right)\right]\\
&\overset{(d)}{=}\frac{4\omega\kappa(1-\rho^{(R+1)T})}{R(S-\rho)(1-\rho^T)}\left(\frac{S(S^T-1)}{S-1}-\frac{\rho(1-\rho^T)}{1-\rho}\right)+\left(\frac{2\sqrt{2\omega\kappa G}(1-\rho^{(R+1)T/2})}{R(1-\rho^{T/2})(S-1)}\right.\\
&\qquad\left.+\frac{2\sqrt{2NG\epsilon}}{S-1}\right)\left(\frac{S(S^T-1)}{S-1}-1\right)\\
&\overset{(e)}{=}\mathcal{O}\left(\frac{T^2(\sqrt{G}+1)}{R}+T^2\sqrt{\frac{NG}{M}}\right)
\end{aligned}
\tag{77}
$$

where $(b),(c),(d)$ are from the summation of geometric series. In addition, (e) comes from the fact that $S\triangleq\frac{(T+1)^2}{T(T-1)}$ (i.e., $S\leq 4.5$), $\frac{S^T-1}{S-1}\leq 11T$ in (62), $\frac{S}{S-1}=\frac{(T+1)^2}{3T+1}=\mathcal{O}\left(T\right)$ and $\epsilon=\mathcal{O}\left(\frac{1}{M}\right)$.

$$
\begin{aligned}
\frac{1}{NR}\sum_{r=0}^{R}\sum_{t=1}^{T}\sum_{i=1}^{N}\Xi_{r+1,t}^{(i)}&\overset{(a)}{=}\frac{1}{R}\sum_{r=0}^{R}\sum_{t=1}^{T}\left(4\omega\kappa\rho^{rT+t-1}+2\sqrt{2\omega\kappa\rho^{rT}G}+2\sqrt{2NG\epsilon}\right)\\
&\overset{(b)}{=}\frac{1}{R}\sum_{r=0}^{R}\left(\frac{4\omega\kappa\rho^{rT}(1-\rho^T)}{1-\rho}+2T\sqrt{2\omega\kappa\rho^{rT}G}+2T\sqrt{2NG\epsilon}\right)\\
&\overset{(c)}{=}\frac{4\omega\kappa(1-\rho^{(R+1)T})}{R(1-\rho)}+\frac{2T\sqrt{2\omega\kappa G}(1-\rho^{(R+1)T/2})}{R(1-\rho^{T/2})}+2T\sqrt{2NG\epsilon}\\
&\overset{(d)}{=}\mathcal{O}\left(\frac{T\sqrt{G}+1}{R}+T\sqrt{NG\epsilon}\right)
\end{aligned}
\tag{78}
$$

where $(c),(d)$ are from the summation of geometric series.

$$
\begin{aligned}
\frac{1}{NR}\sum_{r=0}^{R}\sum_{t=1}^{T}\sum_{i=1}^{N}\sqrt{\Xi_{r+1,t}^{(i)}} &\overset{(a)}{\leq} \frac{1}{R}\sum_{r=0}^{R}\sum_{t=1}^{T}\sqrt{\frac{1}{N}\sum_{i=1}^{N}\Xi_{r+1,t}^{(i)}} \\
&\overset{(b)}{\leq} \frac{1}{R}\sum_{r=1}^{R}\sum_{t=1}^{T}\left(\sqrt{4\omega\kappa\rho^{rT+t-1}}+\sqrt{2\sqrt{2\omega\kappa\rho^{rT}G}}+\sqrt{2\sqrt{2NG\epsilon}}\right) \\
&\overset{(c)}{=} \frac{1}{R}\sum_{r=0}^{R}\left(\frac{\sqrt{4\omega\kappa\rho^{rT}}(1-\rho^{T/2})}{1-\rho^{1/2}}+T\sqrt{2\sqrt{2\omega\kappa\rho^{rT}G}}+T\sqrt{2\sqrt{2NG\epsilon}}\right) \\
&\overset{(d)}{=} \frac{\sqrt{4\omega\kappa}(1-\rho^{T/2})(1-\rho^{(R+1)T/2})}{R(1-\rho^{1/2})(1-\rho^{T/2})}+\frac{T\sqrt[4]{8\omega\kappa G}(1-\rho^{(R+1)T/4})}{R(1-\rho^{T/4})}+T\sqrt[4]{8NG\epsilon} \\
&\overset{(e)}{=} \mathcal{O}\left(\frac{T\sqrt[4]{G}+1}{R}+T\sqrt[4]{\frac{NG}{M}}\right)
\end{aligned}
\tag{79}
$$

where (a) is from Cauchy–Schwarz inequality and (b) is from the inequality of $\sum_j c_j \leq \left(\sum_j \sqrt{c_j}\right)^2$ for any $c_j > 0$. Besides, $(c), (d)$ are from the summation of geometric series.

Subsequently, we proceed to establish the proof for the results in Thm. C.1 that are conditioned on different assumptions of F by systematically demonstrating each case individually as follows.

Strongly Convex F. Define $c \triangleq 1-\alpha\eta T/4$. [3] When $R+1 \geq 4\ln(3/4)/(\alpha\eta T)$, we then have that $p_r \leq \alpha\eta T c^{R-r}$ according to (70), which finally yields the following result

$$
\begin{aligned}
&\frac{1}{N}\sum_{r=1}^{R}p_r\sum_{t=1}^{T}\sum_{i=1}^{N}\sum_{\tau=1}^{t}S^{t-\tau}\Xi_{r,\tau}^{(i)} \\
&\overset{(a)}{=}\sum_{r=1}^{R}\frac{4p_r\omega\kappa\rho^{rT}}{S-\rho}\left(\frac{S(S^T-1)}{S-1}-\frac{\rho(1-\rho^T)}{1-\rho}\right)+\sum_{r=1}^{R}\frac{2p_r\sqrt{2\omega\kappa G}\rho^{rT/2}}{S-1}\left(\frac{S(S^T-1)}{S-1}-1\right) \\
&\qquad+\frac{2\sqrt{2NG\epsilon}}{S-1}\left(\frac{S(S^T-1)}{S-1}-1\right) \\
&\overset{(b)}{\leq}\frac{4\alpha\eta T\omega\kappa(c^{R+1}-\rho^{(R+1)T})}{(S-\rho)(c-\rho^T)}\left(\frac{S(S^T-1)}{S-1}-\frac{\rho(1-\rho^T)}{1-\rho}\right) \\
&\qquad+\frac{2\alpha\eta T\sqrt{2\omega\kappa G}(c^{R+1}-\rho^{(R+1)T/2})}{(S-1)(c-\rho^{T/2})}\left(\frac{S(S^T-1)}{S-1}-1\right)+\frac{2\sqrt{2NG\epsilon}}{S-1}\left(\frac{S(S^T-1)}{S-1}-1\right) \\
&\overset{(c)}{\leq}\mathcal{O}\left(\alpha\eta T^3c^R(\sqrt{G}+1)+T^2\sqrt{\frac{NG}{M}}\right) \\
&\overset{(d)}{=}\mathcal{O}\left(\frac{\alpha T^2c^R}{\beta}(\sqrt{G}+1)+T^2\sqrt{\frac{NG}{M}}\right)
\end{aligned}
\tag{80}
$$

where (a) follows from the derivation in (77) and (b) is due to the fact that $p_r \leq \alpha\eta T c^{R-r}$ as well as the summation of geometric series. Besides, (c) comes from $c^{R+1} > \rho^{(R+1)T/2} > \rho^{(R+1)T}$ and $c > \rho^{T/2} > \rho^T$ when we choose c properly in the proof of (69) as well as $\epsilon = \mathcal{O}\left(\frac{1}{M}\right)$. Finally, (d) results from the fact that $\eta \leq \frac{1}{10\beta T}$ and $\alpha < \beta$.

[3] Note that according to (66), we can always find a $\sqrt{\rho} < c < 1$ such that (69) still holds with only different constant terms. As a result, $c^{R+1} > \rho^{(R+1)T/2} > \rho^{(R+1)T}$ and $c > \rho^{T/2} > \rho^T$.

Following from the derivation above, we also have

$$\begin{aligned}
&\frac{1}{N}\sum_{r=0}^{R} p_r \sum_{t=1}^{T}\sum_{i=1}^{N} \Xi_{r+1,t}^{(i)} \\
=&\sum_{r=0}^{R} p_r \left(\frac{4\omega\kappa\rho^{rT}(1-\rho^T)}{1-\rho} + 2T\sqrt{2\omega\kappa\rho^{rT}G} + 2T\sqrt{2NG\epsilon} \right) \\
\leq& \frac{4\alpha\eta T\omega\kappa(1-\rho^T)(c^{R+1}-\rho^{(R+1)T})}{(1-\rho)(c-\rho^T)} + \frac{2\alpha\eta T^2\sqrt{2\omega\kappa G}(c^{R+1}-\rho^{(R+1)T/2})}{(c-\rho^{T/2})} + 2T\sqrt{2NG\epsilon} \\
=&\mathcal{O}\left(\frac{\alpha c^R}{\beta}(T\sqrt{G}+1) + T\sqrt{\frac{NG}{M}} \right) .
\end{aligned} \tag{81}$$

Finally, by introducing (80) and (81) into Thm. E.1, we have

$$\begin{aligned}
&\min_{r\in[R+1)} F(\boldsymbol{x}_r) - F(\boldsymbol{x}^*) \\
\overset{(a)}{\leq}& 2\alpha \exp\left(-\frac{\alpha\eta TR}{4}\right)\|\boldsymbol{x}_0-\boldsymbol{x}^*\|^2 + \sum_{r=0}^{R}\sum_{i=1}^{N}\sum_{t=1}^{T} p_r \left(\frac{\eta}{NT}\sum_{\tau=1}^{t} S^{t-\tau}\Xi_{r+1,\tau}^{(i)} + \frac{8(\eta T+1/\alpha)}{\alpha NT}\Xi_{r+1,t}^{(i)} \right) \\
\overset{(b)}{\leq}& \mathcal{O}\left(\alpha\exp\left(-\frac{\alpha\eta TR}{4}\right) D_0 + \frac{1}{\beta T^2}\left(\frac{\alpha c^R T^2}{\beta}(\sqrt{G}+1) + T^2\sqrt{\frac{NG}{M}} \right) \right. \\
&\left. + \frac{1/\beta+1/\alpha}{\alpha T}\left(\frac{\alpha c^R}{\beta}(T\sqrt{G}+1) + T\sqrt{\frac{NG}{M}} \right) \right) \\
\overset{(c)}{=}& \mathcal{O}\left(\exp(-\eta RT)D_0 + c^R\sqrt{G} + \sqrt{\frac{NG}{M}} \right)
\end{aligned} \tag{82}$$

where (b) is due to the fact that $\eta \leq \frac{1}{10\beta T}$. Let each item above achieve an $\epsilon/4$ error, we then realize the result in our Thm. C.1 when F is α-strongly convex and β-smooth.

Convex F. By introducing (77), (78) and (79) into Thm. E.1, we have

$$\begin{aligned}
&\min_{r\in[R+1)} F(\boldsymbol{x}_r) - F(\boldsymbol{x}^*) \\
\overset{(a)}{\leq}& \frac{2\|\boldsymbol{x}_0-\boldsymbol{x}^*\|^2}{\eta RT} + \frac{1}{R}\sum_{r=0}^{R}\sum_{i=1}^{N}\sum_{t=1}^{T}\left(\frac{\eta}{NT}\sum_{\tau=1}^{t} S^{t-\tau}\Xi_{r+1,\tau}^{(i)} + \frac{8\eta}{N}\Xi_{r+1,t}^{(i)} + \frac{4\sqrt{d}}{NT}\sqrt{\Xi_{r+1,t}^{(i)}} \right) \\
\overset{(b)}{\leq}& \mathcal{O}\left(\frac{D_0}{\eta RT} + \frac{1}{\beta T^2}\left(\frac{T^2(\sqrt{G}+1)}{R} + T^2\sqrt{\frac{NG}{M}} \right) + \frac{1}{\beta T}\left(\frac{T\sqrt{G}+1}{R} + T\sqrt{\frac{NG}{M}} \right) \right. \\
&\left. + \frac{\sqrt{d}}{T}\left(\frac{T\sqrt[4]{G}+1}{R} + T\sqrt[4]{\frac{NG}{M}} \right) \right) \\
\overset{(c)}{=}& \mathcal{O}\left(\frac{D_0}{\eta RT} + \frac{\sqrt{G}+\sqrt[4]{d^2G}}{R} + \sqrt{\frac{NG}{M}} + \sqrt[4]{\frac{NG}{M}} \right)
\end{aligned} \tag{83}$$

where (b) is due to the fact that $\eta \leq \frac{1}{10\beta T}$. Let each item above achieve an $\epsilon/4$ error, we then realize the result in our Thm. C.1 when F is convex and β-smooth.

Non-Convex F. By introducing (77) and (78) into Thm. E.1, we have

$$\begin{aligned}
&\min_{r\in[R+1)} \left\|\nabla F(\boldsymbol{x}_r)\right\|^2 \\
&\overset{(a)}{\leq} \frac{13(F(\boldsymbol{x}_0)-F(\boldsymbol{x}^*))}{\eta RT} + \frac{13}{\eta RT}\sum_{r=0}^{R}\sum_{i=1}^{N}\sum_{t=1}^{T}\left(\frac{(0.14\eta+1/(2\beta T))}{N}\Xi_{r+1,t}^{(i)}\right. \\
&\qquad\qquad \left. + \frac{1.02\eta^2\beta}{N}\sum_{\tau=1}^{t} S^{t-\tau}\Xi_{r+1,\tau}^{(i)}\right) \\
&\overset{(b)}{\leq} \mathcal{O}\left(\frac{D_1}{\eta RT} + \frac{1}{T}\left(\frac{T\sqrt{G}+1}{R} + T\sqrt{\frac{NG}{M}}\right) + \frac{1}{\beta T^2}\left(\frac{T^2(\sqrt{G}+1)}{R} + T^2\sqrt{\frac{NG}{M}}\right)\right) \\
&\overset{(c)}{=} \mathcal{O}\left(\frac{D_1}{\eta RT} + \frac{\sqrt{G}}{R} + \sqrt{\frac{NG}{M}}\right)
\end{aligned} \tag{84}$$

where (b) is due to the fact that $\eta \leq \frac{7}{100\beta T}$. Let each item above achieve an $\epsilon/3$ error, we then realize the result in our Thm. C.1 when F is non-convex and β-smooth. This hence finally concludes our proof of Thm. C.1.

F. Theoretical Results for Existing Federated ZOO Algorithms

F.1. Gradient Estimation in Existing Federated ZOO Algorithms

We first introduce the following lemma from the Thm. 2.6 in [22] to bound the gradient estimation error of the standard FD method, which usually serves as the foundation of existing federated ZOO baselines, e.g., [2].

Lemma F.1. *Let $\delta \in (0,1)$. Assume that function f is β-smooth in its domain and $\boldsymbol{u}_q \sim \mathcal{N}(\mathbf{0}, \mathbf{I})$ in (7), then the following holds with a probability of at least $1-\delta$,*

$$\|\boldsymbol{\Delta}(\boldsymbol{x}) - \nabla f(\boldsymbol{x})\| \leq \beta\lambda\sqrt{d} + \frac{\epsilon\sqrt{d}}{\lambda} + \sqrt{\frac{3n}{\delta Q}\left(3\|\nabla f(\boldsymbol{x})\|^2 + \frac{\beta^2\lambda^2}{4}(d+2)(d+4) + \frac{4\epsilon^2}{\lambda^2}\right)}$$

where $\sup_{\boldsymbol{x}\in\mathcal{X}} |y(\boldsymbol{x}) - f(\boldsymbol{x})| \leq \epsilon$.

Remark. In our setting (see Sec. 2), we in fact have the following result with a probability of at least $1-\delta$ by applying the Chernoff bound on the Gaussian observation noise ζ:

$$\epsilon = \sqrt{2\ln(2/\delta)}\sigma\ , \tag{85}$$

which is regarded as a constant in our following proofs. By additionally assuming that the gradient of f be bounded (i.e., $\|\nabla f(\boldsymbol{x})\| \leq c$ for any $\boldsymbol{x}$ in the domain of f and some $c > 0$), we have

$$\|\boldsymbol{\Delta}(\boldsymbol{x}) - \nabla f(\boldsymbol{x})\| \leq \Lambda + \mathcal{O}\left(\frac{1}{\sqrt{Q}}\right) \tag{86}$$

where the constant Λ is defined as $\Lambda \triangleq \beta\lambda\sqrt{d} + \frac{\epsilon\sqrt{d}}{\lambda}$. Note that this additional constant term in (86) can not be avoided, which thus is another pitfall of the FD method in addition to its query inefficiency as discussed in our Appx. B.2.

Based on the results above, we can get the following upper bounds for the gradient estimation methods in the existing federated ZOO algorithms. Note that, we usually keep the constant before $\mathcal{O}\left(\frac{1}{Q}\right)$ to deliver a more detailed comparison among different federated ZOO algorithms throughout this section.

FedZO Algorithm. For FedZO [2], it applies the following gradient estimation for every local update in Algo. 1:

$$\widehat{\boldsymbol{g}}_{r,t-1}^{(i)} = \boldsymbol{\Delta}^{(i)}(\boldsymbol{x}_{r,t-1}^{(i)})\ . \tag{87}$$

That is, $\gamma_{r,t-1}^{(i)} = 0$ and $\boldsymbol{g}_{r,t-1}^{(i)} = \boldsymbol{\Delta}^{(i)}(\boldsymbol{x}_{r,t-1}^{(i)})$ in (6). We provide the following gradient disparity bound for such a gradient estimation method when it is applied in Algo. 1.

Proposition F.1. *Assume that $\frac{1}{N}\sum_{i=1}^N \|\nabla f_i(\boldsymbol{x}) - \nabla F(\boldsymbol{x})\|^2 \leq G$ for any $\boldsymbol{x} \in \mathcal{X}$ and f_i is β-smooth with bounded gradient for any $i \in [N]$. When applying (87) in Algo. 1, the following then holds with a constant probability for some $\Lambda > 0$,*

$$\frac{1}{N}\sum_{i=1}^N \Xi_{r,t}^{(i)} \leq 4\Lambda^2 + 2G + 4\mathcal{O}\left(\frac{1}{Q}\right)\ .$$

Proof.

$$\begin{aligned}
\frac{1}{N}\sum_{i=1}^N \Xi_{r,t}^{(i)} &\overset{(a)}{=} \frac{1}{N}\sum_{i=1}^N \left\|\boldsymbol{\Delta}^{(i)}(\boldsymbol{x}_{r,t-1}^{(i)}) - \nabla F(\boldsymbol{x}_{r,t-1}^{(i)})\right\|^2 \\
&\overset{(b)}{=} \frac{1}{N}\sum_{i=1}^N \left\|\boldsymbol{\Delta}^{(i)}(\boldsymbol{x}_{r,t-1}^{(i)}) - \nabla f_i(\boldsymbol{x}_{r,t-1}^{(i)}) + \nabla f_i(\boldsymbol{x}_{r,t-1}^{(i)}) - \nabla F(\boldsymbol{x}_{r,t-1}^{(i)})\right\|^2 \\
&\overset{(c)}{\leq} \frac{1}{N}\sum_{i=1}^N 2\left(\left\|\boldsymbol{\Delta}^{(i)}(\boldsymbol{x}_{r,t-1}^{(i)}) - \nabla f_i(\boldsymbol{x}_{r,t-1}^{(i)})\right\|^2 + \left\|\nabla f_i(\boldsymbol{x}_{r,t-1}^{(i)}) - \nabla F(\boldsymbol{x}_{r,t-1}^{(i)})\right\|^2\right) \\
&\overset{(d)}{\leq} 4\Lambda^2 + 2G + 4\mathcal{O}\left(\frac{1}{Q}\right)
\end{aligned} \tag{88}$$

where (c) comes from Lemma E.5 and (d) is based on Lemma E.5 as well as the result in (86). □

FedProx Algorithm. For FedProx in the federated ZOO setting (i.e., by simply combining FedProx from [16] with the standard FD method in (7)), it has the gradient estimation form as follows:

$$\widehat{\boldsymbol{g}}_{r,t-1}^{(i)} = \boldsymbol{\Delta}^{(i)}(\boldsymbol{x}_{r,t-1}^{(i)}) + \gamma(\boldsymbol{x}_{r,t-1}^{(i)} - \boldsymbol{x}_{r-1}) \tag{89}$$

where γ is a constant. That is, $\gamma_{r,t-1}^{(i)} = \gamma$, $\boldsymbol{g}_{r,t-1}^{(i)} = \boldsymbol{\Delta}^{(i)}(\boldsymbol{x}_{r,t-1}^{(i)})$ and $\boldsymbol{g}_{r-1}(\boldsymbol{x}') - \boldsymbol{g}_{r-1}^{(i)}(\boldsymbol{x}'') = \boldsymbol{x}_{r,t-1}^{(i)} - \boldsymbol{x}_{r-1}$ in (6). We provide the following gradient disparity bound for such a gradient estimation method when it is applied in Algo. 1.

Proposition F.2. *Assume that $\frac{1}{N}\sum_{i=1}^{N}\|\nabla f_i(\boldsymbol{x}) - \nabla F(\boldsymbol{x})\|^2 \leq G$ for any $\boldsymbol{x} \in \mathcal{X}$ and f_i is β-smooth with bounded gradient for any $i \in [N]$. When applying (89) in Algo. 1, the following then holds with a constant probability for some $\Lambda > 0$,*

$$\frac{1}{N}\sum_{i=1}^{N}\Xi_{r,t}^{(i)} \leq 6\Lambda^2 + 3G + \frac{3\gamma^2}{N}\sum_{i=1}^{N}\left\|\boldsymbol{x}_{r,t-1}^{(i)} - \boldsymbol{x}_{r-1}\right\|^2 + 6\mathcal{O}\left(\frac{1}{Q}\right).$$

Proof.

$$\begin{aligned}
\frac{1}{N}\sum_{i=1}^{N}\Xi_{r,t}^{(i)} &\overset{(a)}{=} \frac{1}{N}\sum_{i=1}^{N}\left\|\boldsymbol{\Delta}^{(i)}(\boldsymbol{x}_{r,t-1}^{(i)}) + \gamma\left(\boldsymbol{x}_{r,t-1}^{(i)} - \boldsymbol{x}_{r-1}\right) - \nabla F(\boldsymbol{x}_{r,t-1}^{(i)})\right\|^2 \\
&\overset{(b)}{=} \frac{1}{N}\sum_{i=1}^{N}\left\|\boldsymbol{\Delta}^{(i)}(\boldsymbol{x}_{r,t-1}^{(i)}) - \nabla f_i(\boldsymbol{x}_{r,t-1}^{(i)}) + \nabla f_i(\boldsymbol{x}_{r,t-1}^{(i)}) - \nabla F(\boldsymbol{x}_{r,t-1}^{(i)}) + \gamma\left(\boldsymbol{x}_{r,t-1}^{(i)} - \boldsymbol{x}_{r-1}\right)\right\|^2 \\
&\overset{(c)}{\leq} \frac{1}{N}\sum_{i=1}^{N} 3\left(\left\|\boldsymbol{\Delta}^{(i)}(\boldsymbol{x}_{r,t-1}^{(i)}) - \nabla f_i(\boldsymbol{x}_{r,t-1}^{(i)})\right\|^2 + \left\|\nabla f_i(\boldsymbol{x}_{r,t-1}^{(i)}) - \nabla F(\boldsymbol{x}_{r,t-1}^{(i)})\right\|^2\right) \\
&\qquad + \frac{3\gamma^2}{N}\sum_{i=1}^{N}\left\|\boldsymbol{x}_{r,t-1}^{(i)} - \boldsymbol{x}_{r-1}\right\|^2 \\
&\overset{(d)}{\leq} 6\Lambda^2 + 3G + \frac{3\gamma^2}{N}\sum_{i=1}^{N}\left\|\boldsymbol{x}_{r,t-1}^{(i)} - \boldsymbol{x}_{r-1}\right\|^2 + 6\mathcal{O}\left(\frac{1}{Q}\right).
\end{aligned} \tag{90}$$

Similarly, (c) is from Lemma E.5 and (d) is based on Lemma E.5 as well as the result in (86). □

SCAFFOLD (Type I) Algorithm. For SCAFFOLD using its Type I gradient correction in the federated ZOO setting (i.e., by simply combining SCAFFOLD (Type I) from [8] with the standard FD method in (7)), it has the gradient estimation form as follows:

$$\widehat{\boldsymbol{g}}_{r,t-1}^{(i)} = \boldsymbol{\Delta}^{(i)}(\boldsymbol{x}_{r,t-1}^{(i)}) + \frac{1}{N}\sum_{j=1}^{N}\boldsymbol{\Delta}^{(j)}(\boldsymbol{x}_{r-1}) - \boldsymbol{\Delta}^{(i)}(\boldsymbol{x}_{r-1}). \tag{91}$$

That is, $\gamma_{r,t-1}^{(i)} = 1$, $\boldsymbol{g}_{r,t-1}^{(i)} = \boldsymbol{\Delta}^{(i)}(\boldsymbol{x}_{r,t-1}^{(i)})$ and $\boldsymbol{g}_{r-1}(\boldsymbol{x}') - \boldsymbol{g}_{r-1}^{(i)}(\boldsymbol{x}'') = \frac{1}{N}\sum_{j=1}^{N}\boldsymbol{\Delta}^{(j)}(\boldsymbol{x}_{r-1}) - \boldsymbol{\Delta}^{(i)}(\boldsymbol{x}_{r-1})$ in (6). Of note, similar to our FZooS where an additional transmission is required when we actively query in the neighborhood of $\boldsymbol{x}_r$ in line 7 of Algo. 2, SCAFFOLD (Type I) also needs another server-client transmission of $\frac{1}{N}\sum_{j=1}^{N}\boldsymbol{\Delta}^{(j)}(\boldsymbol{x}_{r-1})$ for gradient correction. We provide the following gradient disparity bound for such a gradient estimation method when it is applied in Algo. 1.

Proposition F.3. *Assume that f_i is β-smooth with bounded gradient for any $i \in [N]$. When applying (91) in Algo. 1, the following then holds with a constant probability for some $\Lambda > 0$,*

$$\frac{1}{N}\sum_{i=1}^{N}\Xi_{r,t}^{(i)} \leq 18\Lambda^2 + \frac{6\beta^2}{N}\sum_{i=1}^{N}\left\|\boldsymbol{x}_{r,t-1}^{(i)} - \boldsymbol{x}_{r-1}\right\|^2 + 18\mathcal{O}\left(\frac{1}{Q}\right).$$

Proof.

$$
\begin{aligned}
\frac{1}{N}\sum_{i=1}^{N}\Xi_{r,t}^{(i)} &\overset{(a)}{=} \frac{1}{N}\sum_{i=1}^{N}\left\|\boldsymbol{\Delta}^{(i)}(\boldsymbol{x}_{r,t-1}^{(i)})+\left(\frac{1}{N}\sum_{j=1}^{N}\boldsymbol{\Delta}^{(j)}(\boldsymbol{x}_{r-1})-\boldsymbol{\Delta}^{(i)}(\boldsymbol{x}_{r-1})\right)-\nabla F(\boldsymbol{x}_{r,t-1}^{(i)})\right\|^2 \\
&\overset{(b)}{=} \frac{1}{N}\sum_{i=1}^{N}\left\|\boldsymbol{\Delta}^{(i)}(\boldsymbol{x}_{r,t-1}^{(i)})-\nabla f_i(\boldsymbol{x}_{r,t-1}^{(i)})+\frac{1}{N}\sum_{j=1,j\neq i}^{N}\left(\boldsymbol{\Delta}^{(j)}(\boldsymbol{x}_{r-1})-\nabla f_j(\boldsymbol{x}_{r,t-1}^{(i)})\right)\right. \\
&\qquad \left.+\frac{N-1}{N}\left(\nabla f_i(\boldsymbol{x}_{r,t-1}^{(i)})-\boldsymbol{\Delta}^{(i)}(\boldsymbol{x}_{r-1})\right)\right\|^2 \\
&\overset{(c)}{\leq} \frac{3}{N}\sum_{i=1}^{N}\left\|\boldsymbol{\Delta}^{(i)}(\boldsymbol{x}_{r,t-1}^{(i)})-\nabla f_i(\boldsymbol{x}_{r,t-1}^{(i)})\right\|^2+\frac{3}{N^3}\sum_{i=1}^{N}\left\|\sum_{j=1,j\neq i}^{N}\left(\boldsymbol{\Delta}^{(j)}(\boldsymbol{x}_{r-1})-\nabla f_j(\boldsymbol{x}_{r,t-1}^{(i)})\right)\right\|^2 \\
&\qquad +\frac{3(N-1)^2}{N^3}\sum_{i=1}^{N}\left\|\nabla f_i(\boldsymbol{x}_{r,t-1}^{(i)})-\boldsymbol{\Delta}^{(i)}(\boldsymbol{x}_{r-1})\right\|^2 \\
&\overset{(d)}{\leq} \frac{3}{N}\sum_{i=1}^{N}\left\|\boldsymbol{\Delta}^{(i)}(\boldsymbol{x}_{r,t-1}^{(i)})-\nabla f_i(\boldsymbol{x}_{r,t-1}^{(i)})\right\|^2+\frac{3(N-1)}{N^3}\sum_{i=1}^{N}\sum_{j=1,j\neq i}^{N}\left\|\boldsymbol{\Delta}^{(j)}(\boldsymbol{x}_{r-1})-\nabla f_j(\boldsymbol{x}_{r,t-1}^{(i)})\right\|^2 \\
&\qquad +\frac{3(N-1)^2}{N^3}\sum_{i=1}^{N}\left\|\nabla f_i(\boldsymbol{x}_{r,t-1}^{(i)})-\boldsymbol{\Delta}^{(i)}(\boldsymbol{x}_{r-1})\right\|^2 \\
&\overset{(e)}{\leq} \frac{3}{N}\sum_{i=1}^{N}\left\|\boldsymbol{\Delta}^{(i)}(\boldsymbol{x}_{r,t-1}^{(i)})-\nabla f_i(\boldsymbol{x}_{r,t-1}^{(i)})\right\|^2+\frac{6(N-1)}{N^2}\sum_{j=1}^{N}\left\|\boldsymbol{\Delta}^{(j)}(\boldsymbol{x}_{r,t-1}^{(i)})-\nabla f_j(\boldsymbol{x}_{r,t-1}^{(i)})\right\|^2 \\
&\qquad +\frac{6\beta^2(N-1)^2}{N^2}\sum_{j=1}^{N}\left\|\boldsymbol{x}_{r,t-1}^{(i)}-\boldsymbol{x}_{r-1}\right\|^2 \\
&\overset{(f)}{\leq} \frac{9}{N}\sum_{i=1}^{N}\left\|\boldsymbol{\Delta}^{(i)}(\boldsymbol{x}_{r,t-1}^{(i)})-\nabla f_i(\boldsymbol{x}_{r,t-1}^{(i)})\right\|^2+6\beta^2\sum_{i=1}^{N}\left\|\boldsymbol{x}_{r,t-1}^{(i)}-\boldsymbol{x}_{r-1}\right\|^2 \\
&\overset{(g)}{\leq} 18\Lambda^2+6\beta^2\sum_{i=1}^{N}\left\|\boldsymbol{x}_{r,t-1}^{(i)}-\boldsymbol{x}_{r-1}\right\|^2+18\mathcal{O}\left(\frac{1}{Q}\right)
\end{aligned}
\tag{92}
$$

Similarly, $(c), (d)$ are from Lemma E.5 and (e) is because of the smoothness of F as well as (28) with $a=\frac{1}{N-1}$. Finally, (g) follows from the results in (86) as well as the result in Lemma E.5. □

SCAFFOLD (Type II) Algorithm. For SCAFFOLD using its Type II gradient correction in the federated ZOO setting (i.e., by simply combining SCAFFOLD (Type II) from [8] with the standard FD method in (7)), it has the gradient estimation form as follows:

$$
\widehat{\boldsymbol{g}}_{r,t-1}^{(i)}=\boldsymbol{\Delta}^{(i)}(\boldsymbol{x}_{r,t-1}^{(i)})+\frac{1}{NT}\sum_{j=1}^{N}\sum_{\tau=1}^{T}\boldsymbol{\Delta}^{(j)}(\boldsymbol{x}_{r-1,\tau-1}^{(j)})-\frac{1}{T}\sum_{\tau=1}^{T}\boldsymbol{\Delta}^{(i)}(\boldsymbol{x}_{r-1,\tau-1}^{(i)})\,. \tag{93}
$$

That is, $\boldsymbol{g}_{r-1}(\boldsymbol{x}')-\boldsymbol{g}_{r-1}^{(i)}(\boldsymbol{x}'')=\frac{1}{NT}\sum_{j=1}^{N}\sum_{\tau=1}^{T}\boldsymbol{\Delta}^{(j)}(\boldsymbol{x}_{r-1,\tau-1}^{(j)})-\frac{1}{T}\sum_{\tau=1}^{T}\boldsymbol{\Delta}^{(i)}(\boldsymbol{x}_{r-1,\tau-1}^{(i)})$, $\boldsymbol{g}_{r,t-1}^{(i)}=\boldsymbol{\Delta}^{(i)}(\boldsymbol{x}_{r,t-1}^{(i)})$ and $\gamma_{r,t-1}^{(i)}=1$ in (6). Interestingly, SCAFFOLD (Type II) servers as an approximation of SCAFFOLD (Type I), which in fact does not require another server-client transmission for gradient correction as discussed in [8]. This is because $\frac{1}{NT}\sum_{j=1}^{N}\sum_{\tau=1}^{T}\boldsymbol{\Delta}^{(j)}(\boldsymbol{x}_{r-1,\tau-1}^{(j)})$ can be computed before the aggregation of $\{\boldsymbol{x}_{r-1,T}^{(i)}\}_{i=1}^{N}$ on server. We provide the following gradient disparity bound for such a gradient estimation method when it is applied in Algo. 1.

Proposition F.4. *Assume that f_i is c-continuous and β-smooth for any $i\in[N]$ and the randomly sampled $\{\boldsymbol{u}_q\}_{q=1}^{Q}$ in (7) are shared across all iterations and rounds. When applying (93) in Algo. 1, the following then holds with a constant*

probability for some $\Lambda, a > 0$*,*

$$\frac{1}{N}\sum_{i=1}^{N}\Xi_{r,t}^{(i)} \leq 18\Lambda^2 + \frac{24ac^2}{\lambda^2 T}\sum_{i=1}^{N}\sum_{\tau=1}^{T}\left\|\boldsymbol{x}_{r,t-1}^{(i)} - \boldsymbol{x}_{r-1,\tau-1}^{(i)}\right\|^2 + 6\mathcal{O}\left(\frac{1}{Q}\right) + 12\mathcal{O}\left(\frac{1}{TQ}\right).$$

Proof. We slightly abuse notation and use $\boldsymbol{\Delta}_T^{(i)}(\boldsymbol{x}_{r,t-1}^{(i)})$ to denote the FD method in (7) using TQ function queries for the gradient estimation at input $\boldsymbol{x}_{r,t-1}^{(i)}$ on client i. Based on this notation, we then have

$$\begin{aligned}
&\frac{1}{N}\sum_{i=1}^{N}\Xi_{r,t}^{(i)} \\
&\overset{(a)}{=}\frac{1}{N}\sum_{i=1}^{N}\left\|\boldsymbol{\Delta}^{(i)}(\boldsymbol{x}_{r,t-1}^{(i)}) + \left(\frac{1}{NT}\sum_{j=1}^{N}\sum_{\tau=1}^{T}\boldsymbol{\Delta}^{(j)}(\boldsymbol{x}_{r-1,\tau-1}^{(j)}) - \frac{1}{T}\sum_{\tau=1}^{T}\boldsymbol{\Delta}^{(i)}(\boldsymbol{x}_{r-1,\tau-1}^{(i)})\right) - \nabla F(\boldsymbol{x}_{r,t-1}^{(i)})\right\|^2 \\
&\overset{(b)}{=}\frac{1}{N}\sum_{i=1}^{N}\left\|\boldsymbol{\Delta}^{(i)}(\boldsymbol{x}_{r,t-1}^{(i)}) - \nabla f_i(\boldsymbol{x}_{r,t-1}^{(i)}) + \frac{N-1}{N}\left(\nabla f_i(\boldsymbol{x}_{r,t-1}^{(i)}) - \frac{1}{T}\sum_{\tau=1}^{T}\boldsymbol{\Delta}^{(i)}(\boldsymbol{x}_{r-1,\tau-1}^{(i)})\right)\right. \\
&\qquad\left. + \frac{1}{NT}\sum_{j=1,j\neq i}^{N}\sum_{\tau=1}^{T}\left(\boldsymbol{\Delta}^{(j)}(\boldsymbol{x}_{r-1,\tau-1}^{(j)}) - \nabla f_j(\boldsymbol{x}_{r,t-1}^{(j)})\right)\right\|^2 \\
&\overset{(c)}{\leq}\frac{3}{N}\sum_{i=1}^{N}\left\|\boldsymbol{\Delta}^{(i)}(\boldsymbol{x}_{r,t-1}^{(i)}) - \nabla f_i(\boldsymbol{x}_{r,t-1}^{(i)})\right\|^2 \\
&\qquad + \frac{3(N-1)^2}{N^3}\sum_{i=1}^{N}\left\|\left(\nabla f_i(\boldsymbol{x}_{r,t-1}^{(i)} - \boldsymbol{\Delta}_T^{(i)}(\boldsymbol{x}_{r,t-1}^{(i)})\right) + \left(\boldsymbol{\Delta}_T^{(i)}(\boldsymbol{x}_{r,t-1}^{(i)}) - \frac{1}{T}\sum_{\tau=1}^{T}\boldsymbol{\Delta}^{(i)}(\boldsymbol{x}_{r-1,\tau-1}^{(i)})\right)\right\|^2 \\
&\qquad + \frac{3}{N^3}\sum_{i=1}^{N}\left\|\sum_{j=1,j\neq 1}^{N}\left[\left(\nabla f_j(\boldsymbol{x}_{r,t-1}^{(j)}) - \boldsymbol{\Delta}_T^{(j)}(\boldsymbol{x}_{r,t-1}^{(j)})\right) + \left(\boldsymbol{\Delta}_T^{(j)}(\boldsymbol{x}_{r,t-1}^{(j)}) - \frac{1}{T}\sum_{\tau=1}^{T}\boldsymbol{\Delta}^{(j)}(\boldsymbol{x}_{r-1,\tau-1}^{(j)})\right)\right]\right\|^2 \\
&\overset{(d)}{\leq}\frac{3}{N}\sum_{i=1}^{N}\left\|\boldsymbol{\Delta}^{(i)}(\boldsymbol{x}_{r,t-1}^{(i)}) - \nabla f_i(\boldsymbol{x}_{r,t-1}^{(i)})\right\|^2 \\
&\qquad + \frac{3(N-1)^2}{N^3}\sum_{i=1}^{N}\left(\left(1+\frac{1}{N-1}\right)\left\|\nabla f_i(\boldsymbol{x}_{r,t-1}^{(i)} - \boldsymbol{\Delta}_T^{(i)}(\boldsymbol{x}_{r,t-1}^{(i)})\right\|^2\right. \\
&\qquad\qquad \left. + N\left\|\boldsymbol{\Delta}_T^{(i)}(\boldsymbol{x}_{r,t-1}^{(i)}) - \frac{1}{T}\sum_{\tau=1}^{T}\boldsymbol{\Delta}^{(i)}(\boldsymbol{x}_{r-1,\tau-1}^{(i)})\right\|^2\right) \\
&\qquad + \frac{3(N-1)}{N^3}\sum_{i=1}^{N}\sum_{j=1,j\neq 1}^{N}\left(\left(1+\frac{1}{N-1}\right)\left\|\nabla f_j(\boldsymbol{x}_{r,t-1}^{(j)}) - \boldsymbol{\Delta}_T^{(j)}(\boldsymbol{x}_{r,t-1}^{(j)})\right\|^2\right. \\
&\qquad\qquad \left. + N\left\|\boldsymbol{\Delta}_T^{(j)}(\boldsymbol{x}_{r,t-1}^{(j)}) - \frac{1}{T}\sum_{\tau=1}^{T}\boldsymbol{\Delta}^{(j)}(\boldsymbol{x}_{r-1,\tau-1}^{(j)})\right\|^2\right)
\end{aligned} \tag{94}$$

Similarly, (c) are from (29) in Lemma E.5 and (d) is because of (28) in Lemma E.5 with $a = \frac{N}{N-1}$.

We then bound $\left\|\boldsymbol{\Delta}_T^{(i)}(\boldsymbol{x}_{r,t-1}^{(i)}) - \frac{1}{T}\sum_{\tau=1}^{T}\boldsymbol{\Delta}^{(i)}(\boldsymbol{x}_{r-1,\tau-1}^{(i)})\right\|^2$ as below

$$
\begin{aligned}
&\left\|\boldsymbol{\Delta}_T^{(i)}(\boldsymbol{x}_{r,t-1}^{(i)}) - \frac{1}{T}\sum_{\tau=1}^{T}\boldsymbol{\Delta}^{(i)}(\boldsymbol{x}_{r-1,\tau-1}^{(i)})\right\|^2 \\
&\overset{(a)}{\leq}\frac{1}{T}\sum_{\tau=1}^{T}\left\|\boldsymbol{\Delta}^{(i)}(\boldsymbol{x}_{r,t-1}^{(i)}) - \boldsymbol{\Delta}^{(i)}(\boldsymbol{x}_{r-1,\tau-1}^{(i)})\right\|^2 \\
&\overset{(b)}{=}\frac{1}{T}\sum_{\tau=1}^{T}\left\|\frac{1}{Q}\sum_{q=1}^{Q}\left(y_i(\boldsymbol{x}_{r-1,\tau-1}^{(i)}+\lambda\boldsymbol{u}_q) - y_i(\boldsymbol{x}_{r,t-1}^{(i)}+\lambda\boldsymbol{u}_q) + y_i(\boldsymbol{x}_{r,t-1}^{(i)}) - y_i(\boldsymbol{x}_{r-1,\tau-1}^{(i)})\right)\frac{\boldsymbol{u}_q}{\lambda}\right\|^2 \\
&\overset{(c)}{\leq}\frac{1}{\lambda^2 TQ}\sum_{\tau=1}^{T}\sum_{q=1}^{Q}\left|y_i(\boldsymbol{x}_{r-1,\tau-1}^{(i)}+\lambda\boldsymbol{u}_q) - y_i(\boldsymbol{x}_{r,t-1}^{(i)}+\lambda\boldsymbol{u}_q) + y_i(\boldsymbol{x}_{r,t-1}^{(i)}) - y_i(\boldsymbol{x}_{r-1,\tau-1}^{(i)})\right|^2\|\boldsymbol{u}_q|^2 \\
&\overset{(d)}{=}\frac{1}{\lambda^2 TQ}\sum_{\tau=1}^{T}\sum_{q=1}^{Q}2\left|f_i(\boldsymbol{x}_{r-1,\tau-1}^{(i)}+\lambda\boldsymbol{u}_q) - f_i(\boldsymbol{x}_{r,t-1}^{(i)}+\lambda\boldsymbol{u}_q) + f_i(\boldsymbol{x}_{r,t-1}^{(i)}) - f_i(\boldsymbol{x}_{r-1,\tau-1}^{(i)})\right|^2\|\boldsymbol{u}_q\|^2 \\
&\qquad+\frac{1}{\lambda^2 TQ}\sum_{q=1}^{Q}2\left|\zeta_{r-1,\tau-1}^{(i)} - \zeta_{r,t-1}^{(i)} + \zeta_{r-1,\tau-1}^{(i)'} - \zeta_{r,t-1}^{(i)'}\right|^2\|\boldsymbol{u}_q\|^2 \\
&\overset{(e)}{\leq}\frac{1}{\lambda^2 TQ}\sum_{\tau=1}^{T}\sum_{q=1}^{Q}4\left(\left|f_i(\boldsymbol{x}_{r-1,\tau-1}^{(i)}+\lambda\boldsymbol{u}_q) - f_i(\boldsymbol{x}_{r,t-1}^{(i)}+\lambda\boldsymbol{u}_q)\right|^2 + \left|f_i(\boldsymbol{x}_{r,t-1}^{(i)}) - f_i(\boldsymbol{x}_{r-1,\tau-1}^{(i)})\right|^2\right)\|\boldsymbol{u}_q\|^2 \\
&\qquad+\frac{1}{\lambda^2 TQ}\sum_{q=1}^{Q}8\epsilon^2\|\boldsymbol{u}_q\|^2 \\
&\overset{(f)}{\leq}\frac{8}{\lambda^2 T}\sum_{\tau=1}^{T}\left(c^2\left\|\boldsymbol{x}_{r,t-1}^{(i)} - \boldsymbol{x}_{r-1,\tau-1}^{(i)}\right\|^2 + \epsilon^2\right)\left(\frac{1}{Q}\sum_{q=1}^{Q}\|\boldsymbol{u}_q\|^2\right) \\
&\overset{(g)}{\leq}\frac{8a}{\lambda^2 T}\sum_{\tau=1}^{T}\left(c^2\left\|\boldsymbol{x}_{r,t-1}^{(i)} - \boldsymbol{x}_{r-1,\tau-1}^{(i)}\right\|^2 + \epsilon^2\right)
\end{aligned}
\tag{95}
$$

where (a), (d), (e) are due to (29) in Lemma E.5. Note that (d) is valid because $\{\boldsymbol{u}_q\}_{q=1}^{Q}$ in (7) is assumed to be shared across all iterations and rounds. In addition, (c) is from the Cauchy–Schwarz inequality and (f) is based on the continuity of F, i.e., $\|F(\boldsymbol{x}) - F(\boldsymbol{x}')\| \leq c$ for any $\boldsymbol{x}, \boldsymbol{x}' \in \mathcal{X}$. Finally, (g) is from Lemma E.2 and $a \triangleq d + 2\sqrt{dQ^{-1}\ln(1/\delta)} + 2Q^{-1}\ln(1/\delta)$.

Finally, by introducing (95) into (94), we have

$$
\begin{aligned}
\frac{1}{N}\sum_{i=1}^{N}\Xi_{r,t}^{(i)} &\overset{(a)}{\leq}\frac{3}{N}\sum_{i=1}^{N}\left\|\boldsymbol{\Delta}^{(i)}(\boldsymbol{x}_{r,t-1}^{(i)}) - \nabla f_i(\boldsymbol{x}_{r,t-1}^{(i)})\right\|^2 + \frac{6(N-1)}{N^2}\sum_{i=1}^{N}\left\|\nabla f_i(\boldsymbol{x}_{r,t-1}^{(i)}) - \boldsymbol{\Delta}_T^{(i)}(\boldsymbol{x}_{r,\tau-1}^{(i)})\right\|^2 \\
&\quad+\frac{24a(N-1)^2}{\lambda^2 TN^2}\sum_{i=1}^{N}\sum_{\tau=1}^{T}\left(c^2\left\|\boldsymbol{x}_{r,t-1}^{(i)} - \boldsymbol{x}_{r-1,\tau-1}^{(i)}\right\|^2 + \epsilon^2\right) \\
&\quad+\frac{24a(N-1)}{\lambda^2 TN^2}\sum_{j=1,j\neq 1}^{N}\sum_{\tau=1}^{T}\left(c^2\left\|\boldsymbol{x}_{r,t-1}^{(j)} - \boldsymbol{x}_{r-1,\tau-1}^{(j)}\right\|^2 + \epsilon^2\right) \\
&\overset{(b)}{\leq}18\Lambda^2 + \frac{24ac^2}{\lambda^2 T}\sum_{i=1}^{N}\sum_{\tau=1}^{T}\left\|\boldsymbol{x}_{r,t-1}^{(i)} - \boldsymbol{x}_{r-1,\tau-1}^{(i)}\right\|^2 + 6\mathcal{O}\left(\frac{1}{Q}\right) + 12\mathcal{O}\left(\frac{1}{TQ}\right)
\end{aligned}
\tag{96}
$$

Finally, (b) follows from the results in (86) as well as the result in Lemma E.5, which finally concludes our proof. □

Comparison and Discussion. By comparing the upper bounds in Prop. F.1, F.2, F.3, and F.4 above with the one in our Thm. 1, we can summarize certain interesting insights as follows, which, to the best of our knowledge, has never been

formally presented in the literature of federated ZOO.

(i) The gradient disparity of existing federated ZOO algorithms consistently has an additional constant error term (i.e., Λ^2) that can not be avoided. Remarkably, no additional constant error term occurs in the gradient disparity bound of our (5).

(ii) The gradient disparity of existing federated ZOO algorithms typically can only be reduced at a polynomial rate of Q whereas our (5) is able to achieve an exponential rate of reduction for its gradient disparity.

(iii) FedProx achieves an even worse gradient disparity when compared with FedZO by introducing an additional error term $\frac{3\gamma^2}{N}\sum_{i=1}^{N}\left\|\boldsymbol{x}_{r,t-1}^{(i)}-\boldsymbol{x}_{r-1}\right\|^2$. This may explain its worst convergence in Sec. 5.

(iv) SCAFFOLD (Type I) and SCAFFOLD (Type II) are typically able to mitigate the impact of client heterogeneity (i.e., G) by enlarging the impact of the gradient estimation error that is resulting from the FD method applied in these two algorithms. This may lead to worse practical performance when the gradient estimation error outweighs the client heterogeneity, as shown in our Sec. 5.

(v) Although SCAFFOLD (Type II) is proposed to approximate SCAFFOLD (Type I) in the original paper [8], SCAFFOLD (Type II) in fact has the advantage of achieving a smaller gradient estimation error for gradient correction by increasing the number of additional function queries (i.e., the term $\mathcal{O}\left(\frac{1}{TQ}\right)$ in Prop. F.4), which is however at the cost of a likely increased input disparity (i.e., the term $\frac{24ac^2}{\lambda^2 T}\sum_{i=1}^{N}\sum_{\tau=1}^{T}\left\|\boldsymbol{x}_{r,t-1}^{(i)}-\boldsymbol{x}_{r-1,\tau-1}^{(i)}\right\|^2$ in Prop. F.4). Interestingly, federated ZOO usually prefers gradient correction of smaller gradient estimation errors, as suggested by the empirical results in our Sec. 5. This explains the reason why SCAFFOLD (Type II) usually outperforms SCAFFOLD (Type I) in federated ZOO, which differs from the scenario of federated FOO and therefore highlights the importance of an accurate gradient correction in federated ZOO.

F.2. Convergence of Existing Federated ZOO Algorithms

To establish the proof for the convergence of existing federated ZOO algorithms, we introduce the upper bound of gradient disparity $\frac{1}{N}\sum_{i=1}^{N}\Xi_{r,t}^{(i)}$ derived from our Prop. F.1, F.2, F.3, and F.4, into Thm. E.1. Particularly, to ease our proof, we mainly prove the convergence of existing federated ZOO algorithms when F is non-convex and β-smooth. Similar to our Thm. C.1, we define $D_0 \triangleq \|\boldsymbol{x}_0-\boldsymbol{x}^*\|^2$ and $D_1 \triangleq F(\boldsymbol{x}_0)-F(\boldsymbol{x}^*)$, and assume that $\frac{1}{N}\sum_{i=1}^{N}\|\nabla f_i(\boldsymbol{x})-\nabla F(\boldsymbol{x})\|^2 \leq G$ for any $\boldsymbol{x}\in\mathcal{X}$.

Theorem F.1. *FedZO enjoys the following convergence with a constant probability for some $\Lambda>0$ when $\eta \leq \frac{7}{100\beta T}$,*

$$\min_{r\in[R+1)}\|\nabla F(\boldsymbol{x}_r)\|^2 \leq \mathcal{O}\left(\frac{D_1}{\eta RT}+\Lambda^2+G+\frac{1}{Q}\right).$$

Proof. Following the proof in our Appx. E.5, we have

$$\begin{aligned}\min_{r\in[R+1)}\|\nabla F(\boldsymbol{x}_r)\|^2 &\leq \frac{13(F(\boldsymbol{x}_0)-F(\boldsymbol{x}^*))}{\eta RT}+\frac{13}{\eta RT}\sum_{r=0}^{R}\sum_{i=1}^{N}\sum_{t=1}^{T}\left(\frac{(0.14\eta+1/(2\beta T))}{N}\Xi_{r+1,t}^{(i)}\right.\\ &\quad\left.+\frac{1.02\eta^2\beta}{N}\sum_{\tau=1}^{t}S^{t-\tau}\Xi_{r+1,\tau}^{(i)}\right)\\ &\leq \mathcal{O}\left(\frac{D_1}{\eta RT}+\left(\Lambda^2+G+\frac{1}{Q}\right)+\frac{1}{\beta}\left(\Lambda^2+G+\frac{1}{Q}\right)\right)\\ &= \mathcal{O}\left(\frac{D_1}{\eta RT}+\Lambda^2+G+\frac{1}{Q}\right),\end{aligned} \tag{97}$$

which concludes our proof. □

Remark. Of note, this convergence aligns with one provided in [2], which hence supports the validity of our Thm. E.1 and Prop. F.1.

Discussion. Of note, the key to proving the convergence of other existing federated ZOO algorithms (i.e., FedProx and SCAFFOLD) lies in the bounded client drift (i.e., Lemma E.11) when additional input disparity is introduced in these algorithms. This in fact takes up a lot of space as shown in their original paper and is also out of the scope of this paper. As a consequence, we leave out the proof of the convergence of FedProx and SCAFFOLD in federated ZOO. Fortunately, the convergence (i.e., Thm. E.1) for the general optimization framework Algo. 1 implies that the key difference among the convergence of various federated ZOO algorithms in fact lies in their difference of gradient disparity. In light of this, based on our theoretical insights about the gradient disparity in different federated ZOO algorithms (Appx. F.1), we are still able to present the following insights into the advantages of our FZooS intuitively from the perspective of convergence:

(i) In general, the convergence of our FZooS in Appx. E.5 avoids the constant error term that can not be omitted in existing federated ZOO algorithms. Note that even the error term caused by RFF approximation (see Thm. C.1) is in fact able to be mitigated by using a large number M of random features.

(ii) Compared with the convergence of FedZO in Thm. F.1, the convergence of FZooS in Appx. E.5 demonstrates that the client heterogeneity can be effectively mitigated in FZooS and the gradient estimation term enjoys a better reduction rate (i.e., exponential rate vs. polynomial rate).

(iii) The bounded client drift in Lemma E.11 for the framework Algo. 1 implies that the additional input disparity from the FedProx in Prop. F.2, the SCAFFOLD (Type I) in Prop. F.3 and the SCAFFOLD (Type II) in Prop. F.4 likely leads to a larger client drift and consequently results in worse convergence compared with our FZooS, which has been empirically supported by the results in our Sec. 5 and Appx. H.

G. Experimental Settings

General Settings. The gradient correction length is set to be $\gamma_{r,t-1}^{(i)} = 1/t$ such that it decays with the iteration of local updates t. We set the learning rate $\eta = 0.01$ and use Adam as the optimizer. As we described in line 7-8 of Algo. 2 and in Sec. 3.2.1, at each local update iteration, we actively query in the neighborhood of the input $\boldsymbol{x}_{r,t}^{(i)}$ on each client. Each time we generate 100 values of $\boldsymbol{x}_{r,t}^{(i)} + \boldsymbol{\delta}$ where each dimension of $\boldsymbol{\delta}'$ is uniformly sampled from $[-0.01, 0.01]$. We select the top 5 values with the highest uncertainty $\left\|\partial(\sigma_{r,t}^{(i)})^2(\boldsymbol{x}_{r,t}^{(i)} + \boldsymbol{\delta})\right\|$. We set the number of random features $M = 10000$ for the squared exponential kernel with a length scale of 1. Each dimension of the function input is normalized to be within $[0, 1]$ using the min-max normalization. The number of clients N, the number of local updates T, and the number of rounds R vary for different experiments.

G.1. Synthetic Experiments

Let input $\boldsymbol{x} = [x_j]_{j=1}^d \in [-10, 10]^d$, $\boldsymbol{a}^{(i)} = [a_j^{(i)}]_{j=1}^d$, and $\boldsymbol{b}^{(i)} = [b_j^{(i)}]_{j=1}^d$, then the quadratic functions on each client i that has been applied in our Sec. 5.1 is in the form of

$$f_i(\boldsymbol{x}) = \frac{1}{10d}\left(\sum_{j\in[d]}\left[\left(1 + C\left(a_j^{(i)} - \frac{1}{N}\right)\right)x_j^2 + \left(1 + C\left(b_j^{(i)} - \frac{1}{N}\right)\right)x_j\right] + 1\right) \tag{98}$$

where every $[a_j^{(i)}]_{i=1}^N$ and $[b_j^{(i)}]_{i=1}^N$ are independently randomly sampled from the same Dirichlet distribution $\text{Dir}(\boldsymbol{\alpha})$ where $\boldsymbol{\alpha} = \frac{1}{N} \cdot \mathbf{1}$. So, given any $C > 0$, the final objective function remains

$$F(\boldsymbol{x}) = \frac{1}{10d}\left(\sum_{j\in[d]}\left[x_j^2 + x_j\right] + 1\right) . \tag{99}$$

Of note, C is the constant that controls the client shift in our federated setting. Specifically, a larger C typically leads to larger client shifts whereas a smaller C usually enjoys smaller client shifts. We set the number of clients to be $N = 5$. We set $C \in \{0.5, 5, 50\}$ to vary the degree of heterogeneity (i.e., client shifts) among the local functions. The dimension of the function input is set to be $d = 300$. We set the number of local updates to be $T = 10$ and the number of rounds to be $R = 50$.

G.2. Federated Black-Box Adversarial Attack

We set the number of clients $N = 10$ in this experiment. Before we conduct the adversarial attack, we need to train $N = 10$ models on different datasets to get the heterogeneous local model functions. To control the degree of heterogeneity among these functions, each time we sample $P \times 10$ classes among the 10 classes of the dataset (i.e., MNIST or CIFAR-10) and construct a dataset that only contains data points from these $P \times 10$ classes where $P \in [0, 1]$. Repeat the above procedures for 10 times to get 10 different datasets. Consequently, a higher P means that the degree of heterogeneity among the local model functions is lower. As an example, when $P = 1$, all the local models of these clients will be exactly the same since they are all trained on the dataset with all 10 classes data points. For MNIST, we train a convolutional neural network (CNN) with two convolution layers followed by two fully connected layers on each dataset. For CIFAR-10, we train a ResNet18 on each dataset.

After obtaining these 10 local model functions for the clients, we proceed to select 15 data points from the test dataset. Specifically, we choose these data points among the ones that have been correctly classified by all of the 10 local models. These selected data points will be used as the targets for our attack. The goal is to find a perturbation $\boldsymbol{x}$, such that the modified image $\boldsymbol{z} + \boldsymbol{x}$ will be classified incorrectly by the model of each client. The local function takes the perturbed image $\boldsymbol{z} + \boldsymbol{x}$ as input and outputs the difference between the logit of the true class and the highest logit among all other classes except the true class. The condition for the attack to be successful is that the averaged output of $N = 10$ models misclassify the image $\boldsymbol{z} + \boldsymbol{x}$. The success rate is the portion of images that are successfully attacked among the selected 15 images. We set the number of local updates $T = 10$ and the number of rounds to be $R = 100$.

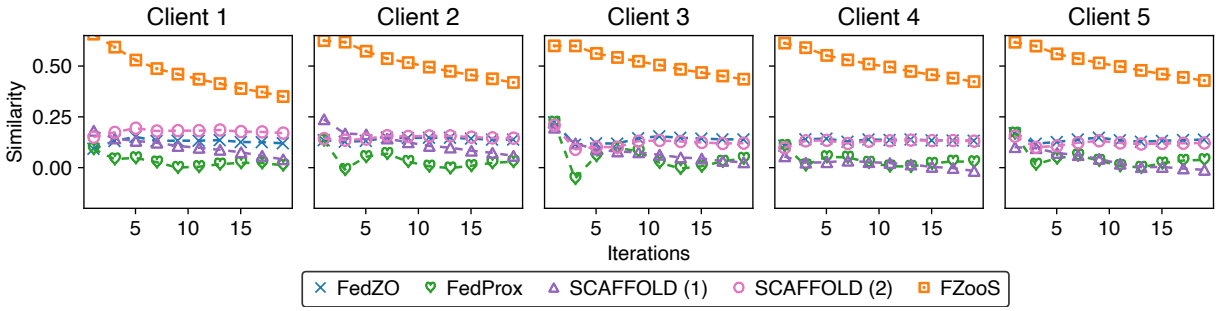

Figure 3. Comparison of the cosine similarity between $\widehat{\boldsymbol{g}}_{r,t-1}^{(i)}$ and $\nabla F(\boldsymbol{x}_{r,t-1})$ within one round (with local iterations $T = 20$) among different federated ZOO algorithms, where the y-axis denotes the cumulatively averaged similarity w.r.t. the x-axis (i.e., the iterations of local updates). Of note, for every iteration, our (5) will actively query only 5 additional function values, which is much fewer than the 20 additional queries in other existing algorithms based on FD methods.

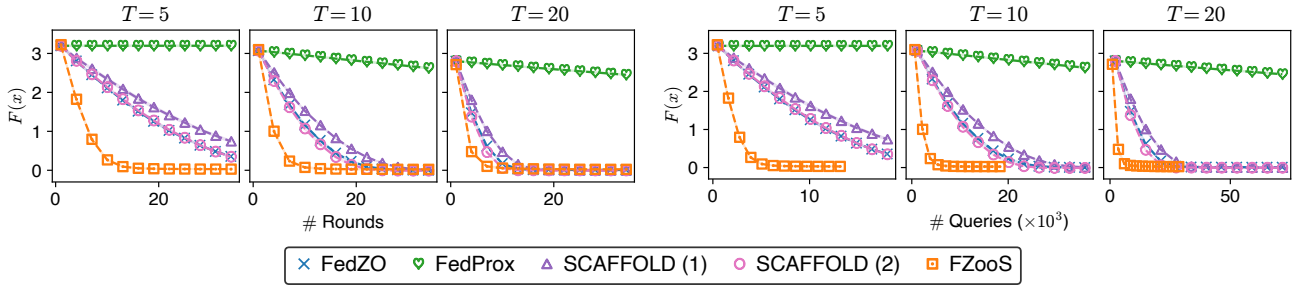

Figure 4. Comparison of the communication round and query efficiency between our FZooS and other existing baselines on the federated synthetic functions with a varying number T of local updates.

G.3. Federated Non-Differentiable Metric Optimization

Following the practice in [3], we first train a 3-layer MLP model on the training dataset of Covertype [26] using the Cross-Entropy loss to obtain its fully converged parameters $\boldsymbol{\theta}^*$. This is to simulate the federated learning (i.e., fine-tuning) of a pre-trained model with other non-differentiable metrics. Similar to the setting in Appx. G.2, we construct $N = 7$ datasets by sampling $P \times 7$ ($P \in [0, 1]$) classes from the test dataset each time. Again, the degree of heterogeneity among the local functions of the clients is controlled by P. The higher the value of P, the more heterogeneous local functions will be. In this experiment, we aim to find a perturbation $\boldsymbol{x}$ to the model parameters $\boldsymbol{\theta}^*$, such that $\boldsymbol{\theta}^* + \boldsymbol{x}$ will yield better performance for other non-differentiable metrics, e.g., precision and recall, by using the distributed datasets on clients. Specifically, the local function takes the perturbed model parameter as input and outputs the result of a non-differentiable metric (e.g., $1 -$ precision) that evaluates the performance of the model on the corresponding constructed dataset. We set $T = 10$ and $R = 50$. As in [3], we conduct experiments on four non-differentiable metrics, namely precision, recall, Jaccard score, and F1 score.

H. More Results

H.1. Synthetic Experiments

In this section, we first compare the gradient disparity of existing federated ZOO algorithms and our FZooS algorithm using the quadratic functions (see Appx. G.1) with $d = 300$, $N = 5$, and $C = 5$. The results are in Fig. 3, showing that our proposed adaptive gradient estimation is indeed able to realize significantly improved estimation quality than other existing methods while requiring fewer function queries. This consequently verified the theoretical insights of Thm. 1. Interestingly, we notice that the quality of our (5) decreases when the number of iterations for local updates is increased, which is likely because the performance of our gradient surrogates suffers when the input $\boldsymbol{x}$ for gradient estimation is far away from the historical function queries (i.e., few function information at $\boldsymbol{x}$ can be used for predictions), as theoretically supported in our Appx. E.3. This also indicates the importance of active queries in our FZooS for consistently high-quality (5) by collecting more function information in the neighborhood of the potential updated inputs within the local updates.

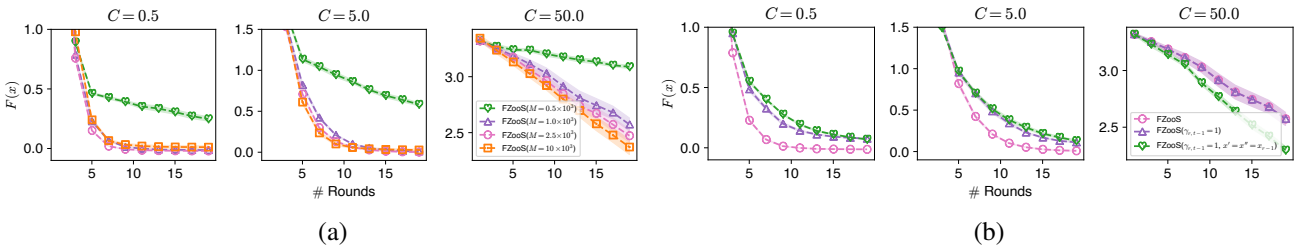

Figure 5. Comparison of the communication round efficiency of our FZooS (a) with a varying number M of random features and (b) without adaptive gradient correction. Of note, $\gamma_{r,t-1} = 1$ means a fixed gradient correction length and $\boldsymbol{x}' = \boldsymbol{x}'' = \boldsymbol{x}_{r-1}$ stands for a fixed gradient correction vector as in SCAFFOLD.

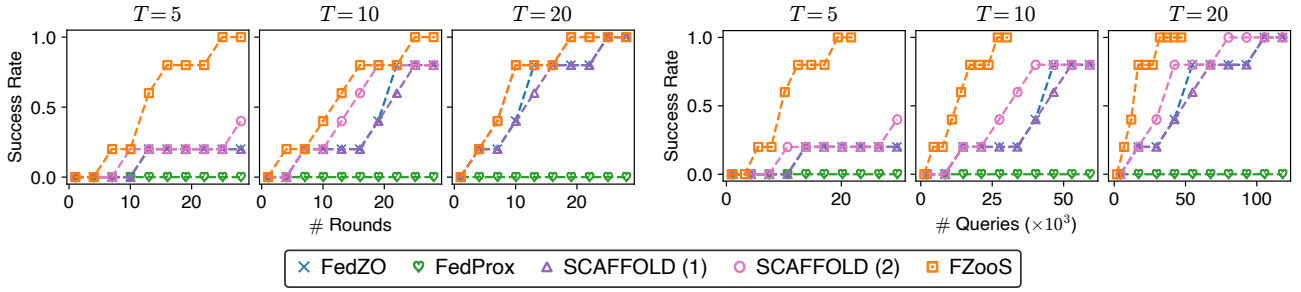

Figure 6. Comparison of the success rate achieved by FZooS and other existing federated ZOO algorithms on CIFAR-10 under a varying number T of local updates.

In addition to the comparison using a quadratic function that is under varying heterogeneity through different C in our Fig. 1, we present the comparison using a quadratic function that is under a varying number T of local updates in Fig. 4. Remarkably, our FZooS still considerably outperforms other baselines in terms of both communication round efficiency and query efficiency. Interestingly, Fig. 4 shows that a larger T usually improves the communication round efficiency of both our FZooS, as theoretically supported in our Thm. C.1. However, such an improvement is usually smaller than the increasing scale of T. This also aligns with our Thm. C.1 since our Thm. C.1 demonstrates that the increasing T fails to mitigate the impact of client heterogeneity. That is, term G in Thm. C.1 can not be reduced when T is increased.

We finally present the comparison of the communication round efficiency of our FZooS (a) with a varying number M of random features and (b) without adaptive gradient correction under varying client heterogeneity in Fig. 5. Of note, in Fig. 5, we only apply $M = 1000$ random features to facilitate a clear and direct comparison. Interestingly, Fig. 5(a) demonstrates that our FZooS of a larger number M of random features generally is preferred for an improved communication round efficiency when the client heterogeneity (i.e., C) is increased, which thus aligns with the theoretical insights from our Thm. C.1 in Appx. C.2. Nevertheless, when client heterogeneity is small (e.g., $C \leq 5.0$), a moderate number of random features can already produce compelling and competitive convergence. Meanwhile, Fig. 5(b) illustrates that, in general, both our adaptive gradient correction vector and adaptive gradient correction length are essential for our FZooS to achieve remarkable convergence in practice. Surprisingly, our FZooS with fixed gradient correction outperforms its counterpart with adaptive gradient correction when client heterogeneity is large (i.e., $C = 50$). This is likely because a small number of random features (i.e., $M = 1000$) are applied when $C = 50$, making adaptive gradient correction generally inaccurate for a long horizon of local updates since the quality of our gradient surrogates decays w.r.t. the horizon (i.e., iterations) as shown in Fig. 3. This can also be verified from Fig. 5(a). On the contrary, the fixed gradient correction is already of reasonably good quality due to the smoothness of the global function F (i.e., its gradients are continuous), which consequently can provide consistently good gradient correction along a long horizon of local updates when client heterogeneity is large (i.e., $C = 50$).

H.2. Federated Black-Box Adversarial Attack

In addition to depicting the success rate of attacks on CIFAR-10 in Fig.2, which accounts for varying client heterogeneity, we also present the success rate of attacks on CIFAR-10 considering a variable number of local updates, as showcased

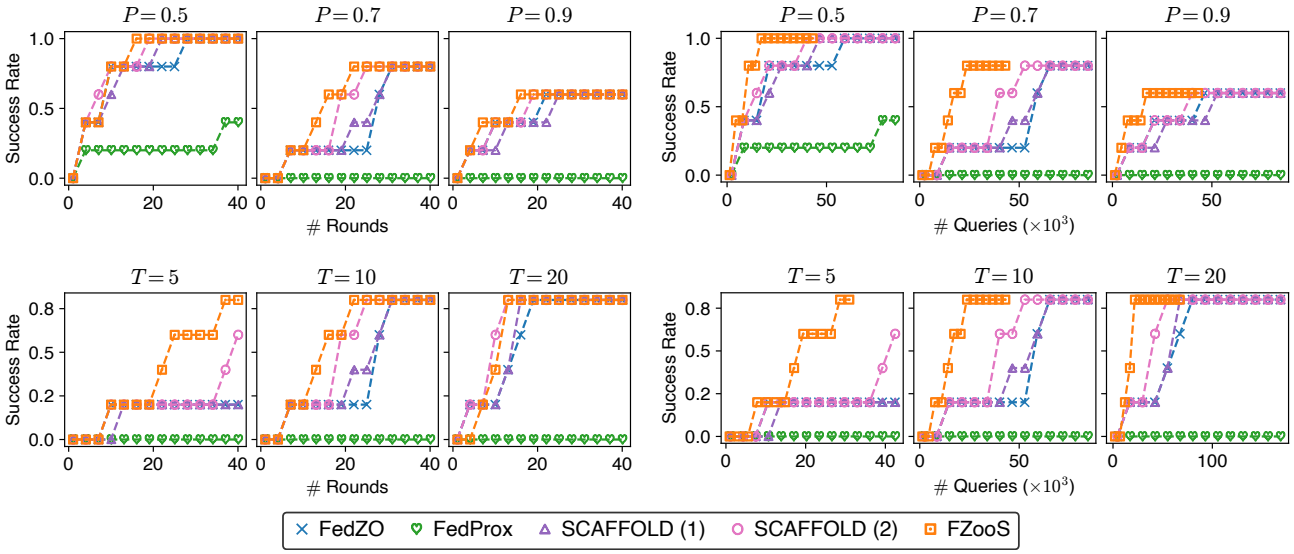

Figure 7. Comparison of the success rate in federated black-box adversarial attack achieved by FZooS and other existing federated ZOO algorithms on MNIST under varying client heterogeneity (controlled by $P \in [0, 1]$, a larger P implies smaller client heterogeneity) and a varying number T of local updates. The x and y-axis are the number of rounds/queries and the corresponding success rate (higher is better).

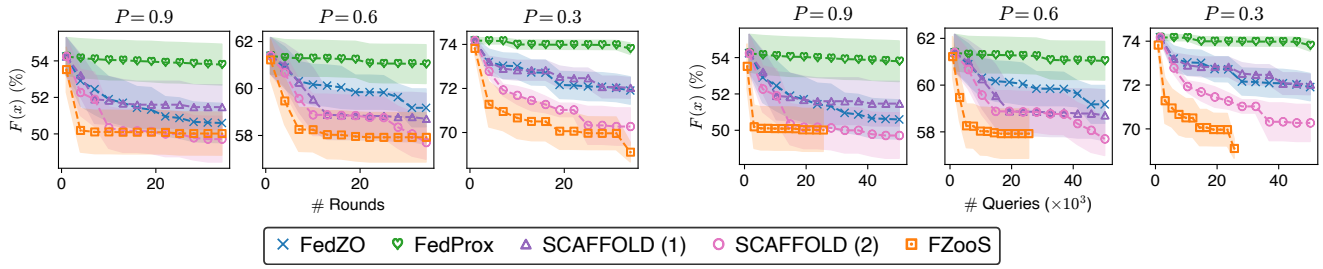

Figure 8. Comparison of the non-differentiable metric optimization between FZooS and other existing federated ZOO algorithms under varying client heterogeneity (controlled by $P \in [0, 1]$, a larger P implies smaller client heterogeneity). The y-axis is $(1-\text{precision}) \times 100\%$ and each curve is the mean $\pm$ standard error from five independent runs.

in Fig.6. Furthermore, we provide an illustration of the attack success rate on MNIST, considering both varying client heterogeneity and a variable number of local updates, as presented in Fig. 7. Notably, our proposed algorithm consistently demonstrates enhanced efficiency in terms of communication rounds when compared to other baselines, across different levels of client heterogeneity and varying numbers of local updates.

H.3. Federated Non-Differentiable Metric Optimization

Besides the non-differentiable metric optimization result for the precision score that is under a varying heterogeneity through different P in Fig. 8, we also report the corresponding result under a varying number T of local updates in Fig. 9. Moreover, we provide results for recall, F1 score, and Jaccard as the non-differentiable metric in Fig. 10, Fig. 11, and Fig. 12 respectively. Notably, our FZooS still consistently outperforms other baselines in terms of both communication round efficiency and query efficiency when under the comparison of varying client heterogeneity and a varying number of local updates with different non-differentiable metrics.

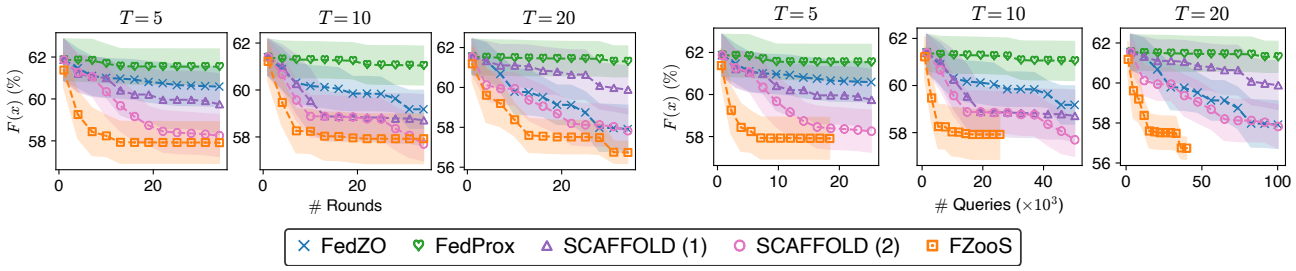

Figure 9. Comparison of the non-differentiable metric optimization between FZooS and other existing federated ZOO algorithms under a varying number T of local updates. Note that the y-axis is $(1 - \text{precision}) \times 100\%$ and each curve is the mean $\pm$ standard error from five independent runs.

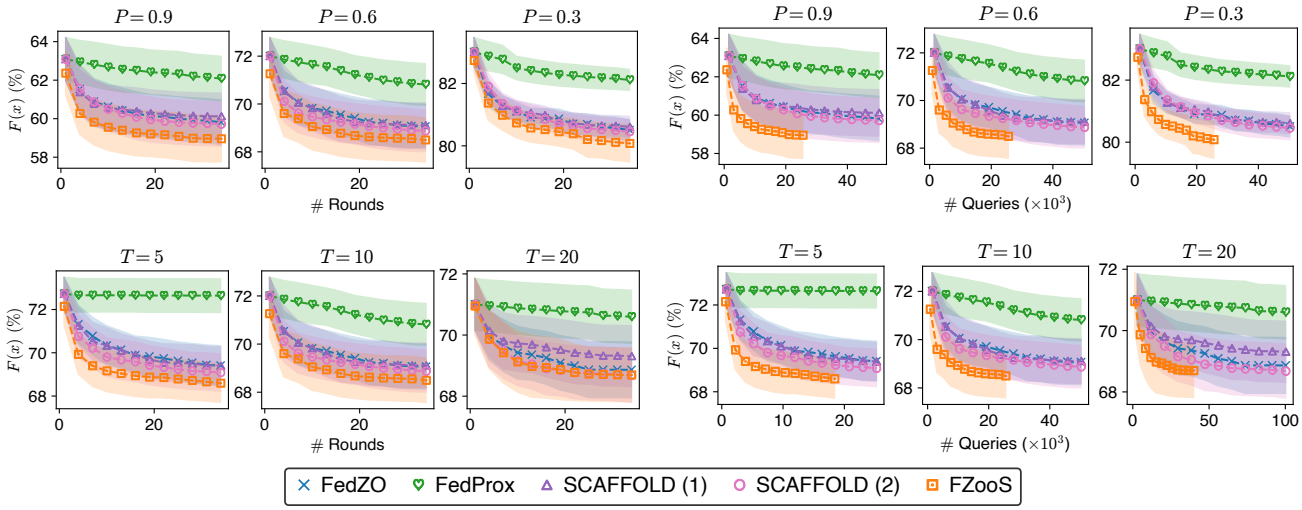

Figure 10. Comparison of the non-differentiable metric optimization between FZooS and other existing federated ZOO algorithms under varying client heterogeneity (controlled by $P \in [0, 1]$, a larger P implies smaller client heterogeneity) and a varying number T of local updates. Note that the y-axis is $(1 - \text{recall}) \times 100\%$ and each curve is the mean $\pm$ standard error from five independent runs.

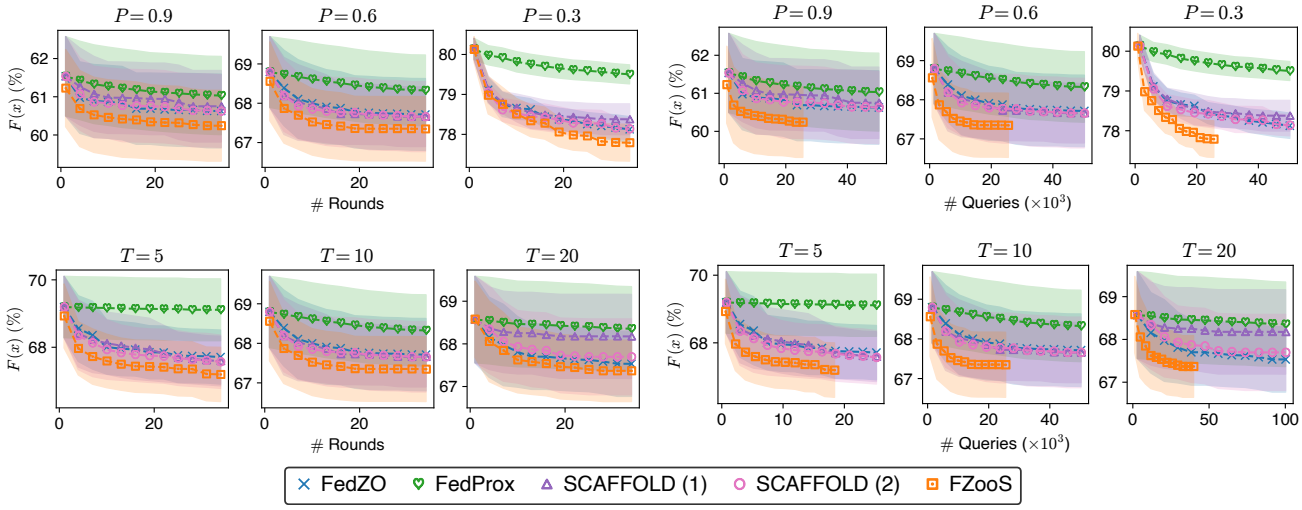

Figure 11. Comparison of the non-differentiable metric optimization between FZooS and other existing federated ZOO algorithms under varying client heterogeneity (controlled by $P \in [0, 1]$, a larger P implies smaller client heterogeneity) and a varying number T of local updates. Note that the y-axis is $(1 - \text{F1 score}) \times 100\%$ and each curve is the mean $\pm$ standard error from five independent runs.

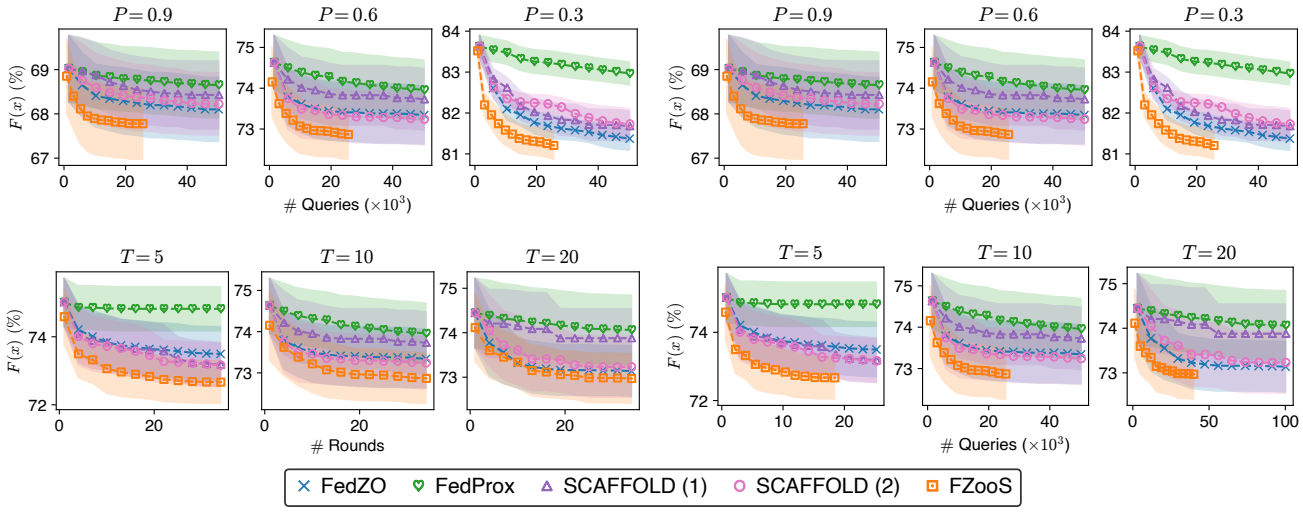

Figure 12. Comparison of the non-differentiable metric optimization between FZooS and other existing federated ZOO algorithms under varying client heterogeneity (controlled by $P \in [0, 1]$, a larger P implies smaller client heterogeneity) and a varying number T of local updates. The y-axis is $(1 - \text{Jaccard score}) \times 100\%$ and each curve is the mean $\pm$ standard error from five independent runs.